QUANTIFYING THE EFFECTS OF MOISTURE CHANGE ON THE SPECTRAL SIGNATURES (350-2500 NM) OF ARCTIC MOSSES, LIVERWORTS, AND LICHENS

A Thesis

by

KATE DIANE VON NESS

Submitted to the Office of Graduate and Professional Studies of
Texas A&M University
in partial fulfillment of the requirements for the degree of

MASTER OF SCIENCE

Chair of Committee,	Julie Loisel
Committee Members,	Anthony Filippi
	Jason West
Head of Department,	David Cairns

May 2021

Major Subject: Geography

ABSTRACT

Increasing temperatures have been altering hydrological conditions and leading to ecological regime shifts across the Arctic biome, with influences on terrestrial carbon cycling. However, the sign, extent, and magnitude of change in Arctic terrestrial carbon cycling from warming is still ambiguous, especially in wetlands and peatlands. Non-vascular vegetation (specifically bryophytes and lichens), which can tolerate low light, extreme cold, desiccation, and waterlogged conditions, are dominant vegetation components in high-latitude ecosystems. As such, they have significant ecological roles in moderating soil temperature and moisture, water flow/retention, nutrient availability, and carbon storage. However, despite their importance and dominance in northern ecosystems, they are still severely neglected or inadequately represented in most Earth System Models.

Remote sensing, being quick and cost-effective, is a popular tool to monitor inaccessible Arctic environments. While the spectral properties of low-latitude vascular vegetation have been of large focus, few have looked at the spectral responses of (sub-)Arctic mosses, lichens, and liverworts, especially how they change with moisture shifts. Using lab water table depth manipulations to simulate shifts from desiccation (0% moisture) to saturation (100% moisture), this project quantified the effects of moisture change on the hyperspectral signatures (350-2500nm) of Arctic mosses, lichens, and liverworts.

Results show that spectral properties vary widely across species and plant types, especially in the VIS and NIR. As moisture was lost, species showed similar patterns in spectral response (primarily in SWIR), with a general increase in reflectance and similar changes in shape; all species developed new peaks and rises in reflectance in SWIR1 and SWIR2 after reaching a certain desiccation point. Furthermore, below 20 to 30% moisture, species eventually became spectrally indistinguishable in the SWIR. Overall, the unique spectral properties in the VIS and NIR can be used to create a "spectral library" to distinguish between some of these non-vascular species; likewise, I show that moisture plays a critical role in the spectral response of these species and, as they get close to desiccation, spectral discrimination in SWIR wavelengths may prove very challenging. This finding may have critical implications for the methods used to map these vegetation types and their unique ecological functions.

ACKNOWLEDGEMENTS

I would like to thank my committee chair, Dr. Julie Loisel, for her encouragement and guidance in completing this research. I would also like to extend gratitude to my committee members, Dr. West and Dr. Filippi, for offering input on this research and reviewing this thesis.

Thanks also go out to the department faculty and staff, and my colleagues for making my graduate education at Texas A&M University a remarkable and unforgettable time in my life. Furthermore, I would like to acknowledge Katherine Beall and Patrick Campbell for their assistance in sample collection, and thank Erin Cox for her time spent identifying these species, both of which were a large part of what made this work possible.

Lastly, I would like to thank my family for their long support of my educational endeavors and above all, I would like to thank my fiancé Bradley for his patience, support, and love at all times throughout this experience.

CONTRIBUTORS AND FUNDING SOURCES

Contributors

This work was supervised by a thesis committee consisting of Professors Julie Loisel (advisor) and Anthony Filippi of the Department of Geography, and Professor Jason West of the Department of Ecosystem Science and Management.

Fieldwork expeditions and sample collection were assisted by Professor Julie Loisel, Katherine Beall (M.S. student in the Department of Geography), Patrick Campbell, and the staff at the Canadian High Arctic Research Station in Cambridge Bay, Nunavut. The spectrometer used to collect the spectral data for this research was provided by the Boise Center Aerospace Laboratory at Boise State University, and species identification was conducted by Erin Cox, M.S. student in the Faculty of Science – Biological Sciences at the University of Alberta.

All other work conducted for the thesis was completed by the student independently.

Funding Sources

Graduate study was supported by an assistantship from Texas A&M University and scholarships from the Marathon Oil Corporation, College of Geosciences, and South Texas Women's Energy Network.

This work was also made possible in part by the National Science Foundation under Grant Number 1802838. Its contents are solely the responsibility of the authors and do not necessarily represent the official views of the National Science Foundation.

NOMENCLATURE

ABoVE	Arctic Boreal Vulnerability Experiment
C	Carbon
CAVM	Circumpolar Arctic Vegetation Map
CO_2	Carbon Dioxide
CH_4	Methane
ESMs	Earth System Models
GPP	Gross Primary Production
LiDAR	Light Detection and Ranging
N	Nitrogen
NDVI	Normalized Difference Vegetation Index
NIR	Near-Infrared range, 700-1400nm
P	Phosphorous
SID	Spectral Information Divergence
SWIR1	Shortwave-Infrared range 1, 1400-1900nm
SWIR2	Shortwave-Infrared range 2, 1900-2500nm
UAVs	Unmanned Aerial Vehicles
VIS	Visible range, 400-700nm

TABLE OF CONTENTS

Page

LIST OF FIGURES

Page

LIST OF TABLES

Page

1. INTRODUCTION AND LITERATURE REVIEW

1.1. Introduction

The Arctic, often termed Earth's last frontier, has been gaining attention due to its significant role in global environmental processes and vulnerability to climate change. The Arctic influences the energy balance of the global climate system in a number of ways. First, its radiative energy deficit is a primary driver in atmospheric circulation that counteracts the radiative excess of the tropics; as such, the Arctic is often viewed as the world's 'air-conditioner' (McGuire et al., 2006). The atmospheric circulation patterns and associated exchanges of heat and energy across the equator-to-pole gradient affect the transport of moisture, and thus the precipitation regimes, across the globe. The Arctic region also plays a key role in ocean circulation: cold and dense polar waters sink deep into the North Atlantic, driving the thermohaline circulation, which distributes energy and nutrients around the world's oceans (Serreze & Barry, 2014; Carmack et al., 2016). Another important and unique role of the Arctic is its capacity for serving as a large soil carbon (C) stock, with estimates of soil C in the circumpolar permafrost region being approximately double the amount of total atmospheric C (van Huissteden & Dolman, 2012; Hugelius et al., 2020).

The Arctic has been experiencing more than twice the warming of the rest of the world, causing concern for its capacity to maintain its aforementioned climate regulating roles at the global scale. At the regional scale, of particular concern is the response of its terrestrial ecosystems to ongoing and projected warming (Post et al., 2019). Indeed,

scientists have been documenting substantial shifts in ecosystem structure and function throughout the high latitudes (Hinzman et al., 2005). For example, evident shifts in vegetation have been termed the Arctic greening phenomenon, in which observations show an increase in aboveground plant biomass, height, abundance, and cover, particularly with shrub expansion, across the tundra (Jia et al., 2003; Tape et al., 2006; Myers-Smith et al., 2020). Likewise, permafrost thaw and ice-wedge degradation are widely-discussed consequences of Arctic warming. Higher temperatures lead to thawing of perennially frozen ground, causing ground subsidence and mass movements (Kokelj et al., 2017; Lewkowicz & Way, 2019). Over the next decades, these changes could lead to landscape-scale drainage and drying in some areas, vs. water ponding and flooding in others (Schuur et al., 2008; Liljedahl et al., 2016; Hugelius et al., 2020). Shifting snowfall patterns have also been observed as a result of warming, with non-uniform variations in snowfall extent, depth, and rates reported across the Arctic (Callaghan et al., 2011; Liu et al., 2012). These changes in snowfall have multiple effects on terrestrial ecosystems, including changes in water provision, soil insulation, and heat exchanges with the atmosphere (Schuur & Mack, 2018). Other impacts associated with warming that may have serious ecological ramifications across the Arctic include increasing insect outbreaks (Kurz et al., 2008) and wildfires (Mack et al., 2011).

While it is known that these environmental changes have, or will have, substantial effects on the Arctic terrestrial C cycling, the extent, magnitude, and sign of these effects are still largely ambiguous (Turetsky et al., 2020). This leaves many questions regarding the role Arctic terrestrial ecosystems will play in the global C cycle under warming

conditions. In particular, the role of wetlands and peatlands is worth evaluating, as these ecosystems are substantive long-term C sinks, but can also be significant C sources to the atmosphere, if they release the C they have stored for millennia (Bridgham et al., 2006). It is often argued that drying conditions (due to post-thaw drainage), coupled with warmer soil temperatures, will lead to intensified microbial activity and thus, greater carbon dioxide (CO_2) emissions to the atmosphere due to peat decomposition (Schuur et al., 2015). Likewise, wetter conditions (due to post-thaw flooding) would lead to greater methane (CH_4) emissions (Liljedahl et al., 2016). Should a large quantity of C be released from peatlands and wetlands, recent debates pertain to whether those greenhouse gasses would be emitted gradually (as thaw depths increase) or abruptly (due to thermokarst collapse) (Turetsky et al., 2020). On the other hand, multiple studies point to an increase in the peatland C sink across the Arctic due to greater plant primary productivity that is driven by longer and warmer growing seasons (Gallego-Sala et al., 2018; Chaudhary et al., 2020; Loisel et al., 2020).

Plant-environmental interactions are of particular interest when trying to understand the fate of peatland and wetland C stocks under warming conditions, because plant composition, extent, and productivity/decay affect biosphere-atmosphere C exchanges. For instance, sedge communities enable the release of belowground CH_4 bubbles to the atmosphere due to their aerenchyma tissues (Lai, 2009), while the recalcitrance of *Sphagnum* mosses to decay slows down peat diagenesis (van Breemen, 1995). As warming changes ecosystem hydrology (e.g., through permafrost thaw), increases growing season length, and promotes northward vegetation migration, Arctic

plants will be subjected to new regimes in terms of soil temperature/moisture, water and nutrient availability, plant and microbial community composition and distribution, and productivity/decay rates. For example, evidence of warming effects on plant community dynamics includes shrubification (or the expansion and increase of shrubs) which, through their litter production and shading, has led to declines in moss and lichen populations (Davis et al., 2020). Yet a large amount of uncertainty still remains in regards to how Arctic plant-environmental interactions are, or will be, changing under warmer temperatures and how these changes can be best monitored or detected (Elmendorf et al., 2012).

Remote sensing techniques are key in tackling the topic of Arctic climate-C feedbacks, offering quick and relatively cheap measurements from otherwise inaccessible lands (Jorgenson & Grosse, 2016). Remote sensing can provide critical ecosystem information across large spatial and temporal extents (Lees et al., 2018). There has been much progress made in using remote sensing to study and monitor Arctic ecosystems with, for example, time-lapse imagery and unmanned aerial vehicles (UAVs) which have proven to be successful ways for supplementing field-based measurements and overcoming limitations presented by optical remote sensing systems (Beamish et al., 2020). However, the analysis of non-vascular vegetation has only been fairly recently given more attention, and thus, these vegetation types are often inadequately represented in, or neglected from, studies and Earth System Models (ESMs) despite their dominance and ecological significance in the Arctic (Beringer et al., 2001; Cornelissen et al., 2007). In fact, most ESMs do not have an adequate representation of Arctic vegetation dynamics,

if any at all, especially in terms of vegetation-C relations (Song et al., 2017; Fisher et al., 2018; Winkler et al., 2019). This omission or inadequate representation is in part due to the lack of ability to identify, classify, and map different non-vascular vegetation types, which causes these plants to be lumped into other plant functional groups (Turetsky et al., 2012). As non-vascular vegetation insulates soil and permafrost (moderating soil temperature/moisture), regulate water flow/retention, impact nutrient availability, compete with vascular vegetation, and drive C storage/emissions (through productivity/decay), these vegetation types are fundamentally important to northern ecosystem dynamics (Longton, 1988; Longton, 1997; Brodo et al., 2001; Turetsky et al., 2012). Therefore, their response to warming has a large capacity to not only shift these ecosystem dynamics, but affect the hydrological, biogeochemical, and surface-energy feedbacks which structure Arctic ecosystems. Improving non-vascular vegetation mapping and identifying taxa-specific traits may be necessary to remedy this issue of their neglect and adequately account for the functional and structural roles that non-vascular vegetation have in Arctic ecosystems (Turetsky et al., 2012). This is particularly relevant when considering how to sufficiently represent bryophytes and lichens, critical plant types in the Arctic, and their response to warming temperatures (Cornelissen et al., 2007; Turetsky et al., 2012; He et al., 2016).

1.2. Arctic Wetlands and Peatlands

Wetlands cover approximately 5-8% of the global land area and include a variety of ecosystem types (e.g., swamps, marshes, peatlands) (Mitsch & Gosselink, 2015). Three

criteria must be fulfilled for an ecosystem to be considered a wetland: 1) there must be a presence of water, either as saturated soil (where water is within the root zone) or as annual or seasonal ground surface flooding; 2) the soil conditions must uniquely differ from nearby upland areas (e.g., accumulated organic matter that slowly decomposes); and 3) the biota supported in this ecosystem should be composed of both terrestrial and aquatic vegetation that are adapted to saturated conditions (Mitsch & Gosselink, 2007). A wetland that has accumulated thick deposits (>30 or 40 cm, depending on country-specific definitions) of organic matter is called a peatland (Gorham, 1991). In these ecosystems, dead/decaying plant material accumulates in waterlogged layers of soil (known as peat) because plant productivity exceeds peat decay (Rydin & Jeglum, 2006). Peatlands account for approximately half of all wetlands and they include a variety of ecosystems themselves, such as marshes, fens, and bogs, and they are also abundant in permafrost-dominated areas. Peatland types are typically determined by local conditions, including substrate, hydrology, chemistry, vegetation, and climate (Yu et al., 2009). For example, fens have seasonal contact with surface or ground-water flow and tend to be more nutrient-rich, while bogs are hydrologically isolated from any local water influences (they rely on rainwater) and are often more nutrient-poor (Vitt, 2006).

Wetlands and peatlands can be found globally in a range of environments (Hu et al., 2017; Xu et al., 2018), but they are most widely found in the boreal and (sub-)Arctic biomes (Figure 1). Over half of the global wetland area is found in the high-latitude regions (above 50°N), with peatlands being a substantial portion of these wetlands (Petrescu et al., 2010; Minayeva et al., 2018).

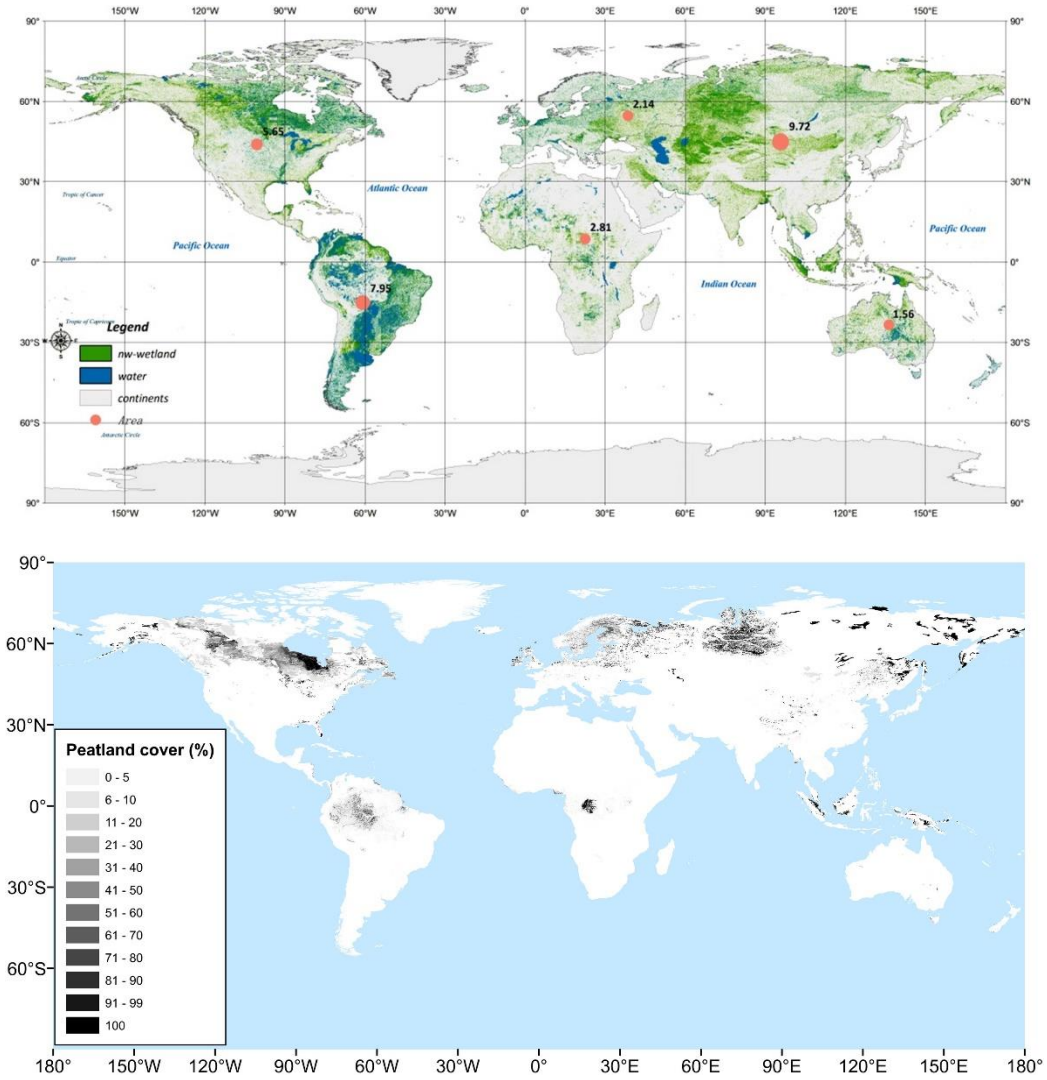

Figure 1: Global wetland and peatland distribution. Top – Modeled wetland distribution, with total wetland area (million km^2) for each continent shown by a red circle; reprinted from Hu et al. (2017). Bottom – PEATMAP-derived peatland distribution, based on national inventories, with shades indicating peatland cover; reprinted from Xu et al. (2018).

Peatlands and wetlands are known for their role in the global C cycle. Throughout most of the Holocene, northern peatlands have acted as net sinks of CO_2 at the millennial timescale (Frolking et al., 2006). Northern peatlands have accumulated approximately 400

to 500 petagrams of C (Gorham, 1991; Yu et al., 2010), but they are also considerable sources of CH_4 to the atmosphere (Frolking et al., 2006). Peatlands have generally been regarded as net C sinks in the high-latitudes, as cold regions offer more conducive conditions for waterlogged, anoxic, and cold soils where organic matter decays slowly, effectively enhancing peat formation and C sequestration despite low plant productivity (Gorham, 1991; Petrescu et al., 2010; Coffer & Hestir, 2019). However, it is also these conditions that make high-latitude wetlands and peatlands CH_4 hotspots, particularly those affected by thawing permafrost (Bubier & Moore, 1994). Indeed, Arctic wetlands are estimated to contain close to half of the world's soil C (Coffer & Hestir, 2019) and presently emit an estimated 27 teragrams of CH_4 annually (Philben et al., 2020), which amounts to ~7% of the world's natural CH_4 emissions (Saunois et al., 2020). These figures are expected to change as the climate warms and permafrost thaws because more soil C will be exposed to decomposition, creating a positive feedback for warming (Andresen et al., 2017; Philben et al., 2020). That said, and as mentioned above, since many other factors play a role in balancing C in peatlands (e.g., microbial community shifts, plant productivity/decay changes), there is still much uncertainty in the fate of the peatland C stock across the high latitudes.

The fate of peatlands and wetlands under warming conditions has been a long-discussed topic (Gorham, 1991; Burkett & Kusler, 2000; White et al., 2008; Sim et al., 2019; Koffi et al., 2020). Rises in temperature are expected to bring about increases in precipitation and permafrost thaw, with the latter leading to land subsidence, thermokarst formation, and wetter conditions themselves leading to wetland expansion (Schuur &

Abbott, 2011; Zhang et al., 2017; Turetsky et al., 2020). A few studies have also suggested enhanced peat accumulation in some areas of the Arctic, where wetter conditions further reduce peat decay and sustain plant productivity, with the latter also aided by warming temperatures (Heffernan et al., 2020; Hugelius et al., 2020). This scenario is expected to increase CH_4 emissions across the Arctic, at least in the short term (Chaudhary et al., 2020). On the other hand, warmer temperatures and thermokarst are also thought to lead to hydrological draining of landscapes, which may lead to drier conditions, accelerating peat decomposition rates, ultimately reducing wetland extent and CH_4 emissions, and enhancing peat degradation (Tarnocai, 2009). Under this alternative scenario, drying may either inhibit or promote plant growth (depending on the intensity of drying) and certainly accelerate peat decay via enhanced microbial activity, which emits CO_2 back to the atmosphere, turning wetlands and peatlands into C sources (Tarnocai, 2009). Overall, while all these scenarios are probably taking place simultaneously in different portions of the Arctic, much uncertainty remains about the CO_2:CH_4 release ration and the overall sign and magnitude of the changes of both gasses. These uncertainties are compounded by the role of climate-induced disturbances, notably fires (Zoltai et al., 1998).

Paleoecological work has shown that high-latitude peatlands likely thrived and sequestered a significant amount of C under past warmer conditions (Jones & Yu, 2010; Charman et al., 2013; Loisel & Yu, 2013; Loisel et al., 2014; Treat et al., 2019). These studies suggest that warmer temperatures increased plant growth and peat burial rates at a greater rate than peat decay. This may indicate that peatlands will continue to sequester C across the Arctic under future warming conditions, yet there is little empirical work that

studies the potential for new peatlands to form under these conditions (but see Zhang et al., 2017 for a modeling study).

Vegetation is a key component to understanding wetland and peatland ecosystem structure and functions. While different types of wetlands and peatlands differ in dominant vegetation types or specific coverages, Arctic communities are typically characterized by a carpet of bryophytes and wet-adapted vascular vegetation (Moor et al., 2017). Vegetation types are important determinants of peatland function, as peat accumulation and degradation (and thus, C sequestration and release) are directly impacted by rates of plant productivity and decay (Acosta et al., 2017). For example, mosses decompose more slowly than vascular plants due to their recalcitrant tissue which is more resistant to microbial breakdown since it has low nitrogen (N) concentration and large concentrations of nonpolar compounds and phenolics (Turetsky, 2003). In terms of ecosystem structure, vegetation types can moderate surface-energy fluxes, nutrient cycling, microtopography, and water storage and flow, all of which directly modify the characteristics and conditions of that environment (Miller & Smith, 2012). For example, moss biomass production, with its low decomposition rates, can produce hummock-hollow formations that physically modifies the ecosystem microtopography, creating individual microhabitats and enhancing community diversity in tundra ecosystems (Turetsky et al., 2012). As such, hummock species are on elevated mounds that may be exposed to drier conditions, while hollow species are in low areas that are often saturated and have higher productivity.

1.3. Non-Vascular Tundra Vegetation

The plant kingdom can broadly be divided into vascular (tracheophytes) and non-vascular (cryptogams) vegetation. Non-vascular vegetation differs from vascular vegetation primarily by their differences in anatomies and morphologies. While vascular vegetation has highly specialized tissues (e.g., xylem/phloem) to transport nutrients and water, non-vascular vegetation lacks any vascular tissue and any true root, stem, or leaf components (Lakatos, 2011; Roos et al., 2019). Perhaps one of the most widely noted differences in non-vascular vegetation is their poikilohydry. While vascular plants evolved to grow roots and have an efficient internal water/nutrient conducting system for extracting resources from the soil, non-vascular plants evolved to use water wherever and whenever available above ground (Proctor, 1982). Therefore, in theory, non-vascular plants have no direct control over their water loss and depend entirely on their environmental conditions. However, in practice, they have developed a unique ability to tolerate desiccation (poikilohydry), as these plants can survive extremely dry conditions and once re-wetted, quickly (within minutes to hours) rebound to a normal metabolism (Proctor & Tuba, 2002). Some have also developed adaptations to further optimize their water retention/attainment, such as capillarity, tight shoot/canopy structures to collectively hold moisture, development of internal water-conducting cells (e.g., *Sphagnum* mosses), and whitening during desiccation to minimize irradiance absorption and limit further cellular damage and evaporative water loss (Proctor, 1982; Elumeeva et al., 2011; May et al., 2018).

While non-vascular vegetation covers a diverse range of biomes and environmental gradients, they (specifically bryophytes and lichens) are critical components in tundra ecosystems, as their tolerance for desiccation/drought, low light, extreme cold, and waterlogged conditions allow them to dominate these landscapes (Cornelissen et al., 2007; Huemmrich et al., 2013). Thus, in many high-latitude ecosystems, non-vascular vegetation significantly contributes to primary productivity and accounts for a considerable portion of tundra C uptake (Huemmrich et al., 2013; Carriqui et al., 2019). In their dominance and unique physiologies, bryophytes and lichens tend to create their own system and habitat apart from vascular vegetation, giving them distinctly critical roles in regulating Arctic soil nutrient, thermal, C, and hydrologic regimes as well as Arctic surface energy exchanges from those of vascular plants (Mägdefrau, 1982; Beringer et al., 2001; Porada et al., 2016). For example, in simulating N deposition events, it was shown that vascular and non-vascular plants have unique roles in the partitioning of ecosystem nutrients, with non-vascular plants assimilating N more quickly (Choudhary et al., 2016). Yet, despite the importance, dominance, and uniqueness of bryophytes and lichens in Arctic ecosystems, they are still severely neglected or inadequately represented in most ESMs (Beringer et al., 2001; Street et al., 2012; Turetsky et al., 2012; Wullschleger et al., 2014; Roos et al., 2019). Furthermore, He et al. (2016) point out that when studying climate change effects on vegetation, there tends to be a bias in the academic community towards vascular vegetation.

Cornelissen et al. (2007) suggest this neglect may be due to historic unfamiliarity with non-vascular vegetation and/or methodological and identification issues. Turetsky et

al. (2012) extend this thought, suggesting that the inattentiveness to specific non-vascular vegetation could be partially due to the general inability to classify and identify non-vascular plant types, which requires detailed analysis. This causes these taxa to be lumped into other plant functional groups that are not as meaningful in characterizing the biophysical characteristics and ecosystem functions of non-vascular plants. Wullschleger et al. (2014) further emphasize this issue, pointing out that even a single plant functional type for one type of non-vascular plant (e.g., moss) is likely going to be insufficient for characterizing their environmental functions, as different species can critically vary in their physiology, morphology, and thus, their plant-environmental interactions. Furthermore, even though bryophytes are particularly abundant in Arctic wetlands (Longton, 1982), Elumeeva et al. (2011) report that their water contents and moisture holding capacities are poorly represented in studies. Turetsky et al. (2012) suggest that identifying species-specific traits (e.g., chlorophyll content, water retention capacity) could remedy this issue and aid in studying their response to a warming climate. Therefore, better understanding the ecosystem functions and interactions of Arctic lichens and bryophytes in the face of a changing climate will depend on a better identification and representation of these plants' species-specific traits (Cornelissen et al., 2007; Turetsky et al., 2012; Bengtsson et al., 2020).

1.3.1. Bryophytes (Mosses and Liverworts)

Bryophytes, which include mosses, liverworts, and hornworts, have over 15,000 species identified across the three lineages (He et al., 2016). Mosses are the most numerous

and diverse species of the bryophyte phyla, with more than 12,000 species identified across the globe (Crandall-Stotler & Bartholomew-Began, 2007; Griffin-Nolan et al., 2018). Liverworts have the second most at 6,000-8,000 species identified, and hornworts have the least at 150 species (Wood, 2007). Still, it is thought that many species within the bryophyte phyla (and therefore the full bryophyte diversity) have not been identified (Lewis et al., 2017).

1.3.1.1. Physiology

Bryophytes are C3 plants (Proctor, 2000a) that exhibit a few key physiological differences when compared to their vascular counterparts. In particular, they have lower net maximal photosynthesis rates than vascular vegetation (He et al., 2016). This can be because of their differing photosynthetic structure, as bryophytes allocate more energy to producing thicker cell walls for their desiccation tolerance and water storage purposes, giving them higher cell wall to volume ratios (Waite & Sack, 2010; He et al., 2016; Carriqui et al., 2019). This could also be from their typically wet environments, as water in their cell walls and on the leaf surfaces increases the resistance to CO_2 diffusion (Proctor, 2000b; Waite & Sack, 2010; Niinemets & Tobias, 2014). As shade-adapted plants that thrive in cool to cold temperatures, bryophytes are also more capable of maintaining photosynthesis under limited light and lower chlorophyll absorption as well as under more restricted temperature ranges than vascular plants (He et al., 2016).

Regarding reproduction, bryophytes are capable of both sexual and asexual reproduction and may actively engage in both activities (Anderson, 1963). In sexual

reproduction, the sperm (male gamete) is produced on the gametophyte in the antheridia, which is a small, often stalked and club-shaped structure, and the eggs are produced in a swollen section of the archegonia, a small flask-like structure on the gametophyte, which the sperm must enter using the neck or tubular section to reach the egg (Goffinet & Shaw, 2009). Once the egg is fertilized, it develops into a sporophyte that may be stalked or non-stalked and that includes a spore-containing capsule; with successful germination, the spore will turn into a new gametophyte (Goffinet & Shaw, 2009). Monoecious bryophytes will produce both the eggs and sperm in their gametophyte while dioecious bryophytes only produce either eggs or sperm and thus, must remain in close proximity to one another to sexually reproduce (Haig, 2016). Water availability is essential to this sexual reproduction process, allowing the sperm to move out of the antheridia and travel into the archegonia to fertilize the egg (Anderson, 1963). However, asexual reproduction in bryophytes does not require water nor does it produce spores (Anderson, 1963). Asexual reproduction can take place by many ways; for example, bryophytes can produce propagules or gemmae that are dispersed to germinate and grow as new individuals, or they may reproduce vegetatively from fragmented leaves and stems (Laaka-Lindberg et al., 2003; Bowden et al., 2007).

In terms of the bryophyte life cycle, the dominant stage is the gametophyte phase, with a short-lived sporophyte phase during which the sporophytes are dependent on the provision of nutrients and protection by the parent gametophyte (Shaw & Renzaglia, 2004). While bryophytes have structures that can resemble stems and roots, they don't have any true vascular plant components or water/food-conducting tissues, although some

species have hydromes and leptomes which act akin to the functions offered by vascular plants' xylem and phloem, respectively (Eckstein & Karlsson, 1999; Beringer et al., 2001; Griffin-Nolan et al., 2018). There is strong variation in bryophyte physiology and structure due to phylogeny differences among species as well as local adaptation; for example, bryophyte leaves are typically one cell thick, but some species can have multicellular leaves (Goffinet & Shaw, 2009).

As bryophytes, mosses and liverworts share many similar functional characteristics, but they can be distinguishable based on their morphological features (see Goffinet & Shaw, 2009 for a full in-depth discussion of these differences). One example would be that, while both have small shoot systems, mosses usually have spirally-arranged leaves that radiate outward from the stem, whereas liverworts (both thalloid and leafy) tend to have a flat appearance, with their leaves usually arranged as rows rather than a spiral (Crandall-Stotler & Bartholomew-Began, 2007; Goffinet & Shaw, 2009). Liverworts are also very different from mosses by their sporophyte morphology: for example, the liverwort sporophyte capsules do not have the columella, cuticle, and stomata that are characteristic of mosses and thus, cannot self-sustain photosynthesis (Goffinet & Shaw, 2009). However, for mosses, a cuticle, stomata, and conducting strand in the seta of their sporophytes create a ventilated photosynthetic tissue (He et al., 2016). Another difference between the two is that liverworts possess oil bodies, unlike mosses who do not have these specialized organelles to accumulate and store oil (Shaw & Renzaglia, 2004).

Mosses are generally classified as acrocarpous and pleurocarpous, with the exception of *Sphagnaceae*, which is often regarded as its own class (Pope, 2016).

Sphagnaceae are upright-growing mosses with branches that grow along the stem in a minimum of three fascicles that cluster at the stem tip to form a clear head (Pope, 2016). Acrocarpous mosses grow upright in tufts/cushions, rarely branch, and have erect stems in which the sporophytes are produced from the tip of a major branch or stem, and the leaves have a spiral arrangement around the stem, with most having a visible single costa (Pope, 2016). A few examples of common acrocarpous moss families include *Aulacomniaceae*, *Bryaceae*, and *Polytrichaceae*. Pleurocarpous mosses, on the other hand, are mat-forming and typically have prostrate main stems that are often long and intertwined, but can have erect tips and branches sometimes (Pope, 2016). These mosses often have extensive branching with spirally-arranged leaves that either do or don't have a single costa (usually have a forked or double costa) and the sporophytes come from the tip of an inconspicuous branch along the stem below a major branch (Pope, 2016). A few examples of common pleurocarpous moss families include *Hypnaceae*, *Hylocomiaceae*, and *Amblystegiaceae*.

Liverworts are generally classified as thalloid (complex vs. simple) or leafy. Thalloid liverworts have a flat, singular body (sometimes appearing raised) that does not have stems or leaves (Pope, 2016). Complex thalloid gametophytes are arranged in clear, distinct layers while simple thalloid gametophytes are, for the most part, anatomically undifferentiated (Wikström et al., 2009). On the other hand, leafy liverworts, which make up the majority of the liverwort class, are characterized by gametophytes that have distinct stem and leaves components (Wikström et al., 2009). Leafy liverworts typically have two rows of leaves with or without a third row of much smaller under-leaves (Pope, 2016).

Their leaves can be toothed, lobed, or intricately folded over into other complicated structures, and do not have a costa (Pope, 2016).

Also apparent on some bryophyte gametophytes are rhizoids and paraphyllia. These are fine structures on the branches and stems produced by the bryophyte to create more surface area for the retention of capillary water (Pope, 2016). Due to a lack of roots, rhizoids (which are filamentous, often branched, non-photosynthetic structures) act to anchor most bryophytes to their substrates and can be present at any interface where the plant meets the substrate (Goffinet & Shaw, 2009). While rhizoids function primarily as an anchoring structure and do not directly serve for water/nutrient uptake, they can strengthen capillary movement of water along the stem's outer surface (Crandall-Stotler & Bartholomew-Began, 2007). While moss rhizoids are multicellular, liverwort rhizoids are often unicellular (Goffinet & Shaw, 2009). For paraphyllia, these can be either filamentous or foliose structures on the stem surface which are thought to photosynthesize and enhance water conductivity along the stem through capillary action (Crandall-Stotler & Bartholomew-Began, 2007). These pseudoparaphyllia are only found in pleurocarpous mosses and only form at the base of branches (Crandall-Stotler & Bartholomew-Began, 2007).

Opposite of vascular plants, bryophytes often grow in groups or colonies rather than as a single stem (Zechmeister et al., 2003). Their dense cushion formation increases their boundary layer resistance and reduces their evaporation rates, enhancing their ability to retain their hydration (Niinemets & Tobias, 2014). Higher packing of shoots also allows the individual plant to increase its water storage capacity and strengthen water transport

by creating capillary spaces among stems, all of which also extend the duration that the plant can perform photosynthesis (Niinemets & Tobias, 2014). Thus, by crowding together, bryophytes are able to reduce their wind exposure and minimize their heat and water losses (Pope, 2016).

Therefore, bryophyte physiology is a key controlling factor to their internal biochemical processes as well as their water relations. Physiological traits (e.g., cellular structure, shoot/canopy morphology) directly affect the storage, retention, and movement of water within and around bryophyte shoots and colonies (Proctor, 1982; Elumeeva et al., 2011). This results in different bryophyte species or taxa having specific hydrological interactions and functional responses with their surrounding environment.

1.3.1.2. Desiccation/Water Relations

Water is a critical component for bryophytes. As a sort of 'amphibian plant', bryophytes often need wet conditions to survive but their poikilohydric strategy to cope with water loss allows them to tolerate desiccation and survive under dry conditions (He et al., 2016; Reski, 2018). The structure of bryophytes allows them to have a larger capacity for holding water – up to 1400% their dry weight – than a majority of other plant types (Michel et al., 2013). However, their dependence on water availability from the environment, either in the air (i.e., humidity), from precipitation, or from their surface substrate, tends to make them sensitive to relatively warm temperatures (Street et al., 2012; He et al., 2016).

The water content of bryophytes is thought to exist in three different parts: water within the cells or cytoplasm (symplast water), water in the free space of cell walls (apoplast water), and external capillary water (water among rhizoid tomentum, that overlaps the bases of leaves, at the inner side of concave leaves, between dense stems and branches, and among paraphyllia) (Proctor, 2000a; Elumeeva et al., 2011). Since bryophyte water conduction is mainly external, and that external water variation directly affects bryophyte total water content (and thus growth and photosynthesis), the external capillary water is a particularly important part to the physiological functions of many bryophytes, with species often having some amount of external water held in their capillary spaces (Proctor et al., 1998; Proctor, 1999; Proctor, 2000b). Elumeeva et al. (2011) found that practically all of their subarctic moss species held higher amounts of external water than water within the cells and cell walls. Proctor (1999) also reported that bryophytes from intermittently dry environments often have significant external water storage, with their cells almost always fully turgid when the plant is actively metabolizing; thus, bryophytes can remain quite hydrated even when found in arid ecosystems.

Water attainment and transport is very diverse in bryophytes. Generally, water can move among an individual bryophyte and between multiple bryophytes through four main pathways: 1) using hydroids, which are specialized cells for water conduction and storage, and are located in a central strand in the stem, 2) through the free areas in cell walls, 3) from cell to cell, i.e., among cellular walls and membranes, and 4) through the external capillary spaces (i.e., between stems and leaf bases, between overlapping leaves, among rhizoids and paraphyllia) which can be very complex and diverse across species (Proctor,

1982). In the leaf lamina and stem cortex of mosses, as well as in the liverwort thalli, a large part of water movement relies on the water transport from cell to cell or along the cell walls (Proctor, 1982). Water movement along the cell wall pathway is particularly important for bryophytes with thick-walled, small cells while water movement from cell to cell may be more important in bryophytes that have thin-walled, large cells (Proctor, 1982).

Species are often grouped as endohydric and ectohydric to generally differentiate between their water acquisition and transport strategies. Endohydric species (e.g., *Polytrichum* spp.) have internal conducting cells (hydroids) that can take water up from the soil similar to vascular plants, and are typically present in nutrient-rich, moist, and porous substrates (Proctor, 1982). In ectohydric species (e.g., *Grimmia* spp.), water over their whole surface can be readily absorbed or lost, as their water movement is mostly based on diffusion and depends more on external capillary conduction (Proctor, 1982). Ectohydric species are typically present on impermeable substrates (e.g., rock) and are loosely connected to the soil (Proctor, 1982). Most thalloid liverworts are endohydric, storing much of their water internally, and primarily relying on internal water conduction; thus, they tend to be less desiccant tolerant, with their predominant water component being symplast water (Proctor, 2000a). The majority of leafy liverworts and mosses, on the other hand, are ectohydric and have much of their symplast water retention exceeded by a larger and more variable external capillary water, and thus are more desiccation-tolerant (Proctor, 2000a; Michel et al., 2013). However, ectohydric/endohydric generalizations

may not fit all species exactly, with many bryophytes employing a variety of combinations that use both ectohydric and endohydric traits (Proctor, 1982).

Once bryophytes begin to lose water, they start desiccating. From their saturated to desiccated states, bryophytes can appear very different: when desiccated and dry, for example, they tend to have much less of their leaf area exposed (He et al., 2016). Most water loss is from evaporation in bryophyte canopies, which depends on air temperature and humidity, but it can also be caused by gravity-induced percolation throughout the canopy as well as capillary loss to adjacent shoots (Elumeeva et al., 2011). When the water table drops, bryophyte plant parts can shrivel and tighten together, narrowing the capillary spaces between branches, leaves, and stems, and if this goes on for too long, the diminished pore spaces can restrict capillary rise and make it more challenging for the plant to access water, enhancing their desiccation intensity and duration (Potvin et al., 2015). When desiccation occurs, cellular water contents equilibrate with the ambient air water levels, with net assimilation rates falling quickly as the water content declines below the threshold needed to maintain full turgor (Turetsky et al., 2012). Furthermore, since plants depend on evaporative cooling to help reduce their radiation load, when they lose water, the plant's temperature increases (He et al., 2016). That said, many bryophytes lose their pigment and pale, increasing their albedo and reducing further evaporation (Proctor et al., 2007). Thus, under desiccation, metabolism is suspended and the plant is physiologically dormant. Their cytoplasm can survive for a long time in this dormancy, yet different species have different tolerances depending on the desiccation intensity and duration (Turetsky et al., 2012; Slate et al., 2019).

Once rehydration occurs, the plant can resume its metabolic activity, but it comes at a high repair cost, as the plant has a burst of respiration (net energy loss) before it recovers and can resume its regular physiological processes (Elumeeva et al., 2011; Turetsky et al., 2012). Less desiccant-tolerant species may be subjected to more damaged cellular membranes when under desiccation, which can leak intracellular contents and nutrients (Slate et al., 2019). From their study of 22 bryophytes species found in the subarctic (*Aulacomnium palustre*, *A. turgidum*, *Dicranum scoparium*, *Hylocomium splendens*, *Limprichtia cossonii*, *Oncophorus wahlenbergii*, *Paludella squarrosa*, *Philonotis caespitosa*, *Plagiomnium ellipticum*, *Pleurozium schreberi*, *Polytrichastrum sexangulare*, *Polytrichum juniperinum*, *P. strictum*, *Ptilidium ciliare*, *Racomitrium fasciculare*, *R. lanuginosum*, *Sphagnum fuscum*, *S. lindbergii*, *S. riparium*, *S. russowii*, *Tomentypnum nitens*, *Warnstorfia pseudostraminea*), Elumeeva et al. (2011) suggest desiccation involves external water loss first, but once it reaches lower water contents, the relative quantities of symplastic and apoplastic water start to critically impact the relationship between water content and potential, and thus, once cellular water is affected, metabolism and photosynthesis rates quickly drop to a standstill (Proctor, 1982). Therefore, desiccant-tolerant bryophytes mostly have water movement in their external capillary spaces (Proctor, 2000a).

The capacity for water retention can significantly affect how bryophytes tolerate desiccation. This capacity mainly depends on the properties of individual shoots in combination with the colony's morphological properties (e.g., the shoot packing within the colony) (Elumeeva et al., 2011). At the species level, differences in capacity for water

retention arises from trait differences, such as lamina cell area and length, stem thickness and cortex, and leaf cell wall thickness (Elumeeva et al., 2011). Therefore, since species have significant differences in their water-holding capacity and physiologies, individual species can exhibit different water retention capabilities even when under similar climate conditions (Porada et al., 2016). Water content differences at the canopy level can be even larger, since external water tends to contribute more to canopy water retention than the symplastic and apoplastic water that is in the individual shoots (Elumeeva et al., 2011). Therefore, water retention capacity differences are also related to the canopy-level traits, such as the turf height and density, density of rhizoids or paraphyllia on branches and stems, and the external water that is contained by the stem and leaf bases of individual shoots as well as that held inside the concave leaves (Elumeeva et al., 2011).

The structure of the colony is particularly important to water retention and desiccation tolerance. For example, tighter cushion-forming colonies are typical of areas usually exposed to frequent drying and thus are more tolerant to desiccation because of the better water retainment in their close shoot interspaces (Slate et al., 2019). On the other hand, more loosely-formed colonies (often characteristic of moist habitats) would not be able to retain water as well in their shoot spaces and thus, are not as tolerant to desiccation (Slate et al., 2019). However, there is still little research done on the extent of upscaling individual shoot-traits that affect internal water content to the canopy-scale (Elumeeva et al., 2011). Furthermore, there is still a need to understand the desiccation-tolerance and hydrological interactions of bryophytes in relation to rhizoids and paraphyllia, as it is thought that the presence of rhizoid tomentums or paraphyllia on bryophytes can also alter

their capacity for water retention, although Elumeeva et al. (2011) did not find a strong impact on the rates of desiccation in their 22 subarctic bryophyte species (see list above).

1.3.1.3. Ecological Significance

Bryophytes have a variety of ecological roles in their environments, particularly in northern ecosystems. They dominate primary productivity in the high-latitudes, contributing 50% of aboveground net primary productivity in wetlands and 20% in boreal forests (Turetsky et al., 2010) As a significant component of the vegetation, bryophytes heavily affect C, energy, nutrient, and water cycling in boreal and arctic ecosystems as well as long-term ecosystem processes (e.g., permafrost stability) (Turetsky et al., 2012; Cerrejón et al., 2020). Bryophytes, especially mosses, are often described as ecosystem engineers, who modify their surroundings through their various interactions with the environment and the abiotic/biotic factors which characterize it.

Sphagnum moss is often regarded as the most proactive ecosystem engineer for its well-documented ability to create cold, acidic, anoxic, and nutrient-poor bogs through the interception of nutrients and slow mineralization, which gives it a considerable competitive advantage to flourish against other plants (van Breemen, 1995; Bengtsson et al., 2020). However, even though *Sphagnum* has been long put on a pedestal as "the only important bryophyte" in peatlands (Hayward & Clymo, 1982), all mosses can reduce ecosystem nutrient availability, create anoxic conditions, increase soil acidity, and enhance cold soil temperatures through permafrost/peat insulation. Their engineering capacities create close and interdependent relationships between bryophytes and vascular

vegetation in most ecosystems (He et al., 2016). Bryophytes also play a critical role for fauna. While bryophytes are often foraged by herbivores in the Arctic such as rodents and migratory birds because of their large availability and biomass (despite their low nutritional value), bryophytes are significant to fauna because they regulate important habitat conditions that are central to the ecosystem food web (Turetsky et al., 2012; Lewis et al., 2017).

Bryophytes can play a critical role in nutrient cycling because they have a low N-use efficiency, a high cation exchange (which causes N interference and retention), slow decomposition rates; they can also moderate soil moisture and temperature (Turetsky et al., 2012). Furthermore, their effective interception of nutrients from the atmosphere, from leachates, and from the litter of the overstory plants allows bryophytes to reduce the available nutrient supply for vascular plants (van Breemen, 1995). Bryophytes seem to primarily rely on atmospheric deposition for N, but because N deposition is often low in high-latitude ecosystems, many northern bryophytes are hosts to symbiotic N_2-fixing cyanobacteria that are capable of fixing considerable amounts of (inert) atmospheric N_2, making up their major source of N (Turetsky, 2003; Lindo et al., 2013). Bryophytes can also affect phosphorous (P) cycling by absorbing phosphate and reducing vascular uptake availability; however, in some areas mosses have created more oxidized conditions and thus allowed for greater vascular P acquisition (Turetsky et al., 2012). Since bryophytes are well-adapted to retrieve nutrients in nutrient-poor ecosystems, they are often able to colonize areas unviable for vascular vegetation (Pope, 2016). Through their cation exchange to acquire nutrients, bryophytes release hydrogen ions which increase the acidity

of their ecosystem, further preventing the viability of other vegetation types, while also limiting rates of litter decomposition (Pope, 2016).

In addition to nutrient-cycling and acidity effects, bryophytes are capable of saturating or waterlogging soils, thanks to their tightly-packed shoots and layers (Bengtsson et al., 2020). In doing so, they create anoxic conditions that negatively affect vascular vegetation but positively feedback to themselves by supporting their hydration and sustaining their photosynthesis and growth (Bengtsson et al., 2020). Waterlogging plays a key role in peat accumulation and C sequestration (with mosses being one of the key facilitators for peat development), because soil saturation (and acidity) significantly decreases decomposition rates, allowing slowly decaying layers of organic matter to build up (Turetsky et al., 2012; Pope, 2016; Bengtsson et al., 2020). Furthermore, some bryophytes can use internal water-conducting tissues to translocate soil water, which may influence soil hydrology and water availability for other plant types (van Breemen, 1995; Hallingbäck & Hodgetts, 2000).

In bryophyte-dominated environments, water retention at the individual and the canopy levels are both critical, because as bryophytes intercept, store, and re-deliver water, they regulate the soil moisture and ecosystem water availability (Michel et al., 2013; Cerrejón et al., 2020). As bryophytes can retain significant amounts of moisture, they also play a mitigating role in flooding, runoff, and soil erosion (Pope, 2016). Their moisture retention also serves to benefit their own resiliency (e.g., cold, wet, low-nutrient soils sustained by bryophytes can prevent deep combustion of fire) as well as that of their close associations with fungi, supplying them with a consistent flow of water that allows them

to perform their decomposing functions (Turetsky et al., 2012; Pope, 2016). By enhancing soil water retention and reducing soil water runoff, bryophytes buffer soil moisture as well as temperature (Slate et al., 2019).

Cold soil temperatures and permafrost or peat stabilization are particularly significant ecological roles of bryophytes in northern ecosystems. Through their thick layer, bryophytes reduce the heat exchange between the soil and the atmosphere, insulating the ground and decreasing soil temperature (Porada et al., 2016). This insulating effect from bryophytes is heavily regulated by their moistures (Porada et al., 2016). From dry to saturated bryophytes, thermal conductivity increases by about one order of magnitude, and heat capacity increases by about two orders of magnitude (Porada et al., 2016). If these bryophyte layers are removed, soil temperatures would increase, leading to higher decomposition rates, degradation of the underlying peat, and enhanced permafrost thaw, which can produce a range of concomitant ecological effects on the Arctic hydrological, thermal, nutrient, and C regimes (Beringer et al., 2001).

Bryophytes are also engineers in the construction sense. Since they produce biomass that often has low decomposition rates, over time they significantly impact the microtopography in northern ecosystems through their construction of hummock-hollow formations (Hallingbäck & Hodgetts, 2000; Turetsky et al., 2012). These hummock-hollow formations create a water-availability gradient, which produces individual microhabitats and niche diversity among species (Turetsky et al., 2012). For example, as elevated mounds, hummock species need to use and retain water efficiently to avoid desiccation (Turetsky et al., 2012). Conversely, the hollow species are often well-hydrated

and highly productive, but tend to be less adapted for desiccation (Turetsky et al., 2012). This diverse microtopography increases functional trait diversity (especially in regards to water balance), which strengthens the ecosystem's resistance to drought or wildfires (Turetsky et al., 2012). Likewise, the diversity of moss communities in high-latitude ecosystems can have a variety of impacts on ecosystem functions, yet identifying and understanding this diversity requires identifying specific-species and individualistic response traits, which is still an issue (Turetsky et al., 2012). Bryophytes are also important in soil construction and formation, colonizing soil or rocks, which allows for the introduction of vascular vegetation (Pope, 2016). Furthermore, bryophytes are significant constituents of biological soil crusts that affect nutrient cycling, infiltration, C sequestration, and soil erosion or stability (Martinez et al., 2006).

Lastly, bryophytes are widely used as environmental indicators. Bryophytes are often small, structurally simple, close to their substratum, and are incapable of regulating their internal systems, so they are especially sensitive to minor shifts in their habitat, such as pH and nutrient levels (Grace, 1995; Pope, 2016). When compared to lichens, bryophytes often grow quicker and are more apparent and larger; thus, they tend to respond to short-term (decadal) environmental shifts (Grace, 1995). In particular, their sensitivity to moisture enables bryophytes to be good proxies for water table position, which can be used to estimate CH_4 emissions (Bubier et al., 1997). Therefore, bryophytes are especially optimal vegetation proxies for studies on northern peatland hydrological conditions and C sequestration and emission (Bubier et al., 1995; Bubier et al., 1997; Hallingbäck & Hodgetts, 2000; Cornelissen et al., 2007).

1.3.2. Lichens

Lichens cover approximately 8% of the global land area (Granlund et al., 2018), with over 20,000 species identified and still more being identified to this day (Allen et al., 2019). Lichens are found in a variety of habitats worldwide and often coexist in the same environments with bryophytes, though the former tends to dominate in drier ecosystems while the latter dominates in wetter ecosystems (Green & Lange, 1995; Hartard et al., 2009; Pope, 2016).

1.3.2.1. Physiology

Lichens, included in the thallophyte class, are composed of green algae/cyanobacteria (the photobiont) and fungi (the mycobiont) which symbiotically function and live together as a single organism (Beringer et al., 2001; Hartard et al., 2009). Their relationship is built upon their mutual benefits: the algae/cyanobacteria synthesizes and excretes a particular carbohydrate that the fungus utilizes and consumes as food, and the fungus offers the algae/cyanobacteria a vegetative body or structure which protects it from abiotic stresses (e.g., from drying out under harsh conditions) (Beringer et al., 2001). This symbiosis is largely what enables lichen to survive under extreme, dry conditions, while still being able to absorb moisture from even the most minimal water vapor (Llano, 1956). Similar to bryophytes, lichens are low-growing, small organisms that produce spores and lack typical plant components (stems, roots, leaves), yet rather than any sort of leafy appearance, they primarily have a singular body known as the thallus (Nash, 1996; Beringer et al., 2001; Pope, 2016). The majority of lichens have an internally stratified

thallus with the cyanobacteria/algae and fungi in various layers throughout the structure, although lichens can also have the cyanobacteria/algae and fungi components mixed together in a large, uniform layer, creating a gelatinous structure (Nash, 1996; Hartard et al., 2009).

There are three main types of lichens, differentiated by their growth form: crustose, foliose, and fruticose. Crustose lichens have small thalli that is often not visible and is securely attached to its substrate, forming a crust-like appearance (Brodo et al., 2001). Foliose lichens have a more leaf-like appearance, with somewhat flattened thalli that have distinct lower and upper surfaces which are often layered (Brodo et al., 2001). Fruticose lichens have a very branched, shrub-like growth form, in which their thalli (even if flat) grows more erect, but does not necessarily have a clearly visible lower and upper surface (Brodo et al., 2001). Like with rhizoid attachments on bryophytes, lichens can also have non-photosynthetic structures (rhizines) that act as attachment threads for their substrate; however, rhizines are more typical in the foliose lichens (Brodo et al., 2001; Vitt, 2007).

While lichens have generally been thought to be C3 plants (Snelgar & Green, 1980), their modes for CO_2 acquisition depend directly on their specific photobiont, which has led to a variety of photosynthesis strategies to be seen in lichens (Palmqvist, 2000). While some lichens do perform photosynthesis similar to C3 plants, others possess a CO_2 concentrating mechanism (Palmqvist, 2000). While there is still much unknown about specific photosynthesis mechanisms in various species of lichens, their photosynthesis is much more comparable to that of algae or cyanobacteria than that of plants (Palmqvist, 2000). Like bryophytes, lichens tend to have lower photosynthetic rates than vascular

vegetation, which is likely due to their low photosynthetic tissue to surface area ratios (Green & Lange, 1995). Furthermore, since lichens tend to be found under low-light and low-temperature conditions, they have lower light compensation and saturation intensities, making them better at photosynthesizing than many vascular plants under restricting temperature ranges and limited light conditions (Green & Lange, 1995; Longton, 1997). That being said, many lichens can also survive in environments with high-light conditions (Palmqvist, 2000; Odland et al., 2018). Lastly, lichens with CO_2 concentrating mechanisms (especially apparent in cyanobacterial lichens) are capable of photosynthesizing at much lower levels of CO_2 than bryophytes (Green & Lange, 1995).

1.3.2.2. Desiccation/Water Relations

In terms of their water relations and morphological functions, lichens are not all that different from bryophytes, as both share poikilohydric characteristics and depend heavily on external ground-water or atmospheric water supplies. However, water storage in lichens is still not completely understood; it is thought that various tissues in the lichen (e.g., medulla, photobiont layer) could be water storage sites (Green & Lange, 1995), although more recently Granlund et al. (2018) only mention that the medulla (which is beneath the algal/cyanobacteria layer) can retain moisture. Despite this ambiguity, it appears that any internal water storage in lichens would be small when compared to that of bryophytes, because lichens have more compact tissues, leaving less space for water storage (Green & Lange, 1995). While Palmqvist (2000) reports that lichens are often able to hold considerable extracellular water, they note that the distribution and size of storage

compartments for extracellular, apoplastic, and symplastic waters remains largely determined by their structural composition. Like bryophytes, lichens face increased resistance to CO_2 diffusion that is caused by water storage and retention in their thallus (Cowan et al., 1992). As for water transport, lichens, unlike bryophytes, are not capable of much lateral water movement along their vegetative body (Green & Lange, 1995). Estimating lichen water content, while still requiring much work, is critical to understand and estimate their photosynthesis, productivity, and impacts on C budgets (Granlund et al., 2018).

Lichen desiccation and rehydration processes are similar to bryophytes. When desiccating, water is first lost in the extracellular components; once the lichen begins to reach lower water contents, their apoplastic and symplastic waters are lost with large quantities of soluble compounds leaking from their mycobiont and photobiont cells, causing their thallus to considerably shrivel and become metabolically dormant (Honegger, 1993; Palmqvist, 2000). Once remoistened, there is a burst of respiration, called the "wetting burst and resaturation respiration" (Proctor, 1982). Any cell damage that occurred during the desiccation is quickly repaired, and metabolic activity resumes (Aubert et al., 2007). Lichens can often fully resume their metabolic activity, even before their cells are completely turgid and the organism is back to an optimal saturated state (Honegger, 1993). Similar to bryophytes, lichens are capable of retaining their internal water until reaching very low water contents because of their significant extracellular water, a relatively high osmotic potential, and less rigid cell walls (Palmqvist, 2000).

Desiccation-tolerance can be quite variable in lichens, just as in bryophytes, as it is related to specific habitat adaptations (Palmqvist, 2000).

1.3.2.3. Ecological Significance

While bryophytes are significant components to Arctic environments, the general aridity of Arctic ecosystems gives lichens a considerable dominating presence and thus, important ecological roles (Llano, 1956). The function of lichen in soil formation is likely one of their most noted ecological roles. In many habitats, lichens are often thought of as the pioneer species for ecosystem formation (Beringer et al., 2001). While bryophytes can also colonize bare rock, lichens are often the first to colonize (Brodo et al., 2001). Lichens play an important role as primary colonizers, because they can grow as far as several millimeters into rock fragments or crevices, speeding the erosion of the rock via weathering processes, which sets the stage for soil formation (Brodo et al., 2001). Furthermore, when the lichen tissues die, their decayed organic matter combines with the rock minerals, increasing nutrient availability and enabling colonization by other plants (Brodo et al., 2001). Lichens, like bryophytes, are also major constituents of soil crusts, which strongly affect ecosystem processes (e.g., C sequestration), particularly in reducing soil erosion through their interception of runoff and regulation of water infiltration (Martinez et al., 2006).

Lichens are also critical resources for fauna in the Arctic. They can be a significant food source; for example, lichen makes up a large majority of reindeer and caribou diet in northern ecosystems, which subjects them to grazing and trampling from herbivory, which

can be highly damaging in the cases where lichens are dry and brittle (Joly et al., 2009; Granlund et al., 2018). Beyond food, lichens can also be important sources of nesting material and shelter for fauna (Esseen et al., 1996). Another significant role played by lichens is in the nutrient cycling of Arctic ecosystems. Like bryophytes, lichens largely affect ecosystem nutrient availability through their N fixation and high cation exchange capacities (Longton, 1997). Furthermore, lichens share bryophytes' ability to impact the ground surface hydrology, as they serve as interception points for moisture (Longton, 1988).

Due to many of the roles mentioned above, akin to bryophytes, lichens share interdependent relationships and undergo direct competition with vascular plants (Joly et al., 2009). Lichens can compete with vascular plants for sunlight and free surface substrate, and due to their hydrologic and nutrient cycling roles, lichens often intercept nutrients and water that would otherwise be taken up by vascular plants (Longton, 1988; Joly et al., 2009). Despite their critical impacts on the surrounding environment and neighboring plants, lichens appear to be viewed as poor competitors, which just take over the areas that bryophytes and vascular plants are incapable of surviving in (Odland et al., 2018).

When abundant, lichens play a critical role in altering ground heat fluxes in northern ecosystems. Similar to bryophytes, high-latitude lichens have a high albedo and high thermal conductance, which reduces the heat exchange between the soil and the atmosphere, insulating permafrost, sustaining cold soil temperatures, and preserving soil moisture (Brodo et al., 2001; Porada et al., 2016; Odland et al., 2018). Therefore, a decline

in lichen cover could lead to increased soil temperatures, permafrost thaw, and less soil moisture (Brodo et al., 2001; Porada et al., 2016; Odland et al., 2018). However, their water content plays a critical effect in this role as they are much more effective in their thermal conductivity when saturated (Porada et al., 2016).

Lichens can also serve as environmental indicators. Like bryophytes, because lichens directly rely on the environment's external conditions for their own resources, they are natural reflections or indicators of that ecosystem's conditions (Hartard et al., 2009). Furthermore, their dependence on environmental conditions for survival as well as their slow growth makes lichens especially vulnerable to climate warming and environmental disturbances, and thus optimal disturbance indicators (Esseen et al., 1996; Joly et al., 2009). Lichens are widely used as air pollution monitors, because they are sensitive to different types of pollutants (Matos et al., 2017; Odland et al., 2018).

1.4. Remote Sensing of the Arctic

Remote sensing is one of the most viable sources of consistent spatiotemporal data collection in the Arctic. As a generally remote and inaccessible region, field expeditions to the Arctic are often expensive and logistically difficult, making *in situ* data challenging to collect (Huemmrich et al., 2013; Malenovský et al., 2017). Remote sensing alleviates these issues by providing quick, economically efficient, and minimally invasive methods for collecting data that are consistent and easily repeated over large spatial and temporal extents (Huemmrich et al., 2013; Malenovský et al., 2017). Remote sensing data can be used to detect and monitor shifts in vegetation composition and structure, distinguish

communities and species, estimate above-ground biomass, examine different vegetation biophysical properties, identify spatial and temporal patterns, and offer input data for models (Laidler & Treitz, 2003; Stow et al., 2004). Remote sensing is also particularly useful because it has significant potential in scaling up field-based measurements and modeling biophysical traits at the landscape, regional, and even global level (Laidler & Treitz, 2003). Having regular spatiotemporal monitoring of ecosystems from remote sensing data is also advantageous because it can provide significant insight into the ecosystem health and potential vulnerabilities from environmental shifts (Malenovský et al., 2017).

Since the early 2000s, terrestrial remote sensing in the Arctic has been a rapidly growing field, largely due to advancements in sensors, increasingly available amounts of data with more advanced spatial, spectral, and temporal scales, and increasing computing and processing capabilities and services (Beamish et al., 2020). Presently, the only consistently termed and circumpolar-scale vegetation map for the Arctic is the CAVM (Circumpolar Arctic Vegetation Map, see Walker et al., 2005). This map, which divides Arctic vegetation into detailed physiognomic classes, was developed from Advanced Very High Resolution Radiometer spectral information (Walker et al., 2005), and while a higher resolution raster version of it has been recently released, the CAVM is still relatively coarse and is limited to the circumpolar extent (Beamish et al., 2020). To enhance remote sensing data quality and versatility, and better infer vegetation biophysical traits in the high-latitudes, studies (Peckham et al., 2009; Huemmrich et al., 2010; Malenovský et al., 2017; Hillman & Nielsen, 2020) are increasingly integrating data from multiple sensor

types with different spectral and/or spatial resolutions and utilizing various types of spectral indices. Beamish et al. (2020) conduct a detailed and comprehensive review of trends in remote sensing research on Arctic vegetation (Table 1).

Application	Example	Remote Sensing Data Types
Time Series Analyses	1 - Change detection (e.g., tundra greening/browning (Jia et al., 2003), photosynthetic activity/productivity (Loranty et al., 2016), and shrub expansion (Fraser et al., 2014)) 2 - Monitoring Arctic vegetation disturbance/recovery after fire (Epting et al., 2005), warming (Bokhorst et al., 2009), anthropogenic and permafrost disturbances (Esau et al., 2016; Nitze et al., 2018), and herbivory (Hogrefe et al., 2017)	Satellite/airborne imagery (e.g., RGB, multispectral, panchromatic), and spectral indices (e.g., Normalized Difference Vegetation Index (NDVI))
Vegetation Properties	1 - Biophysical and biochemical variables (e.g., aboveground biomass (Raynolds et al., 2012), leaf area index (Williams et al., 2008), vegetation pigments/nutrients (Zagajewski et al., 2017), and solar-induced chlorophyll fluorescence (Luus et al., 2017)) 2 - Vegetation seasonality/phenology (Beamish et al., 2016) and primary productivity (Westergaard-Nielsen et al., 2017)	Near-field/field remote sensing systems (e.g., time-lapse cameras), airborne/satellite imagery, spectral indices, and hyperspectral data/imaging spectroscopy
Classification and Mapping	1 – Mapping or identifying ecosystem/plant community cover, composition, structure (Laidler & Treitz, 2003; Stow et al., 2004; Walker et al., 2005; Langford et al., 2019), and plant functional types (Bratsch et al., 2016; Macander et al., 2017) 2 – Scaling up field-based measurements and modeling vegetation properties at the landscape, regional, and global levels (Laidler & Treitz, 2003)	Supervised and unsupervised classifications of spectral reflectance data with ancillary data

Table 1: Overview of Beamish et al. (2020)'s synthesis on the trends seen in Arctic terrestrial optical remote sensing research.

Various remote sensing tools have been used for vegetation characterization. Common tools include: spectral indices, spaceborne/airborne/ground-based passive (e.g., satellite) and active (e.g., Light Detection and Ranging (LiDAR)) remote sensing systems, supervised/unsupervised classifications, and imaging spectroscopy. Spectral indices which use wavelengths that vegetation particularly respond to have been devised to estimate a number of vegetation parameters. For example, NDVI (which relies on near-infrared and red bands) has been used to estimate vegetation green biomass (Bannari et al., 1995). Passive optical imagery has also been an important resource, especially in monitoring time-series or phenological changes in vegetation (Zeng et al., 2020). LiDAR is a popular active remote sensing system for vegetation studies as it can provide a three-dimensional view of vegetation canopy structure and sub-canopy topography, increasing the accuracy of vegetation biophysical measurements such as vegetation height cover (Lefsky et al., 2002). Remote sensing data are often used for identifying and mapping vegetation structural parameters (e.g., leaf area index, fractional cover) (Zhang et al., 2021). Spaceborne remote sensing data have long been used for mapping vegetation structure but have now evolved widely into being used to acquire and characterize canopy/leaf traits and functions (Zhang et al., 2021). The use of imagery coupled with various classification techniques (such as machine learning) is probably one of the most widely used methods for mapping vegetation. It relies on discernable spectral characteristics within the imagery to identify spectral classes which are then translated into various vegetation types (Xie et al., 2008). Imaging spectroscopy has been another critical tool because it provides detailed spectral information that can be used to identify

plant biophysical, morphological, and anatomical properties, making it a particularly useful resource for mapping unique plant functional parameters (Guyot et al., 1992; Zhang et al., 2021). For example, high spectral resolution can be used to identify the shift in the plant's red edge due to stress (Guyot et al., 1992). Solar-induced fluorescence is also becoming an increasingly popular vegetation remote sensing tool, particularly for monitoring plant photosynthesis (Zhang et al., 2021).

The advantages of remote sensing in the Arctic make it an invaluable source of data to answer research questions, and researchers continue to create new methods to overcome current limitations of gathering Arctic data. Still, Arctic terrestrial ecosystems continue to present numerous challenges to remote sensing applications because of their unique characteristics (Beamish et al., 2020). Successful image acquisitions are often limited due to the low solar angle, high cloud coverage, snow/ice cover, standing water, and short summers vs. long and dark winters that characterize Arctic environments; this limits both temporal and spatial comparisons with remote sensing data (Stow et al., 2004; Beamish et al., 2020). Furthermore, the costs and logistical difficulties of Arctic field expeditions create a persistent lack of high-quality, *in situ* data to validate Arctic remote sensing work (Beamish et al., 2020).

Arctic ecosystems also tend to be dominated by temporally dynamic and spatially/spectrally heterogenous (i.e., patchy) distributions and compositions of short-stature non-vascular vegetation that are micro-topographically complex. For example, in the tundra, different communities of vegetation are often interwoven and mixed together at very fine spatial resolutions, such as the decimeter to centimeter scale (Malenovský et

al., 2017; Siewert & Olofsson, 2020). Arctic vegetation is also spectrally heterogenous, as non-vascular and vascular plants have distinct spectral characteristics on their own, creating a mosaic of spectral responses when mixed (Laidler & Treitz, 2003; Huemmrich et al., 2013). Therefore, monitoring Arctic terrestrial ecosystems requires frequent sampling at high spectral/spatial resolutions (Malenovský et al., 2017).

Furthermore, since remote sensing of vegetation methods are typically based upon temperate forest/crop studies, conventional tools of remote sensing (e.g., common vegetative indices) may have ambiguous interpretations and challenges when applied to high-latitude environments (Huemmrich et al., 2013). For example, many widely-used remote sensing indices originated from vascular vegetation applications (Xue & Su, 2017) and while studies (Riedel et al., 2005; Laidler et al., 2008) have explored the suitability of these indices for tundra environments, there appears to still be few studies that explicitly address the specific degree of utility of these conventional indices in monitoring non-vascular tundra vegetation and how this degree may vary by plant functional type and species.

Beamish et al. (2020) emphasize that a key part to advancing the remote sensing of Arctic vegetation and better understanding subsurface characteristics in these high-latitude ecosystems is to improve the identification of non-vascular vegetation (especially, lichens and mosses). Furthermore, it is critical to use their unique spectral properties to devise plant functional types which are based more upon functional diversity than general, traditional diversity; this may help create much more ecologically significant classifications of Arctic vegetation (Beamish et al., 2020). Adequately characterizing plant

functional types (and particularly their ecosystem functions) largely depends on our ability to meaningfully represent and characterize the individual species that constitute these groups. For example, in wetlands/peatlands, each plant functional type can exert a specific and fundamental control on the discharge and sequestration of C depending on their own biomass productivity and decay rate, which are directly related to the community structure, organization, composition, surface moisture, and temperature (Rydin & Jeglum, 2006; Harris & Bryant, 2009). Therefore, improving the detection and identification of plants at the species-level will improve the characterization of ecosystem processes and patterns (Tilman et al., 1997; Díaz & Cabido, 2001; Davidson et al., 2016).

1.5. Spectral Signatures

Spectral signatures are a key solution to this challenge because they provide a high-resolution perspective into the wavelengths and spectral reflectance properties of various vegetation types, which can be used to identify specific biochemical and physiological properties within that vegetation. These high-resolution spectral (or hyperspectral) data are useful for plant studies because they can detect small changes and detailed features in vegetation spectral properties, such as the red edge inflection point which can be used to make accurate detections of minor changes or differences in plant physiological status (Laidler & Treitz, 2003). Plant spectral properties are moderated by their morphological and anatomical structure, and physiological processes (Gates et al., 1965). The visible (VIS) radiation that is absorbed is used for fluorescence and photosynthetic processes, and reflection in this range can be used to detect pigmentation and study chlorophyll,

carotenoid, and xanthophylls absorption (Zagajewski et al., 2018). Reflection in the infrared range (e.g., near-infrared: NIR, shortwave-infrared: SWIR) can depend on the plant's water content, cellular structure, leaf thickness/roughness, chemical components, the canopy structure, and the leaf age/arrangement, as well as any environmental conditions/stress that impact the plant's health and surroundings (Zagajewski et al., 2018). Spectral interactions (absorption, reflection, transmission of light) in plants are dictated by their cellular structures, biochemical characteristics, and pigments, and are critical to monitoring long-term ecosystem shifts and processes (Stow et al., 2004; Zagajewski et al., 2017). Plant canopy, leaf structure, pigment, and water content can cause shifts in vegetation spectral properties, even among similar species. Therefore, unique spectral properties can be used to distinguish and identify different species (Thenkabail et al., 2000). There are limited studies that have examined the spectral properties of individual (sub-)Arctic plant species using hyperspectral data (Rees et al., 2004; Neta et al., 2010a), while the majority of work has focused on vegetation communities in these ecosystems (Vierling et al., 1997; Buchhorn et al., 2013; Bratsch et al., 2016). Detecting pigments and nutrients through remote sensing can play a large role in monitoring plant vitality, but detecting plant phenology and morphology is much more challenging, as different species have unique physiologies, morphologies, and anatomies that produce unique and potentially changing spectral properties (Zagajewski et al., 2017).

1.5.1. Non-Vascular Tundra Vegetation

With different physiological processes and responses from vascular plants, non-vascular plants have different spectral characteristics (Huemmrich et al., 2010). Spectral signatures may be particularly important for non-vascular tundra vegetation because those signatures could provide a detailed spectral perspective on their physiological processes, as well as morphological and anatomical features, which could significantly improve our capabilities for detecting and identifying these vegetation types. Furthermore, the unique spectral properties discerned from these signatures can be used to identify or refine plant functional groups, examine vegetation biophysical properties, and map vegetation patterns (Petzold & Goward, 1988). Indeed, spectral signatures may improve mapping of non-vascular vegetation, which could have important implications for ecosystem monitoring. For example, Bubier et al. (1997) emphasize that if remote sensing could detect mosses, more accurate maps of CH_4 emissions could be developed. Furthermore, for non-vascular vegetation, whose water content largely differs with ecosystem conditions, their short-term moisture shifts may induce a significant shift in their reflectance, bringing large uncertainty when using remote sensing to estimate productivity and biomass (May et al., 2018). Spectral signatures could alleviate this issue by providing species/taxa-specific water content estimates, which will be key as it is well documented that moisture effects on spectral reflectance is largely species dependent (Bubier et al., 1997; Rees et al., 2004; Neta et al., 2010a). This novel application of spectral information may create significant opportunities for using airborne/satellite imagery for comprehensive, detailed monitoring of peatland moisture status (Neta et al., 2010b). The detection of moss desiccation (or

saturation) within the permafrost region could also help, for example, to identify areas that are drying (or flooding) following thaw and monitor their evolution during the growing season.

Huemmrich et al. (2010) also emphasize the importance of monitoring water content changes in vegetation. They point out that, in addition to the potential large-scale shifts in Arctic vegetation, there are significant differences between light use efficiency between wet vs. dry tundra as well as among the mosses within these environments. Therefore, more work should be done to better contrast between plant functional types in the Arctic using remote sensing and to consider how moisture status affects their spectral responses. This is essential to better understand and represent C exchange in tundra ecosystems, as these estimates depend on better spatiotemporal characterization of the distribution of wet/dry tundra ecosystems, with special focus on the plant functional types, microtopography, and permafrost dynamics, which drive their different structures and functions (Huemmrich et al., 2010). In their study, May et al. (2018) point out that moss reflectance spectral features are, indeed, strongly dependent on their moisture status, which may change quickly, and cannot fully be characterized using multispectral data, thus highlighting the importance of hyperspectral data such as spectral signatures. Likewise, Granlund et al. (2018) emphasize that moisture content can also strongly influence lichen spectral reflectance, which does not only complicate the mapping of species/taxa distribution and coverage; it may also limit our ability to estimate their ecological roles. For example, net photosynthesis and C exchanges largely depend on accurately estimating vegetation water content (Granlund et al., 2018).

Despite the dominance and diversity of non-vascular vegetation in the (sub-)Arctic, relatively little work has focused on the spectral properties of northern bryophytes and lichens. Of the few published studies, most are restricted to a limited scope in terms of species types, with even fewer of these studies giving attention to the importance of moisture status in affecting the vegetation spectral reflectance properties. While satellite data have also been a source for identifying reflectance characteristics of specific vegetation types, detailed information regarding bryophyte and lichen spectral properties often comes from studies using spectroradiometers which use narrow band wavelengths.

Regarding tundra bryophytes, most spectral work has focused on *Sphagnum* mosses, with little attention to other (sub-)Arctic mosses. To my knowledge, no work at all has been done on the spectral reflectance properties of (sub-)Arctic liverwort species. Work on the spectral reflectance of tundra lichens appears to have been more widespread, but is still somewhat limited in the number of (sub-)Arctic species included and in the lack of spectral measurements beyond ~1000nm (Rees et al., 2004). Furthermore, out of the vegetation spectral studies that do focus on the (sub-)Arctic, few of these work on both bryophytes and lichens. In terms of spectral differences in bryophytes, many of these studies (Vogelmann & Moss, 1993; Bubier et al., 1997; Arkimaa et al., 2009; Neta et al., 2010a; Stoy et al., 2012) have found that different species/taxa can have very different spectral properties in the VIS and NIR ranges. This is because the VIS and NIR wavelength ranges are moderated by the species' pigment and chlorophyll concentration differences, shoot/canopy morphology and arrangement, biomass, texture, and cellular structure. Furthermore, these differences may be best expressed in bryophytes when at

higher moisture concentrations. For example, Harris et al. (2005) found their moss samples to be most spectrally different when at higher water contents. Absorption features have also been useful for distinguishing bryophytes; for example, unlike regular green vascular vegetation, *Sphagnum* has very pronounced water absorption features at 1000nm and 1200nm (Vogelmann & Moss, 1993) and compared to other mosses, *Sphagnum* had a unique absorption feature at 850nm (Bubier et al., 1997).

For lichen, the usual spectra are thought to have minimal to no reflectance peak in the green range and rather have a gradual reflectance increased from 400-1000nm, although with a visible increase in the reflectance slope around 650nm (Rees et al., 2004; Singh & Prabakaran, 2015). Petzold and Goward (1988) were the first to publish a major dataset of spectra for northern lichens, focusing on three fruticose lichen mats (*Cladonia stellaris*, *Stereocaulon paschale* and *Cetraria ericetorum*), and found that *Cladonia* lichen strongly absorbed radiation in the blue and ultraviolet wavelengths. Rees et al. (2004)'s work notes specific spectral properties within various subarctic lichen types: they found that fruticose lichens had a high reflectance in the VIS range with a gradual increase in the NIR range, while crustose lichens had a gradual increase in reflectance through the VIS to NIR range with a strong spectral structure past 2000nm. Furthermore, crustose lichens rarely had an absorption feature in the blue range while it was weakly therefore for fruticose lichens, and while there was an occasional clear maximum in the green range for fruticose lichens, it was rare for crustose lichens; fruticose lichens also often had a change in their slope in the green range but it was only likely for crustose (Rees et al., 2004). In regards to distinguishing species, Rees et al. (2004) suggest optimal spectral

discrimination in the blue wavelengths less than 450nm, the non-blue wavelengths in the VIS range, the infrared range below the hydroxyl absorption feature at 1400nm, and the infrared wavelengths above 1400nm. Although, more broadly, Singh and Prabakaran (2015) found most variation between species in the NIR and SWIR region (except for 1500-1800nm), while Granlund et al. (2018) and Neta et al. (2010a) suggest the VIS to NIR range more clearly separate different species (due to different pigment concentrations and cellular structure/morphology).

While the SWIR region appears to be less explored than the VIS-NIR ranges for both bryophytes and lichens, it has been found by studies (Bubier et al., 1997; Rees et al., 2004; Arkimaa et al., 2009; Neta et al., 2010a; Granlund et al., 2018) to be very useful in estimating moisture status and in some of those studies, could even be used to separate species because reflectance in this range directly responds to tissue water content (which is driven by species' unique water retention capacities). Neta et al. (2010a) and Stoy et al. (2012) also note that the overall reflectance in the SWIR range for mosses was lower than for lichens, which can be attributed to the higher water carrying capacity of moss tissues compared to the drier (and more reflective) tissue of lichen, with Stoy et al. (2012) additionally noting that *Sphagnum* mosses had a higher water content than the other mosses because of their hyaline cells which can hold large amounts of water.

Yet, many of the studies that do discuss the effects of water on bryophyte and lichen spectra are either not (sub-)Arctic, focus on a limited number and type of taxa/species, and have restricted wavelength ranges. Table 2 provides an overview of these studies' key findings on the effects of moisture on bryophyte/lichen spectral properties.

Study	(Sub-)Arctic?	Species	Spectral Range	Findings
Ager and Milton (1987)	N: Spain	Lichen	400-2500nm	• Largest difference between hydrated and dry lichens were between 1100-1900nm
Vogelmann and Moss (1993)	N: Maine/New Hampshire	Moss	400-2500nm	• With drying, reflectance increased across all wavelengths, depth of water absorption features decreased, but drying also revealed many absorption features not seen at saturation
Bubier et al. (1997)	Y	Moss and Lichen	400-2500nm	• VIS range allowed for easy differentiation of lichens compared to other plant types, and mosses could be separated by VIS, NIR, and SWIR differences • Species within taxa could also be separated by their pigment and tissue water content
Nordberg and Allard (2002)	Y	Lichen	400-2400nm	• When drying, some lichen had decreasing rather than increasing reflectance (similar to what Rees et al. (2004) noted) in wavelengths between 400 to 1200-1400nm
Lovelock and Robinson (2002)	N: Antarctica	Moss	200-900nm	• Characteristic reflectance differences between sites and species were not found to be clearly linked to shifts in pigment concentrations but rather were more heavily linked to water content and canopy/shoot morphological differences
Bryant and Baird (2003)	N: north Scotland	Moss	400-2500nm	• With drying, reflectance increased across all wavelengths (substantially in SWIR) and absorption features/peaks largely disappeared or changed shape
Rees et al. (2004)	Y	Lichen	350-2500nm	• Largest differences between dry and hydrated lichens were near water absorption features (1450 and 1900nm), but they found that when drying, lichens did not invariably have a higher reflectance in all wavelengths (drying effects on lichen spectra seem to be more complex than what was previously thought)
Harris et al. (2005)	N: Cors Fochno, Britain	Moss	350-2500nm	• With drying, reflectance increased across all wavelengths, depth of water absorption features decreased and changed in shape • More differences between sample spectral properties when at higher moisture contents
Van Gaalen et al. (2007)	Y	Moss	400-1000nm	• Decline in water content led to overall increase in reflectance across the spectra
Arkimaa et al. (2009)	Y	Moss	350-2500nm	• Increasing water content produced overall decrease of reflectance, deeper water absorption peaks, and strong decrease in SWIR reflectance
Neta et al. (2010a)	Y	Lichen and Moss	400-2500nm	• Shifts in plant moisture content associated with large variations in SWIR, with a low SWIR reflectance related to high moisture contents • With drying, depth of water absorption bands decreased • VIS and NIR ranges were useful in distinguishing species but were not great for estimating moisture content changes
May et al. (2018)	Y	Moss	350-1100nm	• Shifts in water content can cause quick and substantial shifts in NDVI but changes in biomass may take longer to appear • High red reflectance levels and low NDVI values that appear from low moisture contents may act as mechanisms to minimize absorption of irradiance and diminish any further evaporative water loss and cellular damage • Upon rehydration, *Sphagnum* had a more rapid increase in NDVI, though these values did not reach the magnitude of those at initial saturation, while pleurocarpous communities had a slower increase in NDVI but did recover to their initial saturation NDVI values • They also found that spectral reflectance properties for the different moss communities were very species-specific in their varying resiliencies and responses to drying
Granlund et al. (2018)	Y	Lichen	400-5500nm	• Increasing water had species-specific effects on spectral reflectance properties (especially in VIS-NIR) which were often associated with the unique chemical and structural adaptations to drying and rehydration cycles • Low correlations between lichen water content and reflectance until 1300nm with some strong correlations between 1300-5500nm • Addition of water caused minimal changes in the VIS range, while changes in the NIR range were large for all species because changes in spectral features in this range are associated with shifts in the cellular structure (which appear to be strongly affected by water in lichens) • Water absorption peaks also tended to widen as water content increased, leading to larger reflectance differences in the neighboring wavelengths of those absorption features

Table 2: Key effects of water on bryophyte and lichen spectra seen in the literature.

The majority of these studies (Table 2) find that higher water contents are associated with lower reflectance as well as deeper water absorption peaks across the VIS, NIR, and SWIR ranges (particularly in the SWIR); once drying occurs, reflectance generally increases across all wavelengths (substantially in the SWIR range) and absorption features/peaks largely disappear or change shape, with drying even revealing many absorption features that were not seen at saturation. These higher reflectance levels in response to drying or low moisture have been suggested to act as a mechanism to minimize absorption of irradiance and diminish any further evaporative water loss and cellular damage (May et al., 2018). For example, as lichens lose water content, their cells shrink and form small air cavities which increases the internal scattering of incident radiation, increasing reflectance (Granlund et al., 2018). Despite the general responses of bryophyte and lichen spectra to water changes, many of these studies have also found these responses to be species-specific, due to the unique chemical and structural adaptations to drying and rehydration across various taxa/species. For example, while drying is commonly associated with increasing across VIS, NIR, and SWIR wavelengths in bryophyte and lichen species, some lichen studies (Nordberg & Allard, 2002; Rees et al., 2004) have reported mixed results in this regard, with some of their lichens' reflectance decreasing and others increasing, counteracting this notion of invariably increasing reflectance with drying and emphasizing that different taxa/species will respond uniquely to moisture changes. For changing moisture in their lichen species, Granlund et al. (2018) attribute the species-specific spectral responses to the complex cortical structural

differences within each species, as this affects the manner in which light is scattered internally and reflected.

Furthermore, drying can reveal many absorption features that were not seen at saturation (Vogelmann & Moss, 1993). When water content increases, water absorption peaks tend to widen, producing larger reflectance differences in the neighboring wavelengths of those absorption features at various moisture levels (Granlund et al., 2018). These changing absorption features with moisture shifts likely relate to why lichen studies have seen the largest differences between dry and hydrated lichens near water absorption features (e.g., 1450 and 1900nm) (Rees et al., 2004). Although, Ager and Milton (1987) report the largest difference between their hydrated and dry lichens at a broad wavelength range: between 1100-1900nm.

Species-specific reflectance characteristics are largely the reason for the limited success of common spectral indices in estimating moisture in bryophytes and lichens. While moisture indices (e.g., Moisture Stress Index) have been regarded to be somewhat successful for bryophytes and lichens (Harris et al., 2005; Arkimaa et al., 2009; Neta et al., 2010a; Granlund et al., 2018), many of these studies have found that their success in detecting moisture was dependent on the specific species, especially from differences in canopy branch/leaf architecture which enable some species to better manage decreasing water availability than others, but also from unique shifts in cellular structure with drying/rehydration. That said, many of these studies also confirm that a majority of common indices (e.g., NDVI) do not adequately represent non-vascular plants, highlighting the importance between distinguishing vascular and non-vascular spectral

reflectance properties. For example, May et al. (2018) found that gross primary production (GPP) and NDVI decreased strongly with the loss of water in moss, but this occurred at different rates and magnitudes, creating a mismatch between moss NDVI and productivity levels. Furthermore, for similar NDVI values, GPP values would vary depending on the moisture content of the mosses, showing that NDVI is likely not an accurate index for estimating Arctic moss physiological activity (May et al., 2018). Indices that use NIR and SWIR bands show the strongest correlation between moisture and reflectance, particularly those that use bands near or at major water absorption features (e.g., 1200nm, 1450nm, 1930m) (Harris et al., 2005; Granlund et al., 2018).

Water and shoot/canopy morphological differences exert stronger controls on the spectral responses of different species and sites/microtopographic positions than other factors, such as pigment concentration (Lovelock & Robinson, 2002; Stoy et al., 2012). Thus, not only are spectra often species-specific but they are strongly affected by their environmental conditions, emphasizing the importance of linking species spectra with environmental variables such as water stress (Lovelock & Robinson, 2002). Furthermore, shifts in plant moisture status bring about changes in their surface temperature (Stoy et al., 2012) and directly affect photosynthesis (Van Gaalen et al., 2007), impacting biogeochemical cycles and ground-surface energy fluxes. For example, when water contents are high in *Sphagnum* (above the optimal point for net photosynthesis), the excess water limits CO_2 diffusion into the chloroplast and thus, restricts photosynthetic activity (Van Gaalen et al., 2007). Once water content decreases past an optimal point, net photosynthetic rates decrease despite the increasing CO_2 conductance with less water (Van

Gaalen et al., 2007). Therefore, while excessive drying is detrimental, it is important for bryophytes to maintain some intercellular air space so that cells retain optimum levels of moisture for full physiological functions (May et al., 2018). May et al. (2018) found that their moss communities had their highest GPP when at a moisture content of 70-80%, and drying below these levels progressively dropped the GPP.

1.6. Objectives

As the Arctic is a region quickly changing under warming conditions, tundra vegetation is likely to undergo significant shifts in composition and distribution. Although non-vascular vegetation dominates and largely moderates ecosystem conditions in the high-latitudes, it is often neglected in terms of remote sensing applications. Many remote sensing applications or indices have been built upon vascular vegetation research and thus, can result in misrepresentations of the unique physiological processes within non-vascular vegetation. To discriminate non-vascular vegetation from vascular vegetation, we must understand how their spectral properties differ and what may moderate these spectral differences. While much of the work discussed above has shown that efforts have been made to close this gap, there are many bryophyte and lichen species that are not given attention in these studies, presenting a considerable bias of knowledge towards a few common bryophyte and lichen species (e.g., *Sphagnum*) when tundra ecosystems are characterized by numerous non-vascular plant types and species. Furthermore, as non-vascular vegetation is poikilohydric, shifts in water content directly affect physiology, morphology, and anatomy, producing important changes in spectral properties. While

some of the studies mentioned above have given some focus to the effects of water on bryophyte and lichen spectral signatures, these effects still appear to be ambiguous (particularly when it comes to the type of species being examined) and there is little discussion of how drying may cause these different plant types/species to spectrally appear similar or dissimilar, and how this could affect not only the detection and identification of various bryophyte and lichen species, but also long-term monitoring of Arctic vegetation changes. Furthermore, the neglect of liverworts in any Arctic terrestrial spectral properties studies presents a significant gap in the knowledge on the spectral properties of this plant type.

Considering these knowledge gaps, the overall goal of this study is to examine and compare how the spectral properties of various Arctic moss, liverwort, and lichen species vary under shifting hydrological conditions, giving attention to both within-species shifts but also between-species and -taxa comparisons. Two main objectives will be completed to achieve this goal:

1) Quantify changes in the shape and magnitude of moss, liverwort, and lichen spectral signatures from saturation (100% moisture) to desiccation (0% moisture) through lab water table depth manipulations with daily spectral measurements (350-2500nm).
2) Identify a moisture stress threshold at which different species are no longer spectrally distinguishable from one another in VIS/NIR/SWIR wavelength ranges.

2. METHODOLOGY

2.1. Study Area

This study focuses on southeastern Victoria Island, Nunavut, Canada (Figure 2). Victoria Island is located in the Canadian Arctic Archipelago; it is the 8th largest island in the world. Victoria Island is characterized by continuous permafrost (Brown et al., 2002) and the region belongs to the polar tundra group in the Köppen–Geiger climate classification (Kottek et al., 2006). Two characteristic bioclimate zones (Walker et al., 2005) are represented across the island: (1) Bioclimate zone C has averaged July temperatures of 6-7ºC and is characterized by open patchy vegetation of mosses, herbaceous plants, and dwarf shrubs, with 5-50% of the vegetation being vascular; it encompasses the southern and western portion of the island (see Figure 2), and (2) Bioclimate zone D has averaged July temperatures of 8-9ºC and is characterized by interrupted closed vegetation of mosses, herbaceous plants, and dwarf shrubs with 50-80% of the vegetation being vascular (Walker et al., 2005). While those vegetation assemblages are strongly dependent upon climate, the geological setting also matters as it influences nutrient availability for plants. Most of Victoria Island is underlain by calcareous substrates, including dolomite with some limestone, sandstone, and shale (Washburn, 1947). Lastly, part of the island is included in the domain of the Arctic-Boreal Vulnerability Experiment (ABoVE), which is a large NASA campaign to better explore and understand the effects of climate change on boreal and Arctic ecosystems.

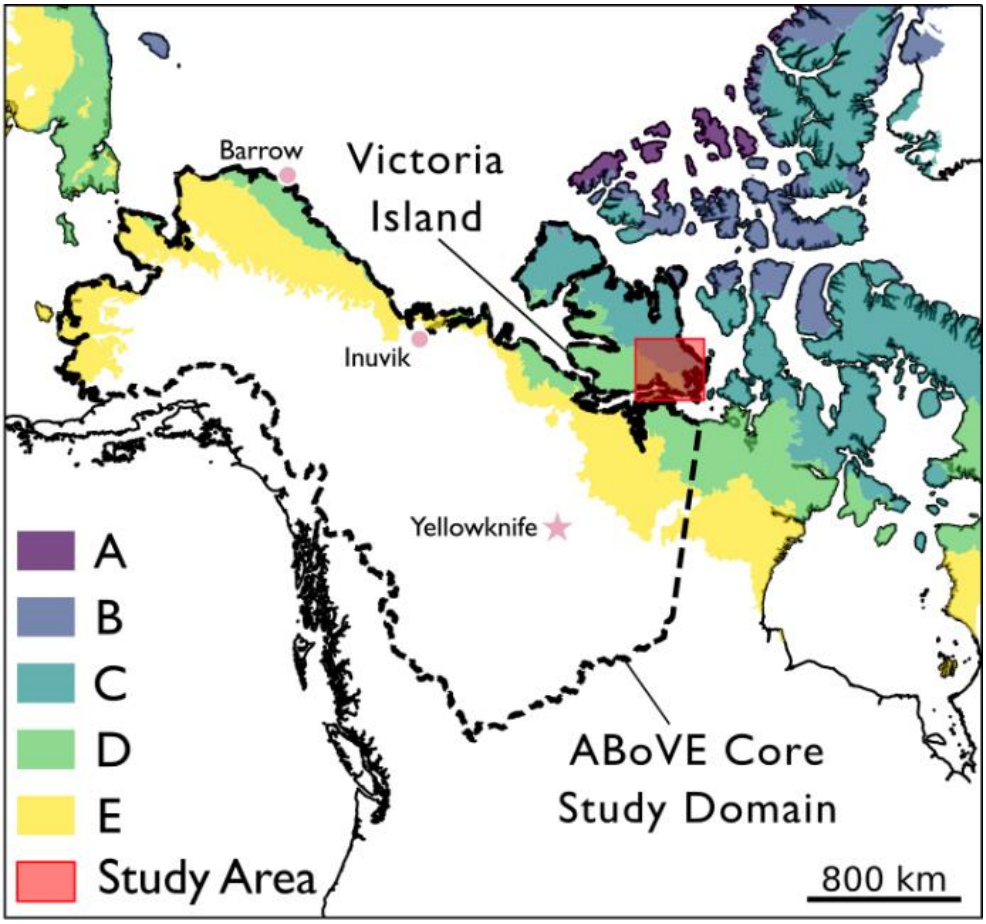

Figure 2: Study area (red), ABoVE core study domain (Loboda et al., 2019), and Arctic tundra bioclimate zones of A (coldest) to E (warmest) (Walker et al., 2005); each zone is characterized by continuous permafrost (Brown et al., 2002).

2.2. Field Sampling

Based on flight reconnaissance over southeastern Victoria Island in July 2019, ten sites representative of the regional ecosystems were chosen to sample vegetation from (Figure 3, Table 3). A majority of these sampling sites were sedge-dominated wetlands (6/10 sites); the others were tussock tundra sites (2/10), 1 inland coastal wetland, and 1 drier rocky upland area (Figure 4). At each field site, one to four surface vegetation

samples were collected which led to a total of 28 samples: 21 mosses, 5 lichens, and 2 liverworts. Note that, despite the team's best efforts, no *Sphagnum* mosses were found within the study area. It is probably due to the weathering of regionally-abundant calcareous parent material, which inhibit *Sphagnum* growth (Donald McLennan, pers. comm. 2019). This confirms similar findings from other regional vegetation surveys (Ponomarenko et al., 2019).

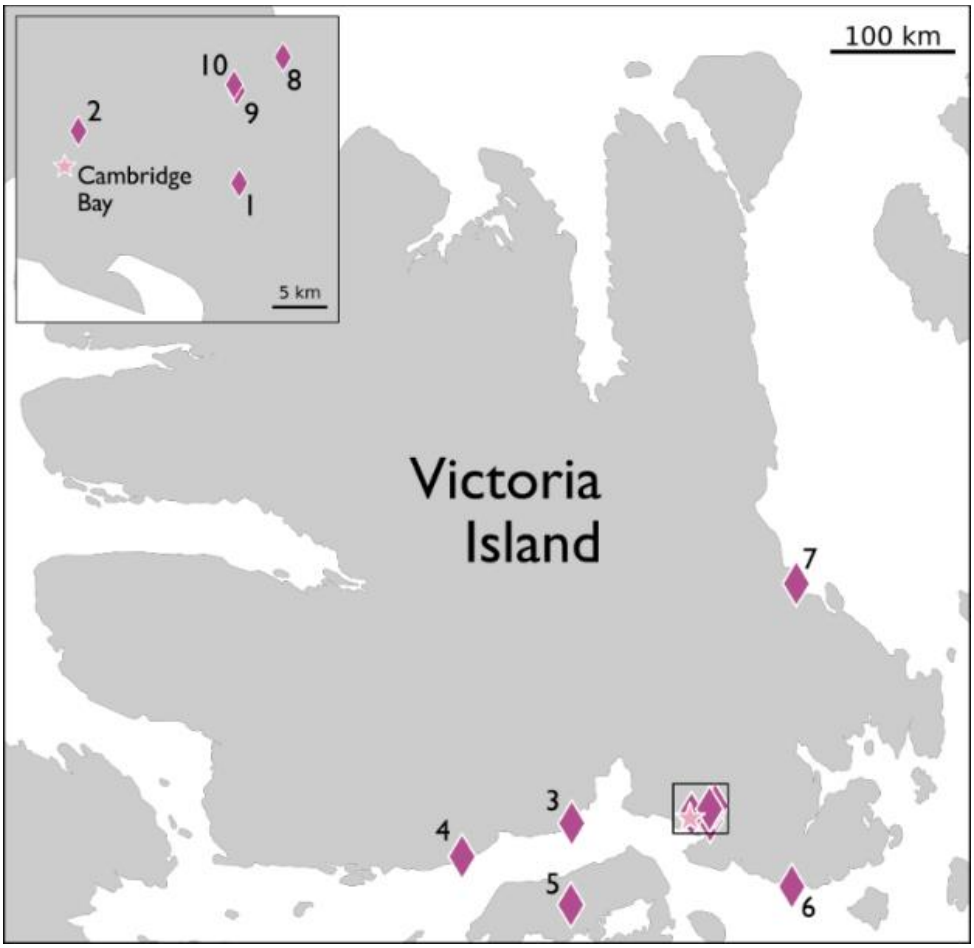

Figure 3: The ten sampling sites (diamonds) selected across southeastern Victoria Island (which correspond to the descriptions, coordinates, and listed species in Table 3).

Site #	Description	Coordinates	Species Collected
1	Wet fen site located in a depression; dominated by *Carex aquatilis* that is largely underlain by *Amblystegiaceae* moss carpets; Shallow ground (dug about 25cm then rock/very deep root).	104.87357°W, 69.16463°N	*Pseudocalliergon brevifolium*
2	Drier fen site; dominated by *Carex aquatilis* and *Salix* spp., with substantial microtopography (e.g., islands of *Salix* spp. with many depressions).	105.20840°W, 69.19037°N	*Pseudocalliergon brevifolium*
3	Inland coastal wetland site on a rocky landscape with shallow wetlands; dominated by *Carex aquatilis* and *Salix* spp. (not as shrublike here: vegetation is much shorter and low-lying to the ground; continuous moss carpets are also present here with moss also growing on the rocks.	107.27458°W, 69.05093°N	*Pseudocalliergon brevifolium, Drepanocladus arcticum*
4	Sedge-dominated, rocky, and disturbed site near a DEW line strip; these surface moss samples were collected near a larger pond.	109.08762°W, 68.75213°N	*Ptychostomum cf. turbinatum, Drepanocladus arcticum*
5	Tussock tundra site (with hummock-hollow formations) located in a depression containing many saturated wetlands that have an oily texture. Lots of lichen, isolated moss carpets, and sedge present at this site.	107.11657°W, 68.54301°N	*Anastrophyllum minutum, Flavocetraria nivalis, cf. Sphaerophorus globosus*
6	Heavily disturbed rocky tussock tundra area that was a previous outpost/station and has a large bird population (lots of oxidized bird feces surrounding shallow ponds); samples were collected in a wet depression here that appears to be an outline of an polygon.	103.35236°W, 68.79739°N	*Pseudocalliergon turgescens*
7	Wet fen site dominated by *Carex aquatilis* and moss carpets; Samples collected in a lower area surrounded by drier upper soil (likely gets flooded from lakes as well as thawing).	103.71999°W, 70.66502°N	*Catoscopium nigritum, Aulacomnium turgidum*
8	This site was on Mount Pelly, which is a rocky, upland, and terraced landscape; there is a large variety of lichen-covered rocks and some small moss patches.	104.81017°W, 69.257903°N	*Xanthoria elegans*
9	Wet wetland site (with a very high water table) dominated by *Carex aquatilis* and a moss understory; being located in a depression, the site is surrounded by upland, rocky areas. The soil in the wetland is highly saturated with lots of bird feces, while the upland area is very dry and barren with many lichen patches.	104.89687°W, 69.23042°N	*Tomentypnum nitens, Xanthoria elegans*
10	Wet wetland site located in a depression near an eddy covariance tower; depression is a very saturated area surrounded by drier upland areas; it is a sedge-dominated area with a moss carpet understory.	104.90330°W, 69.23470°N	*Ptychostomum cf. pseudotriquetrum*

Table 3: Sample site description, coordinates, and species collected (site numbers correspond to those shown in Figure 3).

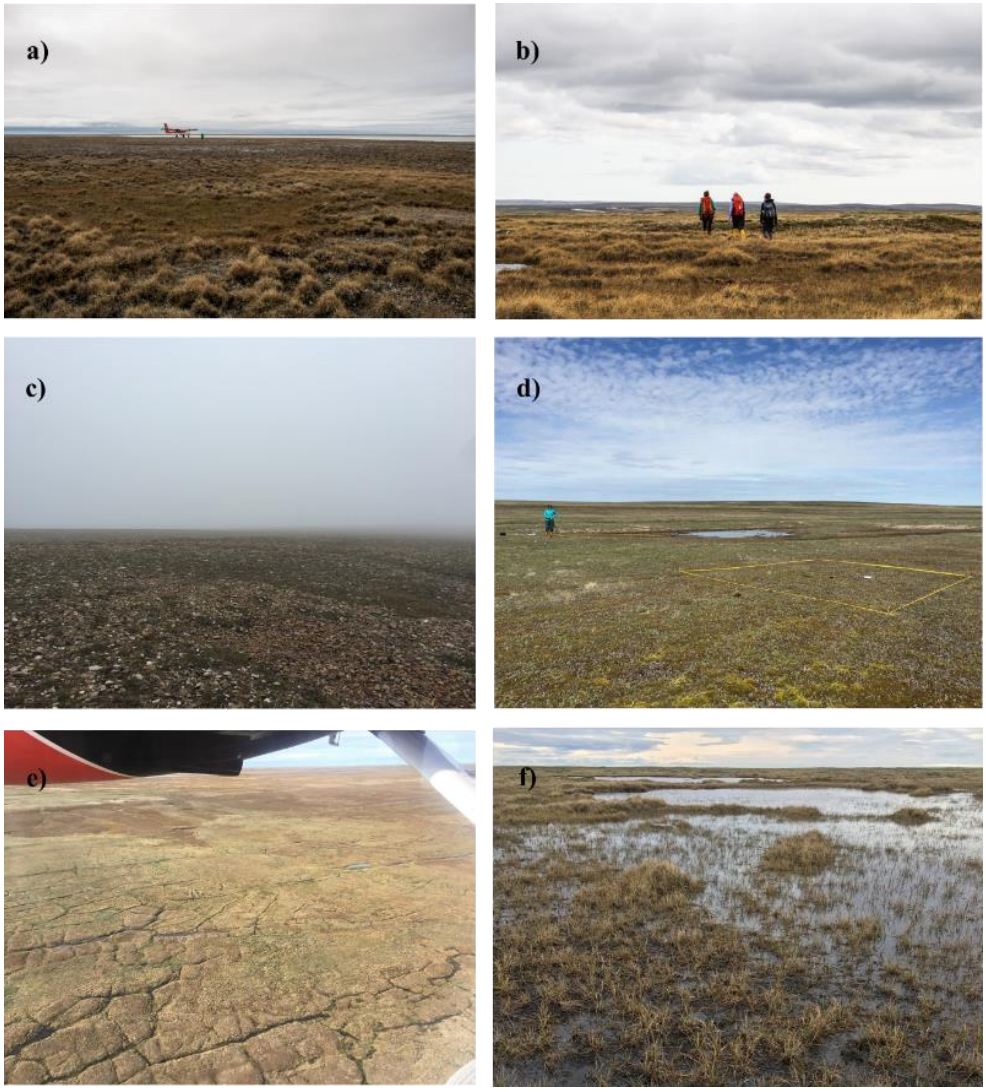

Figure 4: Images of some of the characteristic site types and features observed in the field: a) tussock tundra (photo courtesy of Patrick Campbell), b) hummock-hollow formations (photo courtesy of Patrick Campbell), c) upland, dry rocky areas, d) inland coastal wetland, e) polygonal features (photo courtesy of Julie Loisel), and f) sedge-dominated wetland (photo courtesy of Julie Loisel).

A 13x13cm vegetation block, with ~8cm of underlying litter, was cut for each sample, weighed in the field for a fresh weight, and stored in a sealed plastic container

(Figure 5). Samples were then transported and preserved in a refrigerator under cold, dark conditions until October 2019, when lab measurements took place.

Figure 5: A few action shots of the sampling process: a) identifying and noting representative vegetation patches/species, b) extracting a surface vegetation block from the representative patch, c) transactional view of a surface vegetation block, and d) packing the sample for preservation and transport. Photos courtesy of Patrick Campbell.

All vegetation samples/species were identified by Erin Cox using the taxonomy from the Flora of North America (2007a, 2007b). Ms. Cox is a graduate student in Prof.

Catherine La Farge-England's lab at the University of Alberta. Prof. La Farge-England is one of few Arctic bryologists and is working on an inventory of High-Arctic mosses.

2.3. Laboratory Experiment

In the lab, water table depth manipulations were performed on my samples. Each sample was first put into a black basket (Figure 6); various sizes were used (small – 5cm diameter, medium – 7cm diameter, and large – 9cm diameter). Samples were then "purified": to my best ability, all extraneous interfering vegetation was removed to get the purest single species stand possible. However, some samples were impossible to purify and were left to their natural or 'mixed' state, resulting in 19 pure samples and 13 mixed samples.

Figure 6: Image of some of the moss and liverwort samples in the large black baskets in a tray.

2.3.1. Water Table Depth Manipulations

To achieve full saturation at the beginning of the experiments, samples were flooded overnight with deionized water for ~16 hours in a growth chamber at 10ºC under dark conditions. After removing the samples from the flooded trays, all samples were immediately weighed, pictured, and spectral measurements began. The weights, photos, and spectral measurements were then taken every five hours on the first day, every 11.5 hours the second day, and then daily from the third day throughout the rest of the experiment duration. Samples still had relatively high water contents at the one-week mark, so growth chamber temperatures were set to 25ºC (i.e., increased by 15ºC) to speed up desiccation. This happened once more at the two-week mark, with the growth chamber temperature increased by 5ºC (i.e., set to 30ºC). The small and medium basket samples reached full desiccation at the two-week mark, while weights, pictures, and spectral measurements continued until the 20th day for the large basket samples.

2.3.2. FieldSpec spectroradiometer

Spectral measurements from 350-2500nm were collected using an ASD FieldSpec 4 Hi-Res spectroradiometer and ASD PlantProbe which had a 3nm resolution for VIS-NIR, 8nm resolution for SWIR. The PlantProbe took measurements at a 10mm diameter spot size. Spectral measurements were collected in a dark room where the ASD PlantProbe's internal high-intensity light bulb was the only illumination source. White reference measurements were taken every ~30 minutes during each sampling period using the PlantProbe's Spectralon 100% reflectance white cap, and the PlantProbe was kept at

nadir throughout measurements (refer to Figure 7 for the spectroradiometer set-up). A total of 15 spectral signatures were collected per measurements; two measurements from different spots on the sample surface were taken for the small baskets, three for the medium, and four for the large. The measurements were then averaged to derive a mean spectral signature for each sample. In a few cases, erroneous measurements (e.g., where the spectral signature touched or exceeded 100% reflectance) were excluded from the averaging process.

Figure 7: Lab set-up of spectroradiometer (top), with samples lifted up to contact the probe (bottom). The measurements were collected in a dark room.

2.4. Data Analysis

2.4.1. General Approach and Study Design

Multiple statistical tools were used to analyze the spectral changes that occurred from saturation to desiccation within and between each species. In the following sub-sections, I introduce these different types of analyses.

Since all species lost water content at their own rates and degrees, moisture levels for each species were binned in 10% increments (with the spectra averaged) for direct comparison across species. For example, a species' spectra at 0%, 4%, and 8% moisture were averaged together to produce a mean spectral signature that represents the 0-10% moisture "bin".

The spectral signatures were analyzed using the following spectral ranges: 400-700nm = VIS, 700-1400nm = NIR, 1400-1900nm = SWIR1, 1900-2500nm = SWIR2 (Arkimaa et al., 2009; Ustin et al., 2012; Dennison et al., 2019). These spectral ranges were further divided into 100nm windows (e.g., spectra at 400-500nm, 500-600nm, 600-700nm) to pinpoint the wavelengths of importance within the broader spectral ranges.

Note that these analyses generated a large number of results; in the main text of my thesis, I only present and discuss results from 5 taxa: *Anastrophyllum minutum*, *Xanthoria elegans, Catascopium nigritum*, *Aulacomnium turgidum,* and *Pseudocalliergon turgescens*. I chose these samples to ensure there was at least one of each non-vascular plant type that my thesis touches on (e. g., liverwort, lichen, moss). In addition, these species are common to the study area and/or had interesting features (e.g., *C. nigritum* and

A. turgidum are both acrocarpous mosses yet appear to have quite different spectral features). Results from all other species and taxa can be found in Appendix A.

2.4.2. Within-Species Spectral Analyses

Objective 1 focused on identifying how the shape and magnitude of individual species' spectra change with moisture. A total of two analyses was performed: (1) SID, and (2) Convex Hull maxima.

First derivatives of the average spectra were initially calculated to assess where and when shifts in peaks/troughs and slope occur in the spectra (Lovelock & Robinson, 2002; Harris et al., 2005). To establish and quantify these changes, the Spectral Information Divergence (SID) metric was primarily used. SID is a statistical metric that assesses the discriminability/similarity between two spectral signature vectors by measuring the distance between those spectral signatures' probability distributions (Chang, 2003). Many studies (Chang, 2000; Chang, 2003; Kwan et al., 2006; Zhang et al., 2014) have found SID to be an effective measure for assessing spectral variability when compared to more traditional spectral similarity/distance metrics such as Spectral Angle Mapper or Euclidean Distance. Lower SID values mean the two spectra that are being compared are more similar, and higher SID values mean they are more discriminable or different. SID values were calculated for all moisture level comparisons. For example, a SID value was calculated to compare any given species' 100% vs. 90% moisture spectral signatures; this would continue throughout the desiccation gradient in a stepwise fashion (e.g., 90% vs. 80%, 80% vs. 70%, etc.).

Convex Hull maxima points were also used to quantify shifts in the spectra's local maxima as a function of moisture changes. These maxima were identified by putting a convex hull (or continuum line) over the spectral signature. The convex hull is made up of short line segments that have endpoints at the start/end of the spectral signature and are connected by the local maxima of the spectra (Clark & Roush, 1984; Manevski et al., 2017). These are useful in that they create a standard way to identify maximal features (or the significant, maximal peaks) in the spectra (Figure 8).

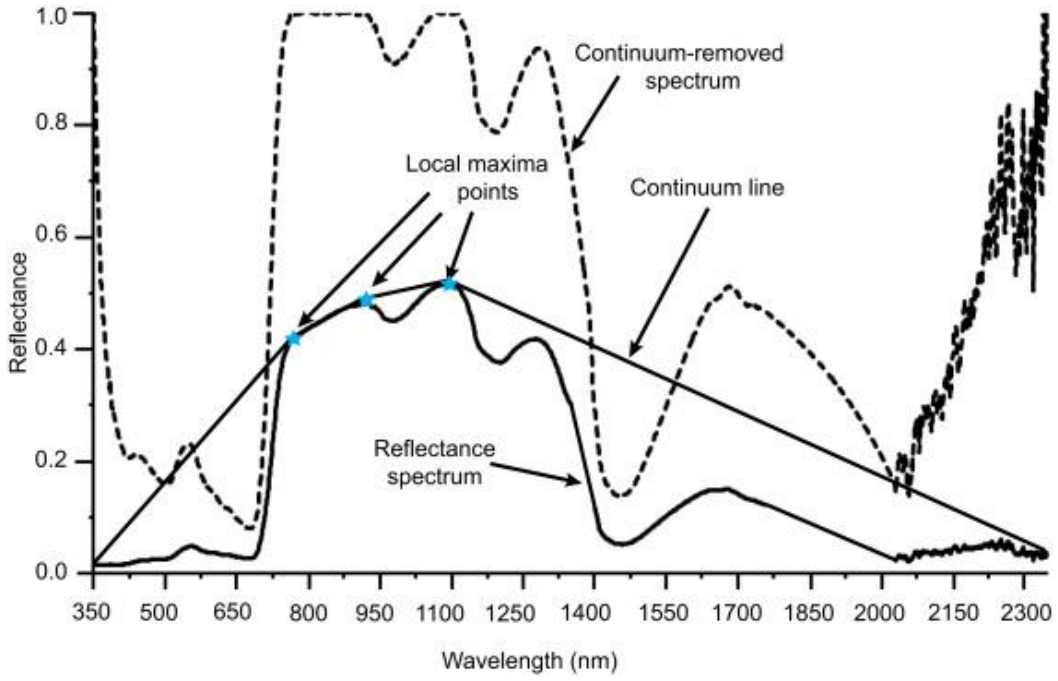

Figure 8: Image depicting what the convex hull maxima points are (blue stars) and how they are a part of the continuum line or convex hull overlayed on a spectral signature. Reprinted from Manevski et al. (2017).

2.4.3. Cross-Species Spectral Analyses

Objective 2 focused on comparing the spectra of different plant types and species against one another to identify similarities/distinctions in their spectral responses at corresponding moisture levels. This objective was also aimed at testing whether there was a moisture level threshold beyond which different plant types and/or species were no longer spectrally distinguishable. A total of two analyses was performed: (1) SID and (2) Convex Hull maxima.

The SID metric was again used to quantify the similarity/discriminability in spectra, but this time, between different plant types and species, at the corresponding binned moisture content classes. For example, each species' spectra at 0-10% moisture content was compared to all the other species' spectra for that same moisture content. Convex Hull maxima points were also used to identify whether there were corresponding shifts in the binned spectra local maxima across plant types and/or species.

3. RESULTS

3.1. Objective 1: Quantify changes in the shape and magnitude of moss, liverwort, and lichen spectral signatures from saturation (100% moisture) to desiccation (0% moisture) through lab water table depth manipulations with daily spectral measurements (350-2500nm)

3.1.1. Average Spectra and First Derivatives

Figure 9 shows the average spectra of the five species at various moisture contents, from saturation (100% moisture) to desiccation (0% moisture), along with the first derivatives of the spectra. Starting at saturation, the following observations can be made:

The liverwort *A. minutum* (Figure 9a) has little reflectance in the VIS range until the red reflectance wavelengths (600-700nm), where a small peak reflectance is observed at 642nm. Reflectance further increases going into the NIR region, which has three main peaks (924nm, 1086nm, and 1267nm). Moving into the SWIR ranges, the reflectance then lowers, but the SWIR1 does contain two peaks: 1670nm and 1818nm, while there is one peak in SWIR2, at 2216nm.

The lichen *X. elegans* (Figure 9b) has a somewhat high reflectance in the blue reflectance wavelengths (400-500nm) compared to the other species, but it does not have peaks in the VIS range until the red reflectance wavelengths (600-700nm), with a small peak at 654nm. Reflectance increases going into the NIR range, with three somewhat flat peaks (928nm, 1116nm, and 1270nm). As reflectance lowers moving into both SWIR

ranges, there are apparent peaks at 1676nm and 1817nm in the SWIR1, and in the SWIR2 range, a peak at 2209nm.

The moss *C. nigritum* (Figure 9c) is characterized by low reflectance and no peaks in the VIS range. Moving into the NIR range, reflectance increases with a slight curve in the spectra at 948nm and two large peaks at 1112nm and 1269nm. Reflectance then decreases going into the SWIR ranges, with two peaks in the SWIR1 range at 1674nm and 1818nm, and a flatter peak in the SWIR2 at 2203nm.

The moss *A. turgidum* (Figure 9d) has an increasing reflectance in the VIS range, from the green to red reflectance wavelengths (500-700nm), with a noticeable peak in the red reflectance wavelengths at 637nm. Reflectance then increases going into the NIR range, which has three main peaks at 922nm, 1094nm, and 1269nm. Going into the SWIR ranges, reflectance lowers, with the SWIR1 range having two peaks at 1674nm and 1815nm, and the SWIR2 range having one peak at 2216nm.

The moss *P. turgescens* (Figure 9e) sees its reflectance increase from the green to the red reflectance wavelengths (500-700nm), with a small peak in the red reflectance wavelengths at 636nm. Reflectance increases going into the NIR range, which has three large peaks at 937nm, 1086nm, and 1266nm, as well as two small peaks at 788nm and 827nm. Moving into the SWIR ranges, reflectance decreases, with the SWIR1 range having two peaks at 1677nm and 1815nm while in the SWIR2 range there is one peak at 2203nm.

Drying affects the spectral features in the VIS range with varied responses in reflectance shape and magnitude (see the different line colors in Figure 9). For *A. minutum*,

drying does not appear to have a dramatic effect on shape or reflectance in the VIS range, but there seems to be a slight increase in reflectance in the red reflectance wavelengths where this species was already having higher reflectance. For *X. elegans*, reflectance more clearly increases in the VIS range with drying, although after reaching 66.67% moisture, the reflectance remains around the same magnitude, with little change in shape. For *C. nigritum*, the VIS range shape does not change with drying, but the reflectance does increase with desiccation (although not invariably, with some decrease in reflectance occurring as well). For *A. turgidum*, the VIS range reflectance increases and decreases variably with drying, though there is little change in shape. For *P. turgescens*, reflectance in the VIS range generally increases with drying (but there are some slight decreases), while the shape remains mainly the same.

Drying also affects NIR features, with shape and magnitude responses somewhat similar across species. The magnitude of reflectance generally increases from saturation to desiccation for all species, though many experienced decreasing reflectance at some points as well (Figure 9). As for the shape of the spectra, there appears to be a pattern among the species in which moving from saturation to desiccation, all species see a disappearance or flattening of their NIR reflectance peaks, with all species appearing to have one major peak in the longer NIR wavelengths by desiccation. Yet, these shape changes start at different moisture levels for each species (*A. minutum*: 49.68%, *X. elegans*: 66.67%, *C. nigritum*: 60.99%, *A. turgidum*: 35.41%, and *P. turgescens*: 21.74%). Many of these changes in the NIR reflectance shape are more evident in the derivative

spectra as the presence of new peaks and deeper (as well as flatter) lines correspond to these slope and peak/trough changes in the NIR reflectance.

Drying also affects full saturation features in the SWIR1 and SWIR2 ranges; a multitude of large shifts, not only in magnitude of reflectance, but in shape as well, are reported for all species, with all five having similar (if not the same) desiccation response patterns. For *A. minutum*, *C. nigritum*, *A. turgidum*, and *P. turgescens*, reflectance magnitude increases from saturation to desiccation for both the SWIR1 and SWIR2 ranges. This is largely the case for *X. elegans* as well, except once it has reached 33.33% moisture, the magnitude of reflectance in the SWIR1 and SWIR2 ranges doesn't appear to change much. As for shape changes in the SWIR1 range, there appears to be the same pattern, with all five species having their two SWIR1 peaks sharpened, and a new slight rise in reflectance around ~1530nm by 0% moisture. That said, these SWIR1 shape changes occur at different moisture points for each species (*A. minutum*: 43.59%, *X. elegans*: 33.33%, *C. nigritum*: 11.52%, *A. turgidum*: 23.74%, and *P.* turgescens: 13.04%). Shape changes in the SWIR2 range have a similar, if not same, pattern for all the species as well. All species see their main SWIR2 peak sharpen, although starting at different moisture points (*A. minutum*: 61.54%, *X. elegans*: 66.67%, *C. nigritum*: 45.29%, *A. turgidum*: 53.31%, and *P. turgescens*: 21.74%). Then, a second peak (between ~2000-2030nm) also takes shape in the SWIR2, which starts at different moisture points for each species (*A. minutum*: 49.68%, *X. elegans*: 66.67%, *C. nigritum*: 11.52%, *A. turgidum*: 23.74%, and *P. turgescens*: 13.04%). Furthermore, all species also see a third small rise in reflectance at ~2390nm, which starts at different moisture points for each species (*A.*

minutum: 36.86%, *X. elegans*: 33.33%, *C. nigritum*: 11.52%, *A. turgidum*: 23.74%, and *P. turgescens*: 13.04%).

As a general interpretation, the five species have unique characteristic reflectance features at higher moisture levels. As they lose moisture, these differences converge, primarily in the NIR, SWIR1, and SWIR2, such that similar patterns of desiccation bring about a general increase in reflectance magnitude (with some decrease) and a shift toward a large, singular peak in the NIR, two sharp peaks in the SWIR1 with a new slight reflectance in the early part of the SWIR1, and a sharpening of the SWIR2 peak that is accompanied by the formation of a new peak in the early SWIR2 wavelengths and a new rise in reflectance in the longer SWIR2 wavelengths. Interestingly, though these changes are similar across the species, they happen at different moisture levels (see details above). For example, the lichen and liverwort most often see these changes at higher moisture levels than the moss species. Lastly, many of these changes in the NIR, SWIR1, and SWIR2 reflectance shape are evident in the derivative spectra, as the presence of new derivative peaks and their steeper slopes correspond to the newly forming or sharpened peak changes in the average spectra.

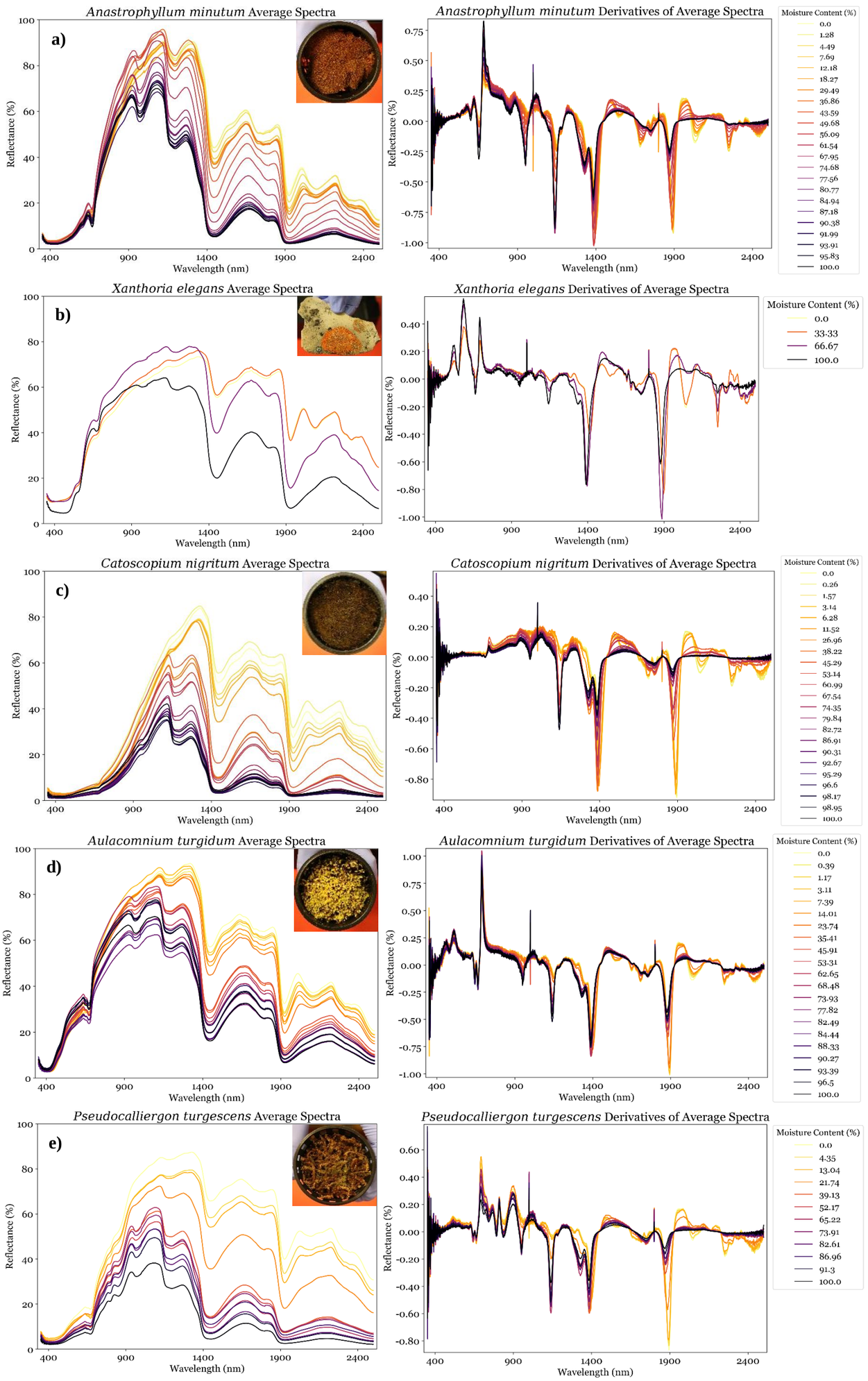

Figure 9: Average spectra (left) and first derivatives (right) for a) a liverwort (Anastrophyllum minutum), b) a lichen (Xanthoria elegans), c/d) two acrocarpous mosses (c: Catascopium nigritum, d: Aulacomnium turgidum), and e) a pleurocarpous moss: Pseudocalliergon turgescens from complete saturation (100% moisture) to complete desiccation (0% moisture). See Appendix A to view the rest of the averaged spectral signatures and first derivatives for species not listed here.

3.1.2. Within-Species SID (Full Spectral Range and 100nm Window) Analyses

The full range analyses of SID for the stepwise moisture comparisons in each species (Figure 10 left panels) show variable patterns in the SID value changes. *A. minutum*, *A. turgidum*, and *P. turgescens* appear to have fairly low and relatively stable SID values as moisture is lost, with a slight jump in the SID (although the spectral range can vary) for a comparison close to the mid to latter end of their moisture loss (A. minutum: 56.09-49.68%, A. turgidum: 35.41-23.74%, P. turgescens: 39.13-21.74%). *X. elegans* and *C. nigritum* see more dramatic SID value changes at some points, but similarly these SID jumps vary with the spectral range, with the largest jumps found for comparisons close to the mid to latter end of their moisture loss (*X. elegans*: 66.67-33.33%, C. nigritum: 26.96-11.52%). Around these SID "jumps", the neighboring moisture comparisons also tend to be characterized by much lower SID values. For example, in the case of *C. nigritum*, the 38.22-26.96% and 11.52-6.28% are its lower neighboring comparisons around its peak at 26.96-11.52%.

The 100nm analyses (Figure 10 right panels) show the different SID value changes in the full range analyses, but pinpoint the specific wavelength ranges in which these spectral differences are strongest in. For all species, the largest SID values are as follows: VIS: 400-500nm (with the exception of *X. elegans* which has its highest SID values in 500-600nm); NIR: 1300-1400nm; SWIR1: 1800-1900nm; and SWIR2: 2000-2100nm.

As a general interpretation, the SID or degree of spectral difference is stronger between some moisture levels than others (e.g., may see a higher SID value between 25-20% moisture than 20-15% moisture). Furthermore, the magnitude of these spectral

differences throughout the moisture gradient varies across species. Still, the SID shows that the highest spectral differences within the species' spectra occur primarily in the mid to latter portion of the moisture gradient. Lastly, the largest SID values for all five species occur in the same wavelength ranges for the NIR, SWIR1, and SWIR2 ranges, but not for the VIS range.

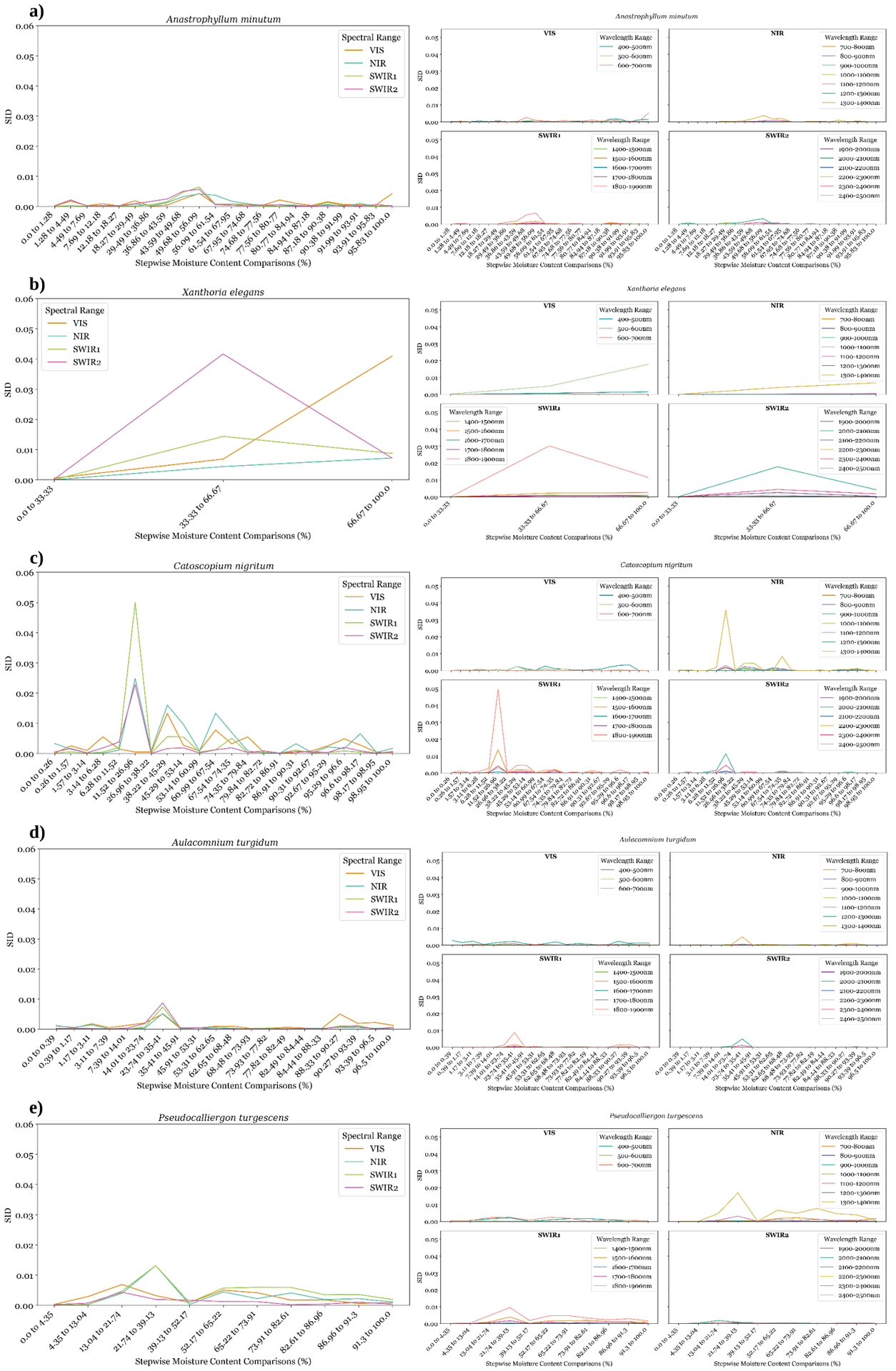

Figure 10: The measure of similarity (SID) in stepwise comparisons of species' spectra across moisture contents (e.g., similarity measure between spectral signature at 100% moisture and spectral signature at 95% moisture) at full spectral ranges (left) and 100nm windows (right) for a) a liverwort (Anastrophyllum minutum), b) a lichen (Xanthoria elegans), c/d) two acrocarpous mosses (c: Catascopium nigritum, d: Aulacomnium turgidum), and e) a pleurocarpous moss: Pseudocalliergon turgescens from complete saturation (100% moisture) to complete desiccation (0% moisture). See Appendix A to view the rest of the within-species SID analyses for species not listed here.

3.1.3. Convex Hull Maxima Points

Plotting the presence and absence of any local maxima or convex hull points in the spectra from saturation to desiccation (Figure 11) shows that all species have unique local maxima at higher moisture points. As moisture is lost, most species start to accumulate more convex hull maxima in the longer wavelengths of the NIR, SWIR1, and SWIR2 ranges, which remain until desiccation. However, for *C. nigritum* in the NIR range, there is a migration of convex hull maxima to the longer NIR wavelengths rather than an accumulation. For example, at 100% saturation, convex hull maxima are present in the 1000-1100nm and 1100-1200nm ranges, but at 0% saturation, convex hull maxima are present in the 1200-1300nm and 1300-1400nm. In the SWIR1 range, all species that do accumulate convex hull maxima have them in the 1800-1900nm, while in the SWIR2 range, the convex hull maxima are accumulated in 2200-2300nm, 2300-2400nm, and 2400-2500nm. However, *A. minutum* mainly has convex hull maxima in the 2400-2500nm for SWIR2. The onset of these convex hull maxima accumulations in each spectral range also varies by moisture level (*A. minutum*: NIR-67.95%, SWIR2-36.86%; *X. elegans*: NIR/SWIR1/SWIR2-66.67%; *C. nigritum*: SWIR-3.14%, SWIR2-11.52%; *A. turgidum*: NIR/SWIR1-23.74%, SWIR2-53.31%; *P. turgescens*: NIR/SWIR2-21.74%, SWIR1-13.04%). Additionally, while most accumulated convex hull maxima persist until desiccation, this is not necessarily the case for all wavelength ranges in all species. To note some exceptions, *A. minutum* does not ever acquire any convex hull maxima in SWIR1 and *X. elegans* has more sporadic convex hull maxima accumulation across the NIR wavelengths.

As a general interpretation, most species see an accumulation of convex hull maxima in the longer wavelengths of the NIR, SWIR1, and SWIR2 ranges, although for some species, namely *C. nigritum*, there is a migration rather than accumulation of convex hull maxima into these longer wavelengths in each spectral range. Furthermore, these convex hull maxima can vary in wavelength location but are mostly similar across the species for SWIR1 and SWIR2, though the onset of convex hull maxima migration or accumulation varies across species by moisture level. Lastly, most of these convex hull maxima do persist until desiccation.

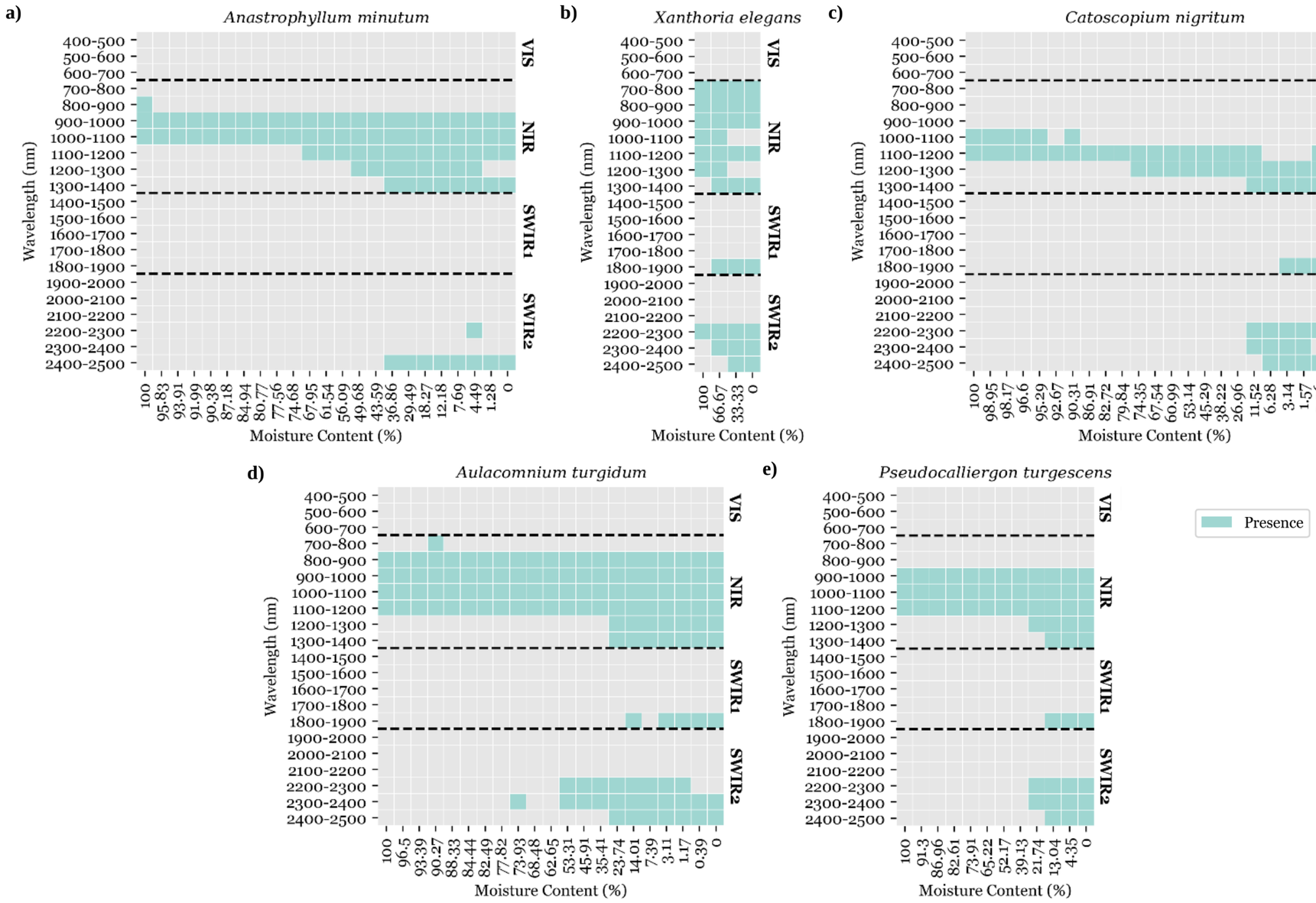

Figure 11: The changing presence of convex hull local maxima points in each 100nm wavelength range of the species' spectra from complete saturation (100% moisture) to complete desiccation (0% moisture) for a) a liverwort (Anastrophyllum minutum), b) a lichen (Xanthoria elegans), c/d) two acrocarpous mosses (c: Catascopium nigritum, d: Aulacomnium turgidum), and e) a pleurocarpous moss: Pseudocalliergon turgescens. See Appendix A to view the other species convex hull point presence plots not listed here.

3.2. Objective 2: Identify a moisture stress threshold at which different species are no longer spectrally distinguishable from one another in VIS/NIR/SWIR wavelength ranges

3.2.1. Convex Hull Maxima Points of Binned Spectra

Comparing all species maxima within my moisture classes (Figure 12), we see that in the NIR, the convex hull maxima never completely match up by wavelength and moisture level, leaving it a spectrally differentiable range. If only looking at the maxima in SWIR1, *A. minutum* never matches up with the other species because it doesn't have any convex maxima, but starting at 10 to 20% moisture, *X. elegans*, *A. turgidum*, and *P. turgescens* would be indistinguishable with their matching maxima at 1800-1900nm, and at 0 to 10% this matching extends to include *C. nigritum*. If only looking at SWIR2 maxima, at 10 to 20% moisture, *X. elegans*, *A. turgidum*, and *P. turgescens* would be indistinguishable with their matching maxima at 2200-2300nm, 2300-2400nm, and 2500nm, and at 0 to 10% this matching extends to include *C. nigritum.*

As a general interpretation, no matter the moisture level, all five species never completely have the same convex hull maxima in the NIR range. However, in the SWIR1 and SWIR2, at 10 to 20% moisture, three of the five species have completely matching convex maxima, and at 0 to 10% moisture this extends to four species being indistinguishable by their maxima. This shows that there is a clear convergence towards an acquiring of the same maxima in the same wavelength regions with drying.

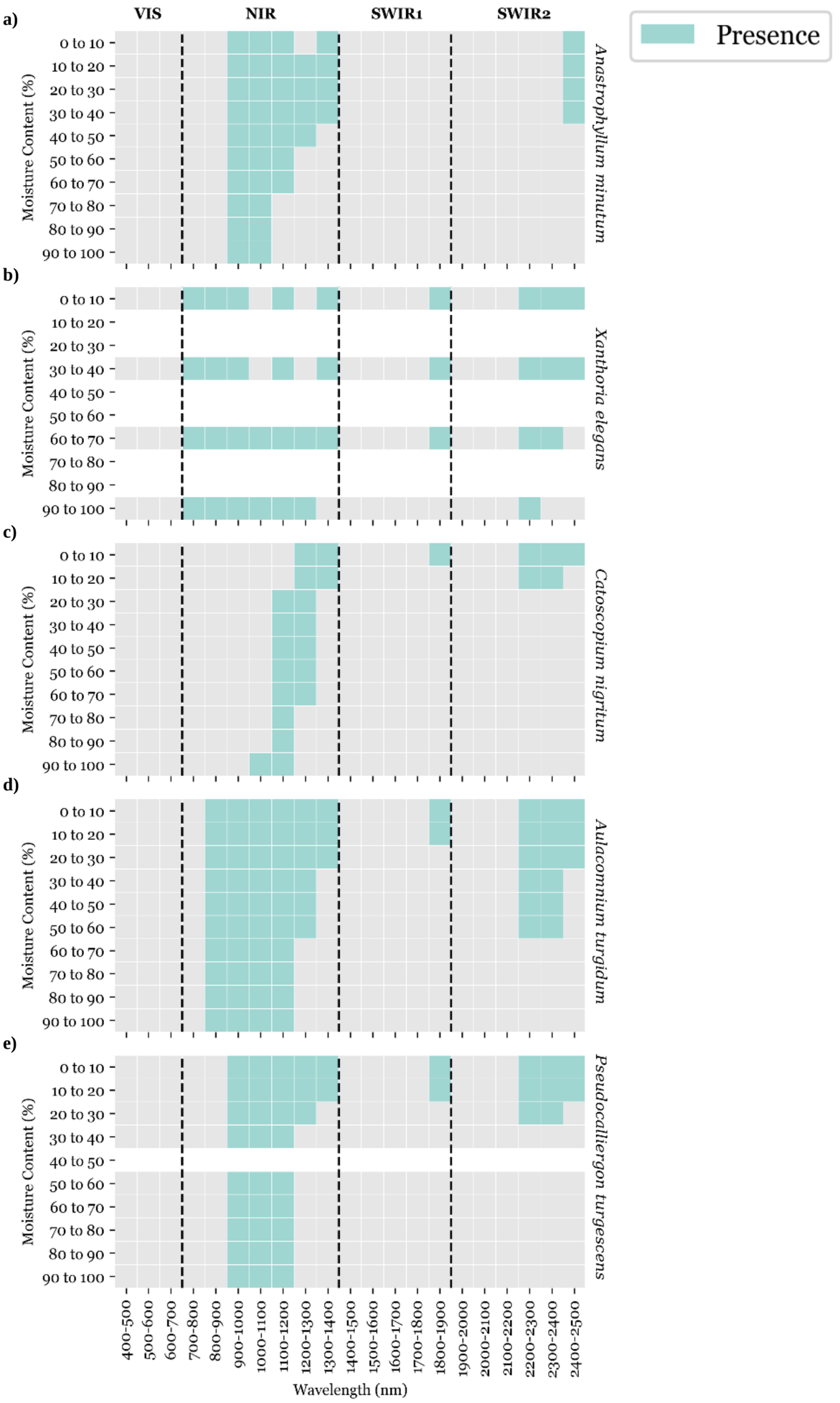

Figure 12: The changing presence of convex hull local maxima points in each 100nm wavelength range of the binned species' spectra from complete saturation (100% moisture) to complete desiccation (0% moisture) for the 5 compared species of a) a liverwort (Anastrophyllum minutum), b) a lichen (Xanthoria elegans), c/d) two acrocarpous mosses (c: Catascopium nigritum, d: Aulacomnium turgidum), and e) a pleurocarpous moss: Pseudocalliergon turgescens. See Appendix A to view all sample binned spectra (none shown here) as well as the other binned convex hull point plots that are not provided here.

3.2.2. Cross-Species SID (Full Spectral Range and 100nm Window) Analyses

3.2.2.1. Boxplots

The full range SID value boxplots for all the species comparisons across the moisture gradients (Figure 13) show that species are most variable in the VIS (Figure 13a) and NIR (Figure 13b) ranges (high SID that have a broad distribution). The SWIR1 (Figure 13c) and SWIR2 (Figure 13d) ranges appear to be less different across species (lower SID values that have a tighter distribution). The 20 to 30% moisture class is particularly interesting in the SWIR1 and SWIR2 ranges, as the majority of comparisons across species are very tight (low SIDs) except for a group of species comparisons.

As a general interpretation, there is no distinct pattern in SIDs between species in the VIS and NIR ranges. This changes in the SWIR ranges, where the level of spectral similarity does vary with moisture, starting at saturation being very similar and increasingly different as moisture is lost. The 40 to 50% moisture bin is an exception, as the spectra briefly become more similar across species, and then, starting at 20 to 30%, the majority of species become spectrally similar again (except for a small group), but from 10 to 20% moisture to desiccation, the distribution is very tight implying species are now spectrally similar in the SWIR1 and SWIR2.

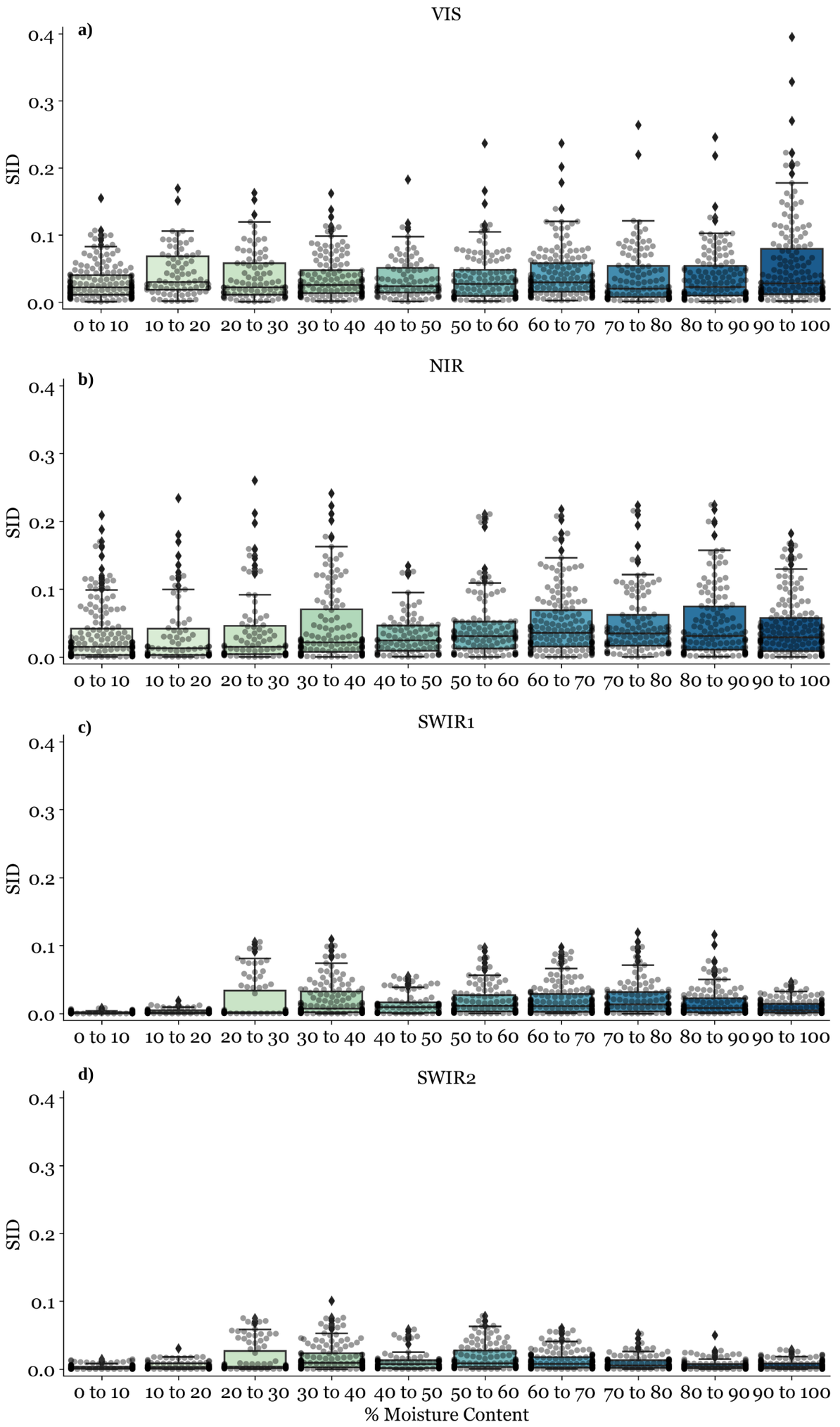

Figure 13: Boxplots of SID values (measure of similarity) between comparisons of species spectra at specific moisture bins in the a) VIS, b) NIR, c) SWIR1, and d) SWIR2 ranges. Each black diamond represents an outlier, which are further analyzed in Figures 15 and 17.

For the 100nm boxplots, the 400-500nm range in the VIS (Figure 14a) has the highest and largest distribution of SID values. 1300-1400nm has the highest and largest distribution of SID values in the NIR (Figure 14b), although these SID values are relatively small. The SWIR1 (Figure 14c) and SWIR2 (Figure 14d) 100nm boxplots have even lower and tighter distributions of SID values, with 1800-1900nm and 2000-2100nm having the highest and largest distribution of SID values in the SWIR1 and SWIR2 ranges, respectively.

The pattern of moisture-related SID distribution changes seen in the full range-boxplots are also seen here, mostly in 1300-1400nm, 1800-1900nm, and 2000-2100nm in which there is much more spectral similarity above 80% and below 20% moisture (and within the 40 to 50% moisture bin).

As a general interpretation, we see the same moisture-related SID distribution changes that were noticeable in the full-range SID boxplots in Figure 13. However, the 100nm boxplots allow us to see that these SID changes are primarily occurring in the 1300-1400nm, 1800-1900nm, and 2000-2100nm wavelength ranges.

.

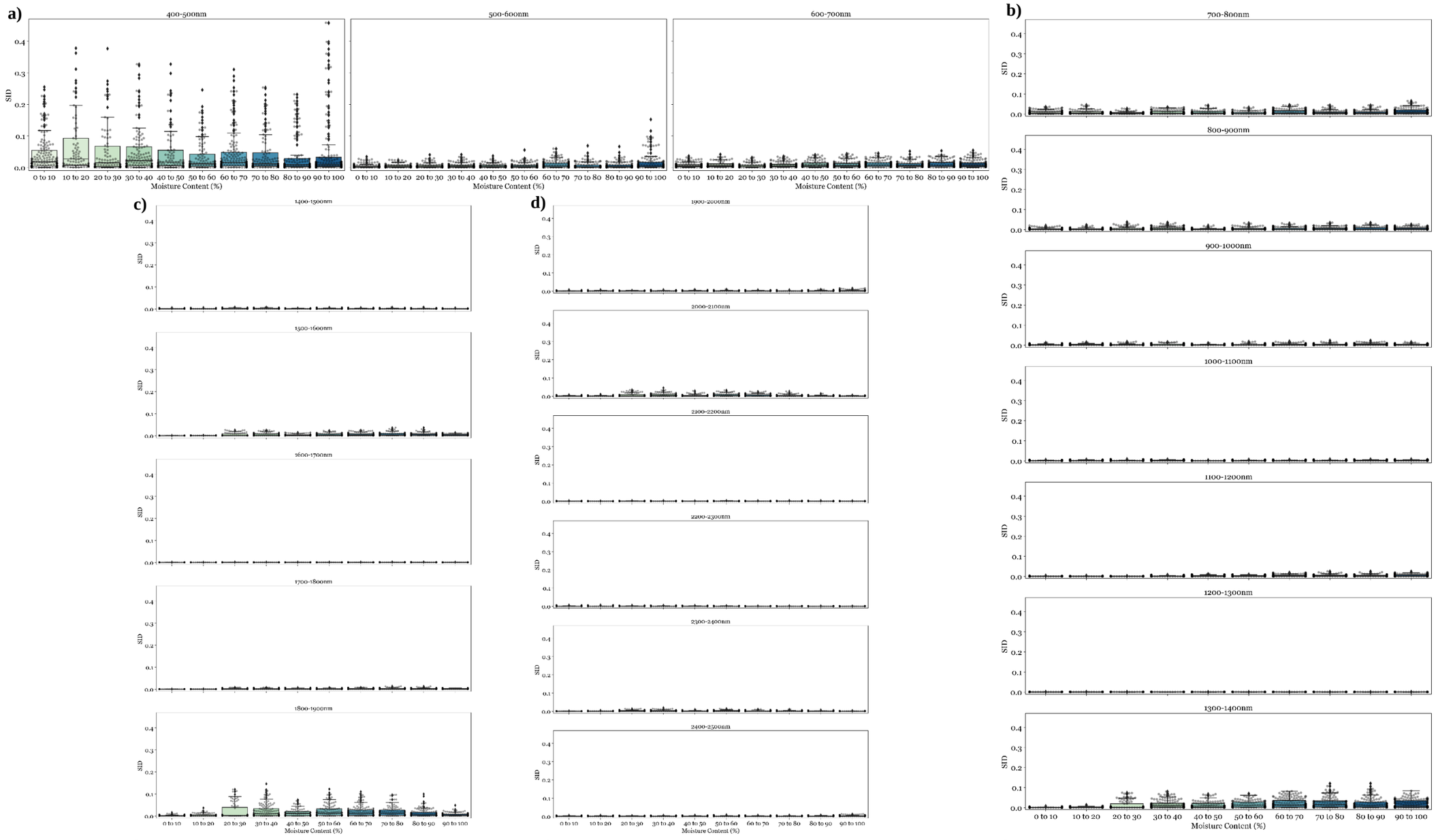

Figure 14: Boxplots of SID values (measure of similarity) between comparisons of species spectra at specific moisture bins in the 100nm windows of the a) VIS, b) NIR, c) SWIR1, and d) SWIR2 ranges. Each black diamond represents an outlier, which are further analyzed in Figures 16 and 18.

3.2.2.2. Outlier Species Frequency

The number of times a species was an outlier ("outlier species frequency" analysis, Figure 15) was calculated for the full range SID species comparison boxplots shown in Figure 13. In the VIS range, the frequency of outliers is small, though *A. minutum* and *F. nivalis* have the most outliers across the moisture range. In the NIR and SWIR1 ranges, *C. nigritum* is the most frequent outlier species, having a higher frequency in the NIR at the higher and lower moisture contents, while in the SWIR1 it has higher frequency in the mid-level moisture points. *P. brevifolium* and *P. turgescens* closely follow as consistent outliers in the SWIR1 range, and while *X. elegans* has the highest outlier frequency of all species in SWIR1, those are only found in the 0 to 10% moisture level. In the SWIR2 range, *C. nigritum*, *P. brevifolium*, and *P. turgescens* follow a similar pattern as in SWIR1, but *A. minutum* also reaches an outlier frequency similar to *C. nigritum* (yet, this is mainly at 0 to 10% moisture).

As a general interpretation, *C. nigritum* appears to be the species that is most consistently an outlier across the spectral ranges, although this is mainly in the NIR, SWIR1, and SWIR2.

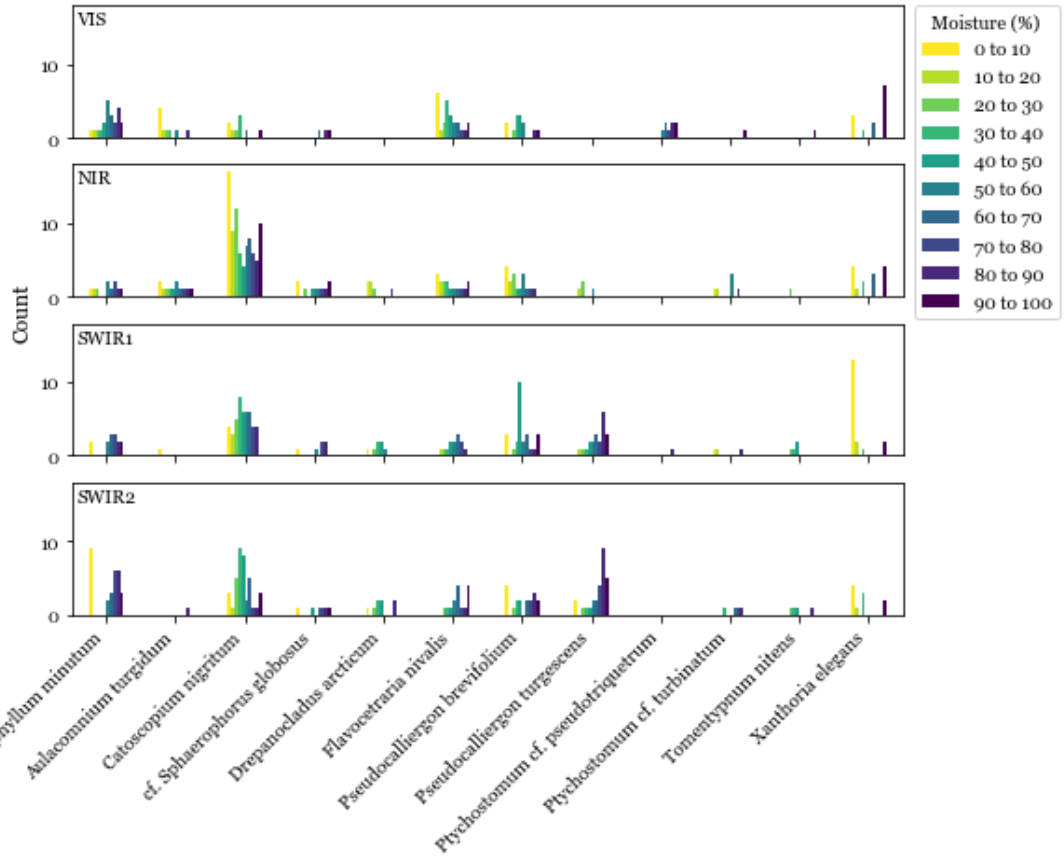

Figure 15: Frequency of a particular species in any comparison that was an outlier in the full range species comparison boxplots (refer to Figure 13) at specific moisture bins for the VIS, NIR, SWIR1, and SWIR2 ranges.

The same analysis, but this time performed on the 100nm window SID species comparison boxplots (Figure 14), also show variable results across the wavelength regions and moisture gradient (Figure 16). In the VIS range (Figure 16a), *A. minutum* and *F. nivalis* are the most consistent outliers (*A. minutum* is high in both 500-600nm and 600-700nm, while *F. nivalis* is high in both 400-500nm and 500-600nm). While all species outlier frequency changes sporadically with moisture, many appear to have higher outlier frequencies at higher moisture levels. In the NIR range (Figure 16b), most species have

low outlier frequencies. *C. nigritum* has the highest frequencies (mainly in 800-900nm, 900-1000nm 1000-1100nm, and 1200-1300nm), although this fluctuates with moisture. In the SWIR1 range (Figure 16c), *C. nigritum* leads the outliers' frequency, followed by *P. brevifolium*, and *P. turgescens* across all the wavelength windows. However, *A. minutum* also has high outlier frequency in the 1400-1500nm and 1600-1700nm ranges, but mostly at lower moisture levels (especially 0 to 10%). In the SWIR2 range (Figure 16d), there is a larger variety of species outliers, with *cf. S. globosus*, *C. nigritum*, *A. minutum, P. brevifolium*, and *P. turgescens* being frequent outliers.

As a general interpretation, the species outlier frequency varies widely, even in 100nm windows, with *C. nigritum* (like in the full range boxplot outlier) being the most common outlier across the NIR, SWIR1, and SWIR2 ranges. Other species that still appear commonly include *A. minutum, P. brevifolium*, and *P. turgescens*, but there is a wide variation of their appearance as outliers in each wavelength window and especially at different moisture levels.

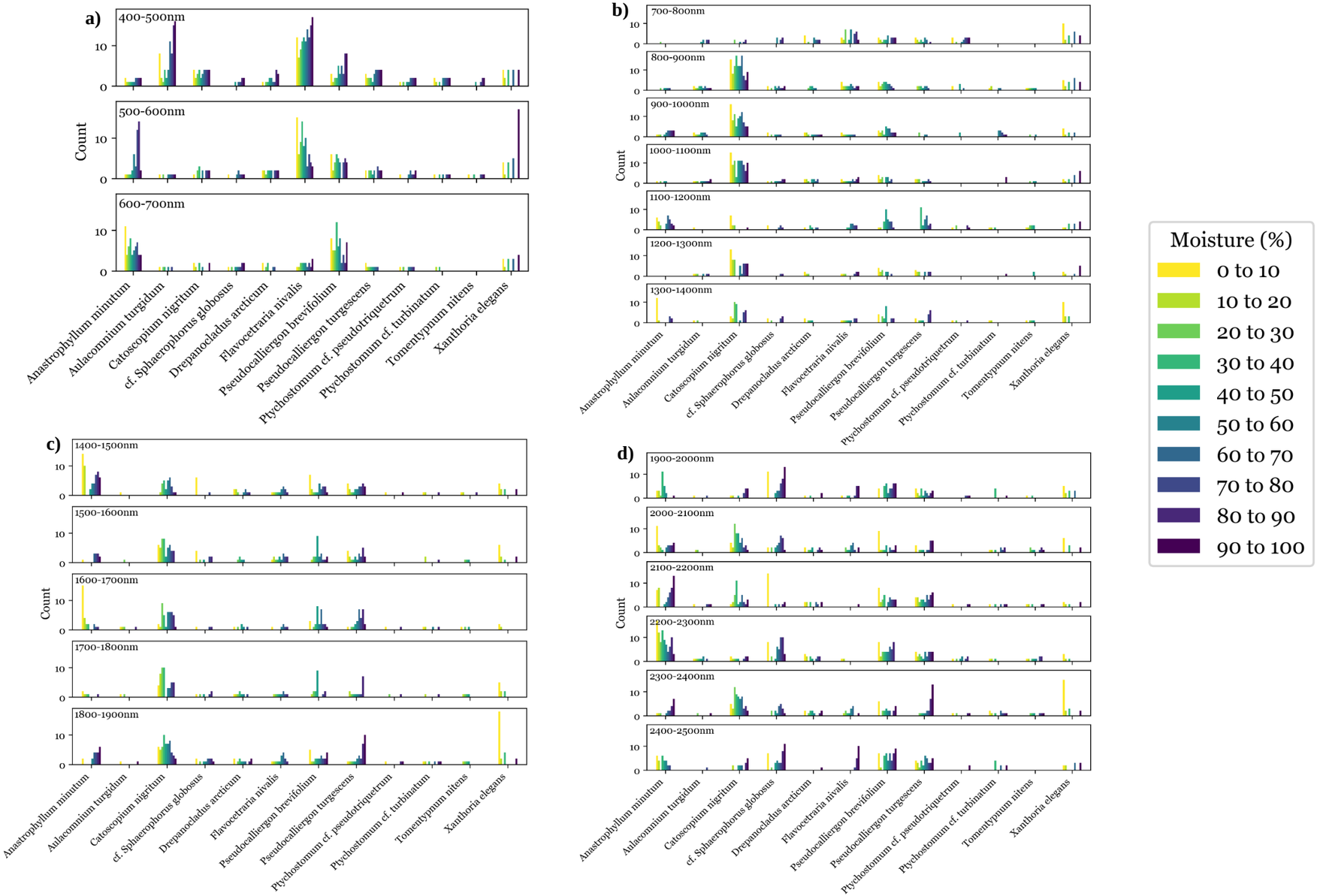

Figure 16: Frequency of a particular species in any comparison that was an outlier in the 100nm window species comparison boxplots (refer to Figure 14) at specific moisture bins for the 100nm windows of the a) VIS, b) NIR, c) SWIR1, and d) SWIR2 ranges.

3.2.2.3. Outlier Comparison Type Frequency

Taking the previous analysis (species outlier frequency) to the next level, here I am looking at the frequency at which the different plant types are outliers (Figure 17). For example, how many times moss vs. lichen comparisons were outliers in the full range SID species comparison boxplots (Figure 13). In the VIS range, the moss vs. lichen comparisons are the most frequent type in the 90 to 100% and 0 to 10% bins. The NIR range however is dominated by moss vs. moss and moss vs. lichen comparisons. In the SWIR1 range, moss vs. moss and moss vs. lichen comparisons are the most frequent outlier types. In the SWIR2, which also has moss vs. moss and moss vs. lichen comparisons as frequent outliers, there is also now moss vs. liverwort comparisons as more frequent outliers, particularly in the 0 to 10% moisture bin.

As a general interpretation, outlier comparison type frequency varies widely across the spectral ranges and moisture bins, but there is a slight pattern, with moss vs. moss and moss vs. lichen being the most common outlier types across all the ranges, with some frequent moss vs. liverwort comparisons as outliers in the SWIR2.

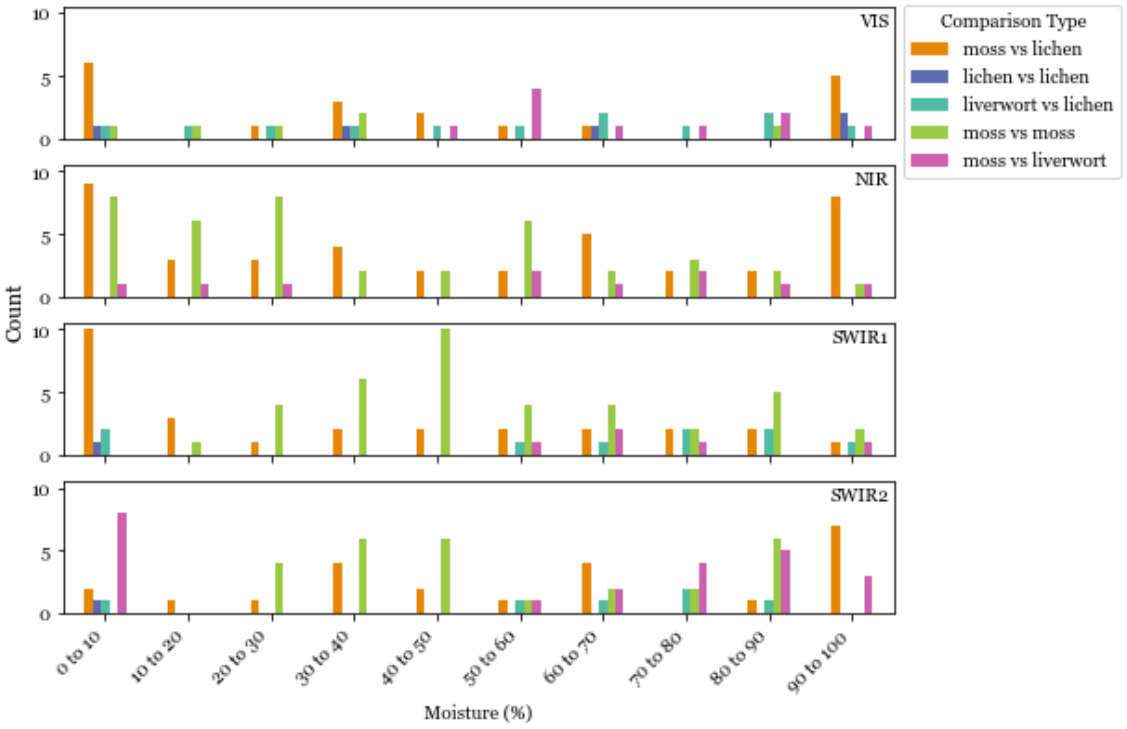

Figure 17: Frequency of the different plant comparison types (e.g., moss vs. lichen, moss vs. liverwort) which were considered outliers in the full range species comparison boxplots (refer to Figure 13) at specific moisture bins for the VIS, NIR, SWIR1, and SWIR2 ranges.

The analysis was repeated on the 100nm SID species comparison boxplots shown in Figure 14. Results show a variety of outlier types and frequencies across the moisture bins and wavelengths (Figure 18). In the VIS range (Figure 18a), 400-500nm and 500-600nm are dominated by moss vs. lichen with some frequent moss vs. moss and moss vs. liverwort comparisons as well (but mainly in the higher moisture bins). In the NIR range (Figure 18b), all wavelengths are dominated by moss vs. moss comparisons and moss vs. lichen comparisons. In the SWIR1 range (Figure 18c), there is a variety of comparison types across all wavelength windows, with (depending on the wavelength) higher

frequencies of moss vs. liverwort, moss vs. moss, and moss vs. lichen comparisons, all of whose frequencies vary across the moisture bins. In the SWIR2 range (Figure 18d), there is also a variety of comparison types, which is dominated by moss vs. liverwort, moss vs. lichen, and moss vs. moss comparisons. Although, the magnitude of these frequencies vary by wavelength range and moisture bin.

As a general interpretation, there are large differences among outlier comparison type frequency when looking at 100nm wavelength ranges, and while most spectral ranges appear to be dominated by moss vs. moss, moss vs. lichen, and moss vs. liverwort comparisons, the magnitude of their dominance does vary across the wavelength windows. Furthermore, moisture causes wide variation of the magnitude of the frequency of these outliers.

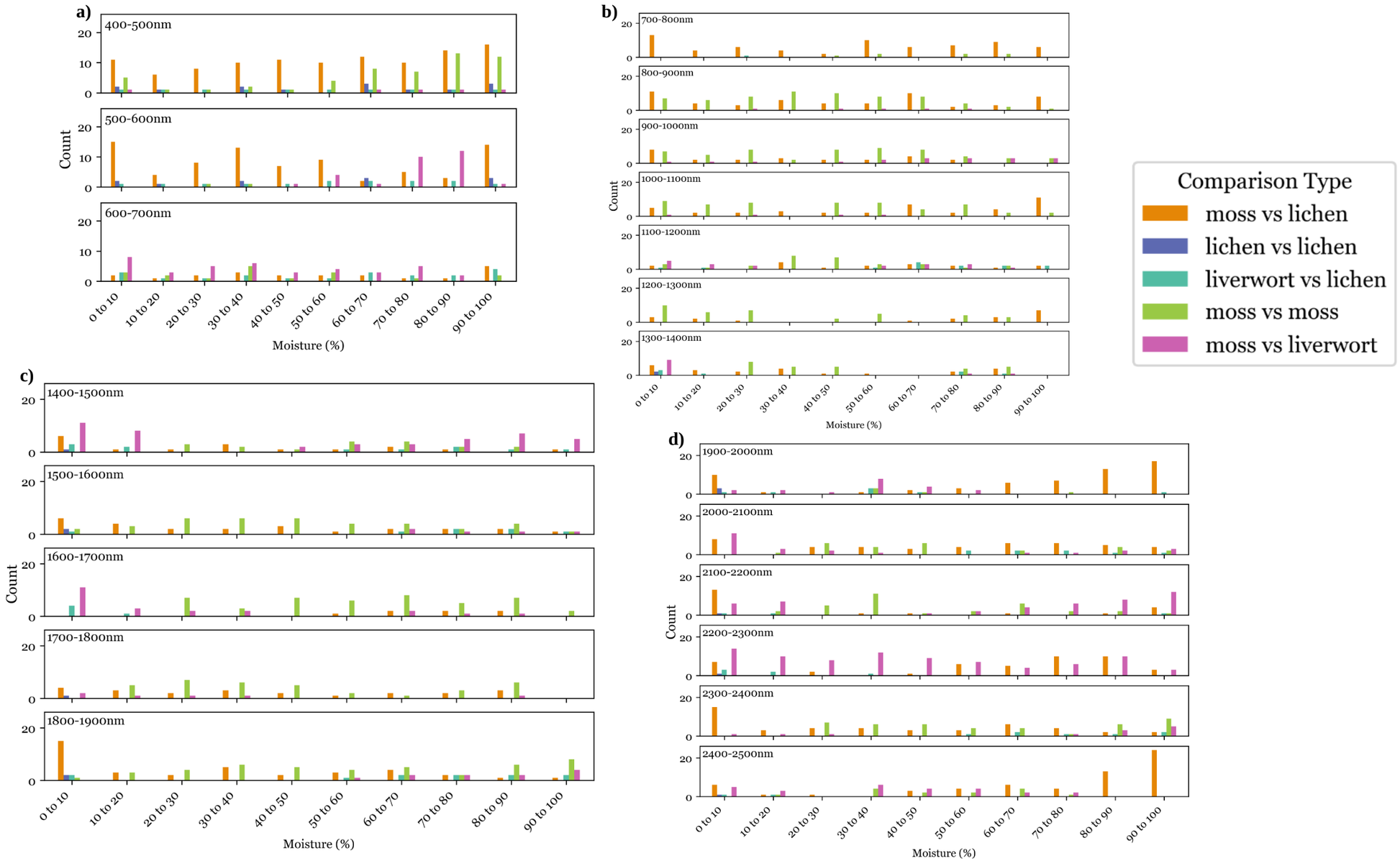

Figure 18: Frequency of the different plant comparison types (e.g., moss vs. lichen, moss vs. liverwort) which were considered outliers in the 100nm window species comparison boxplots (refer to Figure 14) at specific moisture bins for the 100nm windows of the a) VIS, b) NIR, c) SWIR1, and d) SWIR2 range.

4. DISCUSSION

4.1. Species-Specific Spectral Characteristics

All five species displayed unique reflectance characteristics, particularly at higher moisture levels, and particularly in the VIS and NIR ranges. This finding aligns with what is seen in the literature, as Harris et al. (2005) observed the highest differences in moss spectral properties at higher water contents, and many studies on bryophytes (Vogelmann & Moss, 1993; Bubier et al., 1997; Arkimaa et al., 2009; Neta et al., 2010a; Stoy et al., 2012) have observed that there are different spectral properties across different species and taxa in the VIS and NIR ranges. Greater spectral differences in the VIS are likely due to this reflectance being moderated by pigmentation and chlorophyll concentration differences. As for the NIR reflectance, it is moderated by cellular structure, biomass, texture, and shoot/canopy morphology and arrangement. My results showed distinct differences between the lichens and bryophytes in the NIR reflectance range: while the lichen had minimal NIR peaks, the bryophytes had more marked peaks. However, the number, location, and size of the NIR peaks do vary widely between the bryophytes. This likely owes to the variable cellular structure and shoot/canopy biochemical and morphological traits found across bryophyte species, which directly affects the way moisture is retained and incoming radiation is scattered and reflected (Elumeeva et al., 2011; May et al., 2018).

The SWIR1 and SWIR2 reflectance features were much more similar across all the species, since those reflectances are moderated by tissue water content. That said, the

shape and magnitude of reflectance at saturation varied widely, mostly between the lichen and bryophytes. This aligns with what is seen in the literature, as it is noted that reflectance for mosses in the SWIR range is generally lower than for lichens, because moss tissue has a higher water holding capacity than lichen tissue (Neta et al., 2010a; Stoy et al., 2012). This can also differ between bryophytes as well, as different bryophyte species can also have different water retention capacities (Elumeeva et al., 2011; Stoy et al., 2012)

As for the spectral features for each plant type, my results are similar, for the most part, to what is shown in the literature (Nordberg and Allard, 2002; Lovelock and Robinson, 2002; Rees et al., 2004; Van Gaalen et al., 2007; Arkimaa et al., 2009; Neta et al., 2010a; Granlund et al., 2018). That said, a few outstanding differences are worth noting. For example, *X. elegans* (the lichen) exhibited some differences in my study when compared to what has been reported in the literature for the VIS-to-NIR and the SWIR2 ranges. For subarctic crustose lichens, a gradual increase from the VIS to NIR range has previously been documented (Rees et al., 2004); while an increase was observed for *X. elegans*, it does not appear to be gradual. Likewise, a strong spectral structure past 2000nm has previously been documented (Rees et al., 2004), but this was not found in my sample of *X. elegans*. Although *X. elegans* may be treated as a crustose lichen for its rock-encrusting nature, it is a foliose species (Hooker, 1980), which may explain some of these spectral differences; that said, more spectral data for the various subarctic lichen types will be necessary to make stronger conclusions about their spectral properties.

4.1.1. Species Differentiation

My results show that the VIS and NIR are the better spectral ranges for distinguishing species. Indeed, the highest SID values (or highest amounts of spectral differences) and largest distribution of SID values were found within these spectral ranges, meaning that the spectral differences are larger and vary more widely between species in these two ranges. This aligns with what is generally agreed upon in the literature: these ranges tend to more clearly separate species because they are moderated by species-specific features, such as pigment, canopy morphology, or cellular structure (Bubier et al., 1997; Lovelock and Robinson, 2002; Neta et al., 2010a; Granlund et al., 2018). However, Singh and Prabakaran (2015) remark that the SWIR region also could tease apart different species, and while this was not necessarily the case for my study (other than perhaps, separating the lichen and bryophytes), this is still a plausible outcome for species that have very different water retention capacities.

Absorption features can also be useful for distinguishing bryophytes from other plants. Vogelmann and Moss (1993) found that *Sphagnum* had marked water absorption features around 1000nm and 1200nm, unlike typical green vascular vegetation. These absorption features are seen in my bryophytes as well, giving them more pronounced peaks in the NIR range than other (vascular) vegetation. Therefore, these unique water absorption features in the NIR range may be advantageous for teasing apart bryophytes from other plant functional types. They also show potential in distinguishing between bryophyte species, as the shape and depth of these absorption features vary across the

species. For example, *C. nigritum* has a much smaller amplitude and depth in the absorption feature around 1000nm than the other bryophyte species.

4.1.2. Uncertainty in Spectral Measurements

It's important to note that, like in any data, there is a level of uncertainty about the accuracy of the measurements. While precautions were taken to minimize any user or instrument error, there is still a potential for these types of errors to be present in the data. With the resolution of the VNIR being 3nm and SWIR being 8nm, these error ranges should be considered when interpreting specific wavelengths and wavelength ranges. Furthermore, because a majority of the species have never had their spectral measurements reported in the literature, it makes it challenging to compare our spectral results, particularly for the liverwort. Therefore, the measurements collected here serve as a start to a spectral library for these Arctic species, and should be regarded with a degree of caution, until more spectral work is done on these same Arctic species to ensure a higher amount of confidence in their reflectance characteristics.

4.2. Moisture Effects

4.2.1. Species' Spectral Response to Drying

We found that drying impacts each species' characteristic reflectance features, with desiccation bringing clear changes in both the shape and magnitude of the spectra. At higher moisture levels, larger spectral differences were found between the species; this aligns with what is seen in the literature, as Harris et al. (2005) observed the highest

differences in moss spectral properties at higher water contents. My observations of the moisture effects on spectra align well with what many studies (Vogelmann and Moss, 1993; Bryant and Baird et al., 2003; Harris et al., 2005; Van Gaalen et al. 2007; Arkimaa et al., 2009; Neta et al., 2010a; Granlund et al., 2018) in the literature report: at higher moisture levels, we generally see lower reflectance in the VIS, NIR, and SWIR regions, as well as deeper absorption peaks. As drying starts, reflectance generally increases, absorption features weaken, and peaks disappear, change shape, or form (although, just like Granlund et al. (2018) note, I also see that these changes are more minimal in the VIS range). Furthermore, for some species, this general increase in reflectance is not straightforward, with decreasing reflectance at some points; this too has been an observation in the literature for a few studies (Nordberg and Allard, 2002; Rees et al., 2004), yet none have provided a suggestion as to the reasoning behind this, emphasizing that this requires more study and attention. Lastly, even though these general spectral responses to drying occurred for both the bryophytes and lichens, this study also shows these responses are species-specific, and likely driven by canopy branch/leaf architecture differences, which enable some species to better manage decreasing water availability than others, but also these spectral responses are largely driven from unique structural and chemical adaptations in cellular structure to drying and rehydration cycles (Lovelock and Robinson, 2002; Neta et al., 2010a; Granlund et al., 2018; May et al., 2018).

These changes likely occur with drying because, as water is lost (especially reaching sub-optimal points for photosynthesis), a decrease in chlorophyll concentration and an increase in the paleness of the sample might increase the plant reflectance in the

VIS range. As for the NIR range, external and internal water likely decline, changing the cellular structure and shoot/canopy morphology so that there is increased intercellular air space, which increases the scattering and reflection of incoming radiation. In the SWIR range, drying reduces tissue water content, increasing the amount of incident radiation that is scattered throughout the plant and reflected. For example, Granlund et al. (2018) note that when lichens lose water, their cells shrink and create intercellular air spaces that increase the amount of internal scattering of incident radiation, and thereby increase their reflectance. May et al. (2018) suggested that increased reflectance from drying may act as a mechanism to minimize further absorption of irradiance and loss of water by evaporation, and therefore reduce any further cellular damage.

While many moisture-related spectral changes in subarctic bryophytes and lichens have been reported, quantifying the spectral differences between moisture levels is still something absent from the literature. Comparing the spectrum for each moisture level in a stepwise fashion using SID, my results show that most spectral shifts in moisture are fairly gradual for most species, although when getting to the mid to lower end of the moisture gradient, there can be more dramatic changes in spectral shape that cause the SID to jump. The moisture levels at which these dramatic spectral shape changes take place vary widely across the species. For many of the species, dramatic shifts in shape were often observed in 1300-1400nm of the NIR range, 1800-1900nm of the SWIR1 range, and 2000-2100nm of the SWIR2 range. These wavelength windows are close neighboring regions to two major water absorption bands around 1450nm and 1940nm (Jensen, 2007). Granlund et al. (2018) suggest that, as moisture changes, it may directly affect water

absorption band depth and shape, which may cause greater differences in the shape and reflectance of the neighboring wavelength regions. Rees et al. (2004) also suggest that the changing absorption features induced from moisture shifts are likely related to the largest differences between hydrated and dry lichens in the neighboring wavelengths (around 1450nm and 1900nm) of those water absorption features. However, Ager and Milton (1987) do more broadly report that their dry and hydrated lichens had the largest differences between 1100-1900nm.

The convex hull maxima provide another means to evaluate which wavelength regions are impacted by desiccation. In particular, the shape changes in local maxima can be identified and tracked as moisture levels change. As desiccation took place, all species (except *C. nigritum*) had a general accumulation of local maxima towards the longer wavelengths in the NIR, showing that even though NIR peaks appear to flatten in the spectra with a loss of moisture, these peaks still exist. *C. nigritum*, however, with its migration (rather than accumulation) of maxima to the longer NIR wavelengths, shows a different spectral response, implying that this species must have a unique canopy morphology/arrangement and cellular structure. Convex hull maxima also accumulate for most species in the SWIR1 and SWIR2 ranges, with the SWIR1 new local maxima appearing in 1800-1900nm, and in the 2200-2300nm in the SWIR2 range, which continue to accumulate through 2400-2500nm. These maxima points match up closely with where we see new peaks or rises in reflectance. For example, the new accumulation of maxima tends to correspond to the second sharpened peak in SWIR1, the sharpened peak in SWIR2, and the new rise in reflectance in the latter part of the SWIR2.

The fact that these convex hull accumulation or migration changes occur at different moisture loss points is likely due to species-specific water retention capacities and water loss tolerances. The literature has shown that these unique water loss tolerances or water retention capacities are largely moderated by a bryophyte's individual shoot properties as well as colony morphology (Elumeeva et al., 2011). At the shoot-level, this could relate to stem thickness, leaf cell wall thickness, and other shoot trait differences. Canopy-level water content differences can be even larger since external water is more important to the canopy water retention than each individual shoot's symplastic and apoplastic water (Elumeeva et al., 2011). Generally, tightly packed canopies are more capable of retaining water due to the smaller shoot interspaces, and can thus tolerate desiccation better whereas more loosely packed canopies are unable to retain water as strongly and are less tolerant of desiccation (Slate et al., 2019). The lichen *X. elegans* begins to have consistent convex hull changes in the SWIR ranges earliest at 66.67%, which makes sense as lichens would not have the water retention capacities that bryophytes have through their canopy formation as well as typically more spongy tissue. For the bryophytes, *A. turgidum* starts experiencing consistent convex hull changes first in the SWIR ranges at 53.31% moisture, which may be because while the canopy is dense, the shoots were not as tightly packed as in the other species samples. The liverwort *A. minutum* starts convex changes in the SWIR ranges at 36.86% despite appearing to be quite tightly packed, however this could also be from other traits diminishing water retention such as restricted turf height as liverworts are typically smaller in stature. Since *P. turgescens* is the next to begin convex changes in the SWIR ranges at 21.74%, it

suggests that despite having a more loosely packed canopy, this species, with its generally more elongated and densely branched shoots, must be more capable than some of the other bryophytes in retaining its spectral properties until ~20% moisture. *C. nigritum* was the last to experience convex hull changes in the SWIR ranges at 11.52% moisture, which corresponds to the observation that this was an extremely densely packed canopy that clearly was able to retain its water and spectral properties much longer than any of the other species.

4.2.2. Moisture Thresholds

Although the within-species analyses show us that these species have different moisture loss tolerances for desiccation-induced spectral changes, the similar patterns or convergence in the accumulation of their convex maxima leaves it still unaddressed whether at corresponding moisture levels these different species do appear spectrally indistinguishable by their convex maxima. My results do show that at certain moisture bins (particularly those closest to desiccation – 10 to 20% and 0 to 10%), most species do have matching or indistinguishable local maxima in the SWIR1 and SWIR2 wavelengths. While the NIR had some similar trends, none of the convex hull maxima for all the species completely matched from saturation to desiccation. Therefore, it implies that if using SWIR wavelengths to identify maximal regions in the spectra, if these species were below 20% moisture, many would not be spectrally distinguishable from one another. This is likely because of the similar ways that desiccation affects them in the SWIR range. Yet, our results also show this notion may not apply necessarily to all species: for example,

while the liverwort *A. minutum* accumulated convex hull maxima with a loss of moisture, it never reached a point where it had matching or indistinguishable convex hull from any of the other species. Furthermore, many species, based on their NIR local maxima, would appear similar in the NIR range towards desiccation, but they still appear to be spectrally distinguishable.

The SID boxplots, as another perspective on this matter, show that when species are compared, regardless of moisture, they are still widely spectrally different in shape in the VIS and NIR ranges. However, for both the SWIR1 and SWIR2 ranges we see a clear pattern in species' spectral similarity as a function of moisture. Near saturation, species are less spectrally different, and as moisture content starts decreasing (e.g., 70 to 80% moisture), spectral differences increase in amount and range between species. Then, as more moisture is lost, reaching the 40 to 50% moisture bin, spectral similarities between species increase again, with a brief decrease in similarities at 30 to 40%. Lastly, as moisture content decreases to 20 to 30% the majority of species are spectrally similar, except for a small cluster of species comparisons, and then reaching 10 to 20% and 0 to 10% moisture, we see much higher similarities between species spectra.

Therefore, under high (but not the highest) moisture contents, species are more spectrally different from one another. This may align with May et al. (2018)'s observation that moss communities have their highest GPP when at an optimal moisture content of 70-80%. The increase in similarity at 40 to 50% moisture is still something that requires more research to better understand the physiological processes underlying this change; for example the species could be losing moisture here, but then at 30 to 40% are they able to

somehow reacquire or rearrange this moisture (e.g., using capillary action to move moisture) so that they briefly retain their unique spectral properties, until 20 to 30% when the majority are unable to keep this water and become much more spectrally similar again. As for the separate cluster in the 20 to 30% moisture bin, every comparison in this separate group was with *C. nigritum*, which implies that at 20 to 30% moisture this species is still quite spectrally different from other species in both the SWIR1 and SWIR2 ranges. Therefore, moisture clearly does have a role in moderating the amount of spectral differences between species and plant types, although this is mainly in the SWIR wavelengths, as we can see distinct patterns in the spectral similarities with a loss of moisture.

The 100nm boxplots clarify the wavelength windows within which these differences are found. The 400-500nm range has the largest difference within the VIS range. This is likely due to differences with lichens or between lichens and bryophytes. Bubier et al. (1997) point out that lichens commonly have only chlorophyll *a* present in them due to their cyanobacteria, while bryophytes have both chlorophyll *a* and *b*, and so this could explain some of the strong spectral differences seen in the VIS range. This also somewhat aligns with Rees et al. (2004) who found that blue wavelengths (under 450nm) can serve as optimal discrimination of lichen spectra. The 1300-1400nm range in the NIR, the 1800-1900nm range in SWIR1, and the 2000-2100nm range in SWIR2 contain the largest differences within their respective regions. These windows, as mentioned before, may be key areas of spectral changes because they are neighboring wavelength regions to the large water absorption features at this part of the spectra.

It should also be noted that even though there are changes in the spectral similarities between species (with more similarity closer to desiccation), there are marked outliers for each moisture bin. *C. nigritum* was found to be the most common "outlier" species, mainly in the NIR, SWIR1, and SWIR2 ranges, suggesting that this species was the most spectrally different of my samples. This is likely due to a combination of factors relating to its canopy morphological differences as well as shoot anatomy and cellular structure. From direct observation of the samples, *C. nigritum* had a much more low-lying, denser turf than the other samples, and of note, was the only sample to have a small seedling begin growing in its basket towards the latter part of the experiment suggesting that this species was still well-retaining its moisture when other species could not. Furthermore, from the Flora of North America (2007a, 2007b) illustrations of *C. nigritum* and *A. turgidum* (Figure 19), there are apparent differences between their shoot anatomy and cellular structure, suggesting these moss species have quite different internal light interactions.

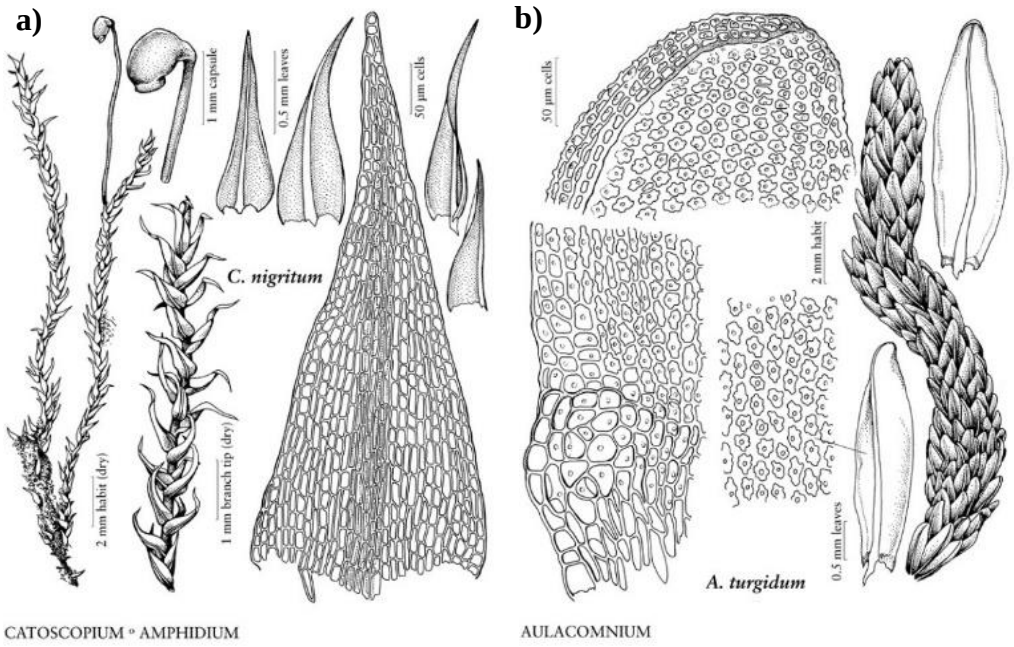

Figure 19: Illustrations of a) C. nigritum and b) A. turgidum shoot anatomy and cellular structure. Reprinted from Flora of North America (2007a, 2007b).

As for the types of plant comparisons themselves, the moss vs. moss and moss vs. lichen were the most common outlier comparison types, with some moss vs. liverwort comparison types also being frequent outliers in the SWIR2 range. This shows that differences in spectra between moss species are to be expected, in addition to differences between mosses, lichens, and liverworts, even when approaching desiccation.

4.3. Implications

4.3.1. Estimating Species Water Content

This study shows the importance of accounting for moisture when using remote sensing, as it clearly affects the spectral properties seen in various species. To estimate

water content in bryophytes and lichens, SWIR has been suggested as the most useful range (Bubier et al., 1997; Rees et al., 2004; Arkimaa et al., 2009; Neta et al., 2010a; Granlund et al., 2018). Moisture is an important feature to assess when using remote sensing to identify and analyze bryophytes, because the plant's canopy/shoot morphological as well as water differences exert the strongest controls on their spectral response (Lovelock & Robinson, 2002; Stoy et al., 2012).

Furthermore, estimating plant moisture status is critical to better estimate their impacts on the ecosystem structure and function (e.g., their ground-surface energy relationships or role in biogeochemical cycles) and overall better monitor these ecosystems in a changing climate. For example, detecting moss moisture status in permafrost ecosystems may help identify areas that flood or dry after thawing, and could be used to detect how these plants evolve throughout the growing season. Achieving a better linkage between non-vascular spectral properties and their physiological processes and traits such as moisture status is still a challenge that has not been resolved; for example, May et al. (2018) found that while GPP more closely followed moisture content changes, there was a disconnect with NDVI, emphasizing that certain indices are not reliable for non-vascular vegetation and that we still need to better identify the spectral responses to water shifts in non-vascular vegetation and assess how to best link these mechanisms with the plant's physiological processes.

4.3.2. Mapping Non-Vascular Vegetation

Another important implication of this study is that it could improve the mapping of non-vascular vegetation, as this high-resolution data at the species-level may be useful to link with airborne/spaceborne imagery to improve the detection and identification of these species or their taxa. A critical problem we have with most remote sensing imagery (UAV being the least problematic) is that it is often too coarse to identify these small plants, especially at the species-level, but these data show what reflectance regions certain species are the most responsive in and how this changes with moisture. These spectral signatures would serve as a more detailed method for estimating water content in various non-vascular species and thereby, could expand the amount of opportunities and use provided by airborne/spaceborne imagery so that there is a more detailed and comprehensive method for monitoring wetland and peatland moisture status.

Furthermore, species identification on the basis of their spectral signatures is important because each species has a unique structural and functional role in the ecosystem, based upon its own unique structural and chemical adaptations to drying and rehydration. This is particularly the case for mosses, which the literature has widely concluded need a more refined identification beyond the plant functional type level since moss species vary so widely in their traits and thus, ecosystem functions. This will also enable for not just a better mapping of the species, but a better mapping of the ecological functions that are driven by these species.

5. CONCLUSION

The results from this study have confirmed that Arctic bryophytes and lichens have distinct and uniquely characteristic reflectance features. As desiccation brings about similar shifts in shape and reflectance magnitude for all species (primarily in the SWIR ranges), moisture does play a key role on the spectral similarity or dissimilarity between different species and plant types. Therefore, moisture does impact the way we are able to detect these species and monitor them through remote sensing. This suggests that when we use remote sensing to identify these plant types from airborne/spaceborne imagery, we must consider the hydrological conditions of the surrounding environment they belong too, as it could affect how their spectra appear. This is particularly important in areas where plants are subjected to lower moisture, because as my result have shown, when close to desiccation, SWIR spectral differences drop drastically between a majority of species (i.e., they become indistinguishable), despite them having unique water retention capacities.

While my results align well with the literature, this research is providing novel hyperspectral work on a series of Arctic mosses, lichens, and liverworts, which have yet to be featured in previously published work. Many of these Arctic bryophyte and lichen species have never had their spectral properties measured and discussed in previously published studies. Therefore, this study contributes a new set of data for these neglected species. This is particularly the case for the liverwort species, with no studies (to my knowledge) that look at the spectral properties of (sub-)Arctic liverworts. Furthermore,

my study provides information on how moisture changes affect the spectral properties of non-vascular vegetation, which may be used to better understand species' hydrological interactions and biophysical changes. Better identifying each species' role in the ecosystem structure will pave a more comprehensive way to estimate and better understand that ecosystem's biogeochemical, hydrological, and surface-energy cycles (Beamish et al., 2020). Lastly, there is yet to be a comprehensive analysis on the spectral differences between moss, lichen, and liverwort spectra in response to moisture stress. Therefore, this research is addressing, for the first time, whether different plant species (or types) are spectrally distinguishable when under moisture stress, which could be potentially transformative in terms of future monitoring efforts, as non-vascular plants could be severely subjected to moisture stress from a warmer and drier climate in the future.

REFERENCES

Acosta, M., R. Juszczak, B. Chojnicki, M. Pavelka, K. Havrankova, J. Lesny, L. Krupkova, M. Urbaniak, K. Machacova, and J. Olejnik. 2017. "CO2 Fluxes from Different Vegetation Communities on a Peatland Ecosystem." *Wetlands* 37 (3): 423-435.

Ager, C. M. and N. M. Milton. 1987. "Spectral Reflectance of Lichens and their Effects on the Reflectance of Rock Substrates." *Geophysics* 52 (7): 898-906.

Allen, J. L., R. T. McMullin, E. A. Tripp, and J. C. Lendemer. 2019. "Lichen Conservation in North America: A Review of Current Practices and Research in Canada and the United States." *Biodiversity and Conservation* 28 (12): 3103-3138.

Anderson, L. E. 1963. "Mosses." *The Bryologist* 66 (3): 107-119.

Andresen, C. G., M. J. Lara, C. E. Tweedie, and V. L. Lougheed. 2017. "Rising Plant-Mediated Methane Emissions from Arctic Wetlands." *Global Change Biology* 23 (3): 1128-1139.

Arkimaa, H., J. Laitinen, R. Korhonen, M. Moisanen, T. Hirvasniemi, and V. Kuosmanen. 2009. "Spectral Reflectance Properties of Sphagnum Moss Species in Finnish Mires." *In 6th EARSeL SIG IS workshop, Imaging Spectroscopy: Innovative tool for scientific and commercial environmental applications,* 16-19.

Aubert, S., C. Juge, A. Boisson, E. Gout, and R. Bligny. 2007. "Metabolic Processes Sustaining the Reviviscence of Lichen Xanthoria Elegans (Link) in High Mountain Environments." *Planta* 226 (5): 1287-1297.

Bannari, A., D. Morin, F. Bonn, and A. R. Huete. 1995. "A Review of Vegetation Indices." *Remote Sensing Reviews* 13 (1-2): 95-120.

Beamish, A., W. Nijland, M. Edwards, N. C. Coops, and G. H. R. Henry. 2016. "Phenology and Vegetation Change Measurements from True Colour Digital Photography in High Arctic Tundra." *Arctic Science* 2 (2): 33-49.

Beamish, A., M. K. Raynolds, H. Epstein, G. V. Frost, M. J. Macander, H. Bergstedt, A. Bartsch, et al. 2020. "Recent Trends and Remaining Challenges for Optical Remote Sensing of Arctic Tundra Vegetation: A Review and Outlook." *Remote Sensing of Environment* 246: 111872.

Bengtsson, F., G. Granath, N. Cronberg, and H. Rydin. 2020. "Mechanisms Behind Species-Specific Water Economy Responses to Water Level Drawdown in Peat Mosses." *Annals of Botany* 126 (2): 219-230.

Beringer, J., A. H. Lynch, F. S. Chapin, M. Mack, and G. B. Bonan. 2001. "The Representation of Arctic Soils in the Land Surface Model: The Importance of Mosses." *Journal of Climate* 14 (15): 3324-3335.

Bokhorst, S. F., J. W. Bjerke, H. Tømmervik, T. V. Callaghan, and G. K. Phoenix. 2009. "Winter Warming Events Damage Sub-Arctic Vegetation: Consistent Evidence from an Experimental Manipulation and a Natural Event." *Journal of Ecology* 97 (6): 1408-1415.

Bowden, W. B., J. M. Glime, and T. Riis. 2007. "CHAPTER 18 - Macrophytes and Bryophytes." In *Methods in Stream Ecology (Second Edition)*, edited by F. R. Hauer and G. A. Lamberti, 381-406. San Diego: Academic Press.

Bratsch, S. N., H. E. Epstein, M. Buchhorn, and D. A. Walker. 2016. "Differentiating among Four Arctic Tundra Plant Communities at Ivotuk, Alaska using Field Spectroscopy." *Remote Sensing* 8 (1): 51.

Bridgham, S. D., J. P. Megonigal, J. K. Keller, N. B. Bliss, and C. Trettin. 2006. "The Carbon Balance of North American Wetlands." *Wetlands* 26 (4): 889-916.

Brodo, I. M., S. D. Sharnoff, and S. Sharnoff. 2001. *Lichens of North America.* Yale University Press.

Brown, J., O. Ferrians, J. A. Heginbottom, and E. Melnikov. 2002. "Circum-Arctic Map of Permafrost and Ground-Ice Conditions, Version 2." *NSIDC: National Snow and Ice Data Center*.

Bubier, J. and T. Moore. 1994. "An Ecological Perspective on Methane Emissions from Northern Wetlands." *Trends in Ecology & Evolution* 9 (12): 460-464.

Bubier, J., T. Moore, and S. Juggins. 1995. "Predicting Methane Emission from Bryophyte Distribution in Northern Canadian Peatlands." *Ecology* 76 (3): 677-693.

Bubier, J., B. Rock, and P. Crill. 1997. "Spectral Reflectance Measurements of Boreal Wetland and Forest Mosses." *Journal of Geophysical Research-Atmospheres* 102 (D24): 29483-29494.

Buchhorn, M., D. Walker, B. Heim, M. K. Raynolds, H. Epstein, and M. Schwieder. 2013. "Ground-Based Hyperspectral Characterization of Alaska Tundra Vegetation Along Environmental Gradients." *Remote Sensing* 5: 3971-4005.

Burkett, V. and J. Kusler. 2000. "Climate Change: Potential Impacts and Interactions in Wetlands of the United States." *Journal of the American Water Resources Association* 36 (2): 313-320.

Callaghan, T. V., M. Johansson, R. D. Brown, P. Y. Groisman, N. Labba, V. Radionov, R. G. Barry, et al. 2011. "The Changing Face of Arctic Snow Cover: A Synthesis of Observed and Projected Changes." *Ambio* 40: 17-31.

Carmack, E. C., M. Yamamoto-Kawai, T. W. N. Haine, S. Bacon, B. A. Bluhm, C. Lique, H. Melling, et al. 2016. "Freshwater and its Role in the Arctic Marine System: Sources, Disposition, Storage, Export, and Physical and Biogeochemical Consequences in the Arctic and Global Oceans." *Journal of Geophysical Research-Biogeosciences* 121 (3): 675-717.

Carriqui, M., M. Roig-Oliver, T. J. Brodribb, R. Coopman, W. Gill, K. Mark, U. Niinemets, et al. 2019. "Anatomical Constraints to Nonstomatal Diffusion Conductance and Photosynthesis in Lycophytes and Bryophytes." *New Phytologist* 222 (3): 1256-1270.

Cerrejón, C., O. Valeria, N. Mansuy, M. Barbé, and N. J. Fenton. 2020. "Predictive Mapping of Bryophyte Richness Patterns in Boreal Forests using Species Distribution Models and Remote Sensing Data." *Ecological Indicators* 119: 106826.

Chang, C. 2000. "An Information-Theoretic Approach to Spectral Variability, Similarity, and Discrimination for Hyperspectral Image Analysis." *IEEE Transactions on Information Theory* 46 (5): 1927-1932.

Chang, C. 2003. "Hyperspectral Measures for Spectral Characterization." In *Hyperspectral Imaging: Techniques for Spectral Detection and Classification*, edited by C. Chang, 15-35. Boston, MA: Springer US.

Charman, D. J., D. W. Beilman, M. Blaauw, R. K. Booth, S. Brewer, F. M. Chambers, J. A. Christen, et al. 2013. "Climate-Related Changes in Peatland Carbon Accumulation during the Last Millennium." *Biogeosciences* 10 (2): 929-944.

Chaudhary, N., S. Westermann, S. Lamba, N. Shurpali, B. K. Sannel, G. Schurgers, P. A. Miller, and B. Smith. 2020. "Modelling Past and Future Peatland Carbon Dynamics Across the Pan-Arctic." *Global Change Biology* 26 (7): 4119-4133.

Choudhary, S., A. Blaud, A. M. Osborn, M. C. Press, and G. K. Phoenix. 2016. "Nitrogen Accumulation and Partitioning in a High Arctic Tundra Ecosystem from Extreme Atmospheric N Deposition Events." *Science of the Total Environment* 554-555: 303-310.

Clark, R. N. and T. L. Roush. 1984. "Reflectance Spectroscopy: Quantitative Analysis Techniques for Remote Sensing Applications." *Journal of Geophysical Research: Solid Earth* 89: 6329-6340.

Coffer, M. M. and E. L. Hestir. 2019. "Variability in Trends and Indicators of CO2 Exchange Across Arctic Wetlands." *Journal of Geophysical Research-Biogeosciences* 124 (5): 1248-1264.

Cornelissen, J. H., S. I. Lang, N. A. Soudzilovskaia, and H. J. During. 2007. "Comparative Cryptogam Ecology: A Review of Bryophyte and Lichen Traits that Drive Biogeochemistry." *Annals of Botany* 99 (5): 987-1001.

Cowan, I. R., O. L. Lange, and T. G. A. Green. 1992. "Carbon-Dioxide Exchange in Lichens: Determination of Transport and Carboxylation Characteristics." *Planta* 187 (2): 282-294.

Crandall-Stotler, B. and S. E. Bartholomew-Began. 2007. "Morphology of Mosses (Phylum Bryophyta)." In *Flora of North America: Bryophytes: Mosses*, edited by Flora of North America Editorial Committee. Vol. 27. New York and Oxford: Oxford University Press.

Davidson, S. J., M. J. Santos, V. L. Sloan, J. D. Watts, G. K. Phoenix, W. C. Oechel, and D. Zona. 2016. "Mapping Arctic Tundra Vegetation Communities using Field Spectroscopy and Multispectral Satellite Data in North Alaska, USA." *Remote Sensing* 8 (12): 978.

Davis, E., A. Trant, L. Hermanutz, R. G. Way, A. G. Lewkowicz, L. S. Collier, A. Cuerrier, and D. Whitaker. 2020. "Plant–Environment Interactions in the Low Arctic Torngat Mountains of Labrador." *Ecosystems*.

Dennison, P. E., Y. Qi, S. K. Meerdink, R. Kokaly, D. R. Thompson, C. S. T. Daughtry, M. Quemada, et al. 2019. "Comparison of Methods for Modeling Fractional Cover using Simulated Satellite Hyperspectral Imager Spectra." *Remote Sensing* 11 (18).

Díaz, S. and M. Cabido. 2001. "Vive La Différence: Plant Functional Diversity Matters to Ecosystem Processes." *Trends in Ecology & Evolution* 16 (11): 646-655.

Eckstein, R. L. and P. S. Karlsson. 1999. "Recycling of Nitrogen among Segments of Hylocomium Splendens as Compared with Polytrichum Commune: Implications for Clonal Integration in an Ectohydric Bryophyte." *Oikos* 86 (1): 87-96.

Elmendorf, S. C., G. H. R. Henry, R. D. Hollister, R. G. Bjork, A. D. Bjorkman, T. V. Callaghan, L. S. Collier, et al. 2012. "Global Assessment of Experimental Climate

Warming on Tundra Vegetation: Heterogeneity Over Space and Time." *Ecology Letters* 15 (2): 164-175.

Elumeeva, T. G., N. A. Soudzilovskaia, H. J. During, and J. H. C. Cornelissen. 2011. "The Importance of Colony Structure Versus Shoot Morphology for the Water Balance of 22 Subarctic Bryophyte Species." *Journal of Vegetation Science* 22 (1): 152-164.

Epting, J., D. Verbyla, and B. Sorbel. 2005. "Evaluation of Remotely Sensed Indices for Assessing Burn Severity in Interior Alaska using Landsat TM and ETM+." *Remote Sensing of Environment* 96 (3): 328-339.

Esau, I., V. V. Miles, R. Davy, M. W. Miles, and A. Kurchatova. 2016. "Trends in Normalized Difference Vegetation Index (NDVI) Associated with Urban Development in Northern West Siberia." *Atmospheric Chemistry and Physics* 16 (15): 9563-9577.

Esseen, P., K. Renhorn, and R. B. Pettersson. 1996. "Epiphytic Lichen Biomass in Managed and Old-Growth Boreal Forests: Effect of Branch Quality." *Ecological Applications* 6 (1): 228-238.

Fisher, J. B., D. J. Hayes, C. R. Schwalm, D. N. Huntzinger, E. Stofferahn, K. Schaefer, Y. Luo, et al. 2018. "Missing Pieces to Modeling the Arctic-Boreal Puzzle." *Environmental Research Letters* 13 (2): 020202.

Flora of North America. 2007a. *Bryophyta, Part 1.* Flora of North America: North of Mexico., edited by Flora of North America Editorial Committee. Vol. 27 New York and Oxford.

Flora of North America. 2007b. *Bryophyta, Part 2.* Flora of North America: North of Mexico., edited by Flora of North America Editorial Committee. Vol. 28 New York and Oxford.

Fraser, R. H., T. C. Lantz, I. Olthof, S. V. Kokelj, and R. A. Sims. 2014. "Warming-Induced Shrub Expansion and Lichen Decline in the Western Canadian Arctic." *Ecosystems* 17 (7): 1151-1168.

Frolking, S., N. Roulet, and J. Fuglestvedt. 2006. "How Northern Peatlands Influence the Earth's Radiative Budget: Sustained Methane Emission Versus Sustained Carbon Sequestration." *Journal of Geophysical Research: Biogeosciences* 111.

Gallego-Sala, A., D. J. Charman, S. Brewer, S. E. Page, I. C. Prentice, P. Friedlingstein, S. Moreton, et al. 2018. "Latitudinal Limits to the Predicted Increase of the Peatland Carbon Sink with Warming." *Nature Climate Change* 8 (10): 907-913.

Gates, D. M., H. J. Keegan, J. C. Schleter, and V. R. Weidner. 1965. "Spectral Properties of Plants." *Applied Optics* 4 (1): 11-20.

Goffinet, B. and A. J. Shaw. 2009. *Bryophyte Biology.* 2nd ed. Cambridge University Press.

Gorham, E. 1991. "Northern Peatlands - Role in the Carbon-Cycle and Probable Responses to Climatic Warming." *Ecological Applications* 1 (2): 182-195.

Grace, M. 1995. "A Key to the Growthforms of Mosses and Liverworts and Guide to their Educational Value." *Journal of Biological Education* 29 (4): 272-278.

Granlund, L., S. Keski-Saari, T. Kumpula, E. Oksanen, and M. Keinänen. 2018. "Imaging Lichen Water Content with Visible to Mid-Wave Infrared (400–5500 nm) Spectroscopy." *Remote Sensing of Environment* 216: 301-310.

Green, T. and O. Lange. 1995. "Photosynthesis in Poikilohydric Plants: A Comparison of Lichens and Bryophytes." In *Ecophysiology of Photosynthesis*, edited by M. Caldwell and E. Schulze, 319-341. Berlin, Heidelberg: Springer.

Griffin-Nolan, R., A. Zelehowsky, J. G. Hamilton, and P. J. Melcher. 2018. "Green Light Drives Photosynthesis in Mosses." *Journal of Bryology* 40 (4): 342-349.

Guyot, G., F. Baret, and S. Jacquemoud. 1992. "Imaging Spectroscopy for Vegetation Studies." In *Imaging Spectroscopy: Fundamentals and Prospective Applications*, edited by F. Toselli and J. Bodechtel. Vol. 2, 145-165. Netherlands: Springer.

Haig, D. 2016. "Living Together and Living Apart: The Sexual Lives of Bryophytes." *Philosophical Transactions of the Royal Society B: Biological Sciences* 371 (1706): 20150535.

Hallingbäck, T. and N. Hodgetts. 2000. *Mosses, Liverworts, and Hornworts : Status Survey and Conservation Action Plan for Bryophytes.* IUCN/SSC Action Plans for the Conservation of Biological Diversity. Gland: IUCN.

Harris, A., R. G. Bryant, and A. J. Baird. 2005. "Detecting Near-Surface Moisture Stress in Sphagnum Spp." *Remote Sensing of Environment* 97 (3): 371-381.

Harris, A. and R. G. Bryant. 2009. "A Multi-Scale Remote Sensing Approach for Monitoring Northern Peatland Hydrology: Present Possibilities and Future Challenges." *Journal of Environmental Management* 90 (7): 2178-2188.

Hartard, B., M. Cuntz, C. Maguas, and M. Lakatos. 2009. "Water Isotopes in Desiccating Lichens." *Planta* 231 (1): 179-193.

Hayward, P. M. and R. S. Clymo. 1982. "Profiles of Water-Content and Pore-Size in Sphagnum and Peat, and their Relation to Peat Bog Ecology." *Proceedings of the Royal Society Series B-Biological Sciences* 215 (1200): 299-325.

He, X., K. S. He, and J. Hyvonen. 2016. "Will Bryophytes Survive in a Warming World?" *Perspectives in Plant Ecology Evolution and Systematics* 19: 49-60.

Heffernan, L., C. Estop-Aragonés, K. Knorr, J. Talbot, and D. Olefeldt. 2020. "Long-Term Impacts of Permafrost Thaw on Carbon Storage in Peatlands: Deep Losses Offset by Surficial Accumulation." *Journal of Geophysical Research: Biogeosciences* 125 (3): e2019JG005501.

Hillman, A. C. and S. E. Nielsen. 2020. "Quantification of Lichen Cover and Biomass using Field Data, Airborne Laser Scanning and High Spatial Resolution Optical Data-A Case Study from a Canadian Boreal Pine Forest." *Forests* 11 (6).

Hinzman, L. D., N. D. Bettez, W. R. Bolton, F. S. Chapin, M. B. Dyurgerov, C. L. Fastie, B. Griffith, et al. 2005. "Evidence and Implications of Recent Climate Change in Northern Alaska and Other Arctic Regions." *Climatic Change* 72 (3): 251-298.

Hogrefe, K. R., V. P. Patil, D. R. Ruthrauff, B. W. Meixell, M. E. Budde, J. W. Hupp, and D. H. Ward. 2017. *Normalized Difference Vegetation Index as an Estimator for Abundance and Quality of Avian Herbivore Forage in Arctic Alaska.* Vol. 9.

Honegger, R. 1993. "Developmental Biology of Lichens." *New Phytologist* 125 (4): 659-677.

Hooker, T. N. 1980. "Factors affecting the growth of Antarctic crustose lichens." *British Antarctic Survey Bulletin* 50: 1-19.

Hu, S., Z. Niu, Y. Chen, L. Li, and H. Zhang. 2017. "Global Wetlands: Potential Distribution, Wetland Loss, and Status." *Science of the Total Environment* 586: 319-327.

Huemmrich, K. F., J. A. Gamon, C. E. Tweedie, S. F. Oberbauer, G. Kinoshita, S. Houston, A. Kuchy, et al. 2010. "Remote Sensing of Tundra Gross Ecosystem Productivity and Light use Efficiency Under Varying Temperature and Moisture Conditions." *Remote Sensing of Environment* 114 (3): 481-489.

Huemmrich, K. F., J. A. Gamon, C. E. Tweedie, P. K. E. Campbell, D. R. Landis, and E. M. Middleton. 2013. "Arctic Tundra Vegetation Functional Types Based on Photosynthetic Physiology and Optical Properties." *Ieee Journal of Selected Topics in Applied Earth Observations and Remote Sensing* 6 (2): 265-275.

Hugelius, G., J. Loisel, S. Chadburn, R. B. Jackson, M. Jones, G. MacDonald, M. Marushchak, et al. 2020. "Large Stocks of Peatland Carbon and Nitrogen are Vulnerable to Permafrost Thaw." *Proc Natl Acad Sci USA* 117 (34): 20438.

Jensen, J. R. 2007. *Remote Sensing of the Environment.* 2nd ed. New Jersey: Pearson Prentice Hall.

Jia, G., H. E. Epstein, and D. A. Walker. 2003. "Greening of Arctic Alaska, 1981-2001." *Geophysical Research Letters* 30 (20): 2067.

Joly, K., R. R. Jandt, and D. R. Klein. 2009. "Decrease of Lichens in Arctic Ecosystems: The Role of Wildfire, Caribou, Reindeer, Competition and Climate in North-Western Alaska." *Polar Research* 28 (3): 433-442.

Jones, M. C. and Z. Yu. 2010. "Rapid Deglacial and Early Holocene Expansion of Peatlands in Alaska." *Proc Natl Acad Sci USA* 107 (16): 7347.

Jorgenson, M. T. and G. Grosse. 2016. "Remote Sensing of Landscape Change in Permafrost Regions." *Permafrost and Periglacial Processes* 27 (4): 324-338.

Koffi, E. N., P. Bergamaschi, R. Alkama, and A. Cescatti. 2020. "An Observation-Constrained Assessment of the Climate Sensitivity and Future Trajectories of Wetland Methane Emissions." *Science Advances* 6 (15): eaay4444.

Kokelj, S. V., T. C. Lantz, J. Tunnicliffe, R. Segal, and D. Lacelle. 2017. "Climate-Driven Thaw of Permafrost Preserved Glacial Landscapes, Northwestern Canada." *Geology* 45 (4): 371-374.

Kottek, M., J. Grieser, C. Beck, B. Rudolf, and F. Rubel. 2006. "World Map of the Koppen-Geiger Climate Classification Updated." *Meteorologische Zeitschrift* 15 (3): 259-263.

Kurz, W. A., C. C. Dymond, G. Stinson, G. J. Rampley, E. T. Neilson, A. L. Carroll, T. Ebata, and L. Safranyik. 2008. "Mountain Pine Beetle and Forest Carbon Feedback to Climate Change." *Nature* 452 (7190): 987-990.

Kwan, C., B. Ayhan, G. Chen, J. Wang, B. Ji, and C. Chang. 2006. "A Novel Approach for Spectral Unmixing, Classification, and Concentration Estimation of Chemical and Biological Agents." *IEEE Transactions on Geoscience and Remote Sensing* 44 (2): 409-419.

Laaka-Lindberg, S., H. Korpelainen, and M. Pohjamo. 2003. "Dispersal of Asexual Propagules in Bryophytes." *The Journal of the Hattori Botanical Laboratory* 93: 319-330.

Lai, D. Y. F. 2009. "Methane Dynamics in Northern Peatlands: A Review." *Pedosphere* 19 (4): 409-421.

Laidler, G. J. and P. Treitz. 2003. "Biophysical Remote Sensing of Arctic Environments." *Progress in Physical Geography: Earth and Environment* 27 (1): 44-68.

Laidler, G. J., P. Treitz, and D. M. Atkinson. 2008. "Remote Sensing of Arctic Vegetation: Relations between the NDVI, Spatial Resolution and Vegetation Cover on Boothia Peninsula, Nunavut." *Arctic* 61 (1): 1-13.

Lakatos, M. 2011. "Lichens and Bryophytes: Habitats and Species." In *Plant Desiccation Tolerance*, edited by U. Lüttge, E. Beck and D. Bartels, 65-87. Berlin, Heidelberg: Springer Berlin Heidelberg.

Langford, Z. L., J. Kumar, F. M. Hoffman, A. L. Breen, and C. M. Iversen. 2019. "Arctic Vegetation Mapping using Unsupervised Training Datasets and Convolutional Neural Networks." *Remote Sensing* 11 (1): 69.

Lees, K. J., T. Quaife, R. R. E. Artz, M. Khomik, and J. M. Clark. 2018. "Potential for using Remote Sensing to Estimate Carbon Fluxes Across Northern Peatlands - A Review." *Science of the Total Environment* 615: 857-874.

Lefsky, M. A., W. B. Cohen, G. G. Parker, and D. J. Harding. 2002. "Lidar Remote Sensing for Ecosystem Studies: Lidar, an Emerging Remote Sensing Technology that Directly Measures the Three-Dimensional Distribution of Plant Canopies, can Accurately Estimate Vegetation Structural Attributes and should be of Particular Interest to Forest, Landscape, and Global Ecologists." *Bioscience* 52 (1): 19-30.

Lewis, L. R., S. M. Ickert-Bond, E. M. Biersma, P. Convey, B. Goffinet, K. Hassel, H. Kruijer, et al. 2017. "Future Directions and Priorities for Arctic Bryophyte Research." *Arctic Science* 3 (3): 475-497.

Lewkowicz, A. G. and R. G. Way. 2019. "Extremes of Summer Climate Trigger Thousands of Thermokarst Landslides in a High Arctic Environment." *Nature Communications* 10 (1): 1329.

Liljedahl, A. K., J. Boike, R. P. Daanen, A. N. Fedorov, G. V. Frost, G. Grosse, L. D. Hinzman, et al. 2016. "Pan-Arctic Ice-Wedge Degradation in Warming Permafrost and its Influence on Tundra Hydrology." *Nature Geoscience* 9 (4): 312-+.

Lindo, Z., M. Nilsson, and M. J. Gundale. 2013. "Bryophyte-Cyanobacteria Associations as Regulators of the Northern Latitude Carbon Balance in Response to Global Change." *Global Change Biology* 19 (7): 2022-2035.

Liu, J., J. A. Curry, H. Wang, M. Song, and R. M. Horton. 2012. "Impact of Declining Arctic Sea Ice on Winter Snowfall." *Proceedings of the National Academy of Sciences of the United States of America* 109 (11): 4074-4079.

Llano, G. A. 1956. "Utilization of Lichens in the Arctic and Subarctic." *Economic Botany* 10 (4): 367-392.

Loboda, T. V., E. E. Hoy, and M. L. Carroll. 2019. *ABoVE: Study Domain and Standard Reference Grids, Version 2.* Oak Ridge, Tennessee, USA.: ORNL Distributed Active Archive Center.

Loisel, J. and Z. Yu. 2013. "Recent Acceleration of Carbon Accumulation in a Boreal Peatland, South Central Alaska." *Journal of Geophysical Research-Biogeosciences* 118 (1): 41-53.

Loisel, J., Z. Yu, D. W. Beilman, P. Camill, J. Alm, M. J. Amesbury, D. Anderson, et al. 2014. "A Database and Synthesis of Northern Peatland Soil Properties and Holocene Carbon and Nitrogen Accumulation." *Holocene* 24 (9): 1028-1042.

Loisel, J., A. Gallego-Sala, M. J. Amesbury, G. Magnan, G. Anshari, D. W. Beilman, J. C. Benavides, et al. 2020. "Expert Assessment of Future Vulnerability of the Global Peatland Carbon Sink." *Nature Climate Change*.

Longton, R. E. 1982. "Bryophyte Vegetation in Polar Regions." In *Bryophyte Ecology*, edited by A. J. E. Smith, 123-165. Dordrecht: Springer Netherlands.

Longton, R. E. 1988. *The Biology of Polar Bryophytes and Lichens.* New York: Cambridge University Press.

Longton, R. E. 1997. "The Role of Bryophytes and Lichens in Polar Ecosystems." In *Ecology of Arctic Environments: 13th Special Symposium of the British Ecological Society*, edited by S. J. Woodin and M. Marquiss. Vol. 13, 69-96. New York: Cambridge University Press.

Loranty, M. M., W. Lieberman-Cribbin, L. T. Berner, S. M. Natali, S. J. Goetz, H. D. Alexander, and A. L. Kholodov. 2016. "Spatial Variation in Vegetation Productivity Trends, Fire Disturbance, and Soil Carbon Across Arctic-Boreal Permafrost Ecosystems." *Environmental Research Letters* 11 (9): 095008.

Lovelock, C. E. and S. A. Robinson. 2002. "Surface Reflectance Properties of Antarctic Moss and their Relationship to Plant Species, Pigment Composition and Photosynthetic Function." *Plant, Cell & Environment* 25 (10): 1239-1250.

Luus, K. A., R. Commane, N. C. Parazoo, J. Benmergui, E. S. Euskirchen, C. Frankenberg, J. Joiner, et al. 2017. "Tundra Photosynthesis Captured by Satellite-Observed Solar-Induced Chlorophyll Fluorescence." *Geophysical Research Letters* 44 (3): 1564-1573.

Macander, M. J., G. V. Frost, P. R. Nelson, and C. S. Swingley. 2017. "Regional Quantitative Cover Mapping of Tundra Plant Functional Types in Arctic Alaska." *Remote Sensing* 9 (10): 1024.

Mack, M. C., M. Bret-Harte, T. N. Hollingsworth, R. R. Jandt, E. A. G. Schuur, G. R. Shaver, and D. L. Verbyla. 2011. "Carbon Loss from an Unprecedented Arctic Tundra Wildfire." *Nature* 475 (7357): 489-492.

Mägdefrau, K. 1982. "Life-Forms of Bryophytes." In *Bryophyte Ecology*, edited by A. J. E. Smith, 45-58. Dordrecht: Springer Netherlands.

Malenovský, Z., A. Lucieer, D. H. King, J. D. Turnbull, and S. A. Robinson. 2017. "Unmanned Aircraft System Advances Health Mapping of Fragile Polar Vegetation." *Methods in Ecology and Evolution* 8 (12): 1842-1857.

Manevski, K., M. Jabloun, M. Gupta, and C. Kalaitzidis. 2017. "Chapter 6 - Field-Scale Sensitivity of Vegetation Discrimination to Hyperspectral Reflectance and Coupled Statistics." In *Sensitivity Analysis in Earth Observation Modelling*, edited by G. P. Petropoulos and P. K. Srivastava, 103-121: Elsevier.

Martinez, I., A. Escudero, F. T. Maestre, A. de la Cruz, C. Guerrero, and A. Rubio. 2006. "Small-Scale Patterns of Abundance of Mosses and Lichens Forming Biological Soil Crusts in Two Semi-Arid Gypsum Environments." *Australian Journal of Botany* 54 (4): 339-348.

Matos, P., L. Geiser, A. Hardman, D. Glavich, P. Pinho, A. Nunes, A. Soares, and C. Branquinho. 2017. "Tracking Global Change using Lichen Diversity: Towards a Global-Scale Ecological Indicator." *Methods in Ecology and Evolution* 8 (7): 788-798.

May, J. L., T. Parker, S. Unger, and S. F. Oberbauer. 2018. "Short Term Changes in Moisture Content Drive Strong Changes in Normalized Difference Vegetation Index and Gross Primary Productivity in Four Arctic Moss Communities." *Remote Sensing of Environment* 212: 114-120.

McGuire, A. D., F. S. Chapin III, J. E. Walsh, and C. Wirth. 2006. "Integrated Regional Changes in Arctic Climate Feedbacks: Implications for the Global Climate System." *Annual Review of Environment and Resources* 31: 61-91.

Michel, P., I. J. Payton, W. G. Lee, and H. J. During. 2013. "Impact of Disturbance on Above-Ground Water Storage Capacity of Bryophytes in New Zealand Indigenous Tussock Grassland Ecosystems." *New Zealand Journal of Ecology* 37 (1): 114-126.

Miller, P. A. and B. Smith. 2012. "Modelling Tundra Vegetation Response to Recent Arctic Warming." *Ambio* 41 (3): 281-291.

Minayeva, T., A. Sirin, P. Kershaw, and O. Bragg. 2018. "Arctic Peatlands." In *The Wetland Book: II: Distribution, Description, and Conservation*, edited by C. M. Finlayson, G. R. Milton, R. C. Prentice and N. C. Davidson, 275-288. Dordrecht: Springer Netherlands.

Mitsch, W. J. and J. G. Gosselink. 2007. *Wetlands.* 4th ed. John Wiley & Sons.

Mitsch, W. J. and J. G. Gosselink. 2015. *Wetlands.* 5th ed. Wiley.

Moor, H., H. Rydin, K. Hylander, M. B. Nilsson, R. Lindborg, and J. Norberg. 2017. "Towards a Trait-Based Ecology of Wetland Vegetation." *Journal of Ecology* 105 (6): 1623-1635.

Myers-Smith, I. H., J. T. Kerby, G. K. Phoenix, J. W. Bjerke, H. E. Epstein, J. J. Assmann, C. John, et al. 2020. "Complexity Revealed in the Greening of the Arctic." *Nature Climate Change* 10 (2): 106-117.

Nash, T. H. 1996. *Lichen Biology.* Cambridge University Press.

Neta, T., Q. Cheng, R. L. Bello, and B. Hu. 2010a. "Lichens and Mosses Moisture Content Assessment through High-Spectral Resolution Remote Sensing Technology: A Case Study of the Hudson Bay Lowlands, Canada." *Hydrological Processes* 24 (18): 2617-2628.

Neta, T., Q. Cheng, R. L. Bello, and B. Hu. 2010b. "Upscaling Reflectance Information of Lichens and Mosses using a Singularity Index: A Case Study of the Hudson Bay Lowlands, Canada." *Biogeosciences* 7 (8): 2557-2565.

Niinemets, U. and M. Tobias. 2014. "Scaling Light Harvesting from Moss ``Leaves" to Canopies." In *Photosynthesis in Bryophytes and Early Land Plants*, edited by D. T. Hanson and S. K. Rice. Vol. 37, 151-171. Dordrecht, Netherlands: Springer.

Nitze, I., G. Grosse, B. M. Jones, V. E. Romanovsky, and J. Boike. 2018. "Remote Sensing Quantifies Widespread Abundance of Permafrost Region Disturbances Across the Arctic and Subarctic." *Nature Communications* 9 (1): 5423-3.

Nordberg, M. and A. Allard. 2002. "A Remote Sensing Methodology for Monitoring Lichen Cover." *Canadian Journal of Remote Sensing* 28 (2): 262-274.

Odland, A., S. A. Sundstøl, and D. K. Bjerketvedt. 2018. "Alpine Lichen-Dominated Heaths: Ecology, Effects of Reindeer Grazing, and Climate Change. A Review." *Oecologia Montana* 27 (2).

Palmqvist, K. 2000. "Tansley Review no. 117. Carbon Economy in Lichens." *The New Phytologist* 148 (1): 11-36.

Peckham, S. D., D. E. Ahl, and S. T. Gower. 2009. "Bryophyte Cover Estimation in a Boreal Black Spruce Forest using Airborne Lidar and Multispectral Sensors." *Remote Sensing of Environment* 113 (6): 1127-1132.

Petrescu, A. M. R., L. P. H. van Beek, J. van Huissteden, C. Prigent, T. Sachs, C. A. R. Corradi, F. J. W. Parmentier, and A. J. Dolman. 2010. "Modeling Regional to Global CH4 Emissions of Boreal and Arctic Wetlands." *Global Biogeochemical Cycles* 24 (4).

Petzold, D. E. and S. N. Goward. 1988. "Reflectance Spectra of Subarctic Lichens." *Remote Sensing of Environment* 24 (3): 481-492.

Philben, M., L. Zhang, Z. Yang, N. Taş, S. D. Wullschleger, D. E. Graham, and B. Gu. 2020. "Anaerobic Respiration Pathways and Response to Increased Substrate Availability of Arctic Wetland Soils." *Environmental Science Processes & Impacts* 22 (10): 2070-2083.

Ponomarenko, S., D. McLennan, D. Pouliot, and J. Wagner. 2019. "High Resolution Mapping of Tundra Ecosystems on Victoria Island, Nunavut – Application of a Standardized Terrestrial Ecosystem Classification." *Canadian Journal of Remote Sensing* 45 (5): 551-571.

Pope, R. 2016. *Mosses, Liverworts, and Hornworts: A Field Guide to Common Bryophytes of the Northeast.* Comstock Publishing Associates.

Porada, P., A. Ekici, and C. Beer. 2016. "Effects of Bryophyte and Lichen Cover on Permafrost Soil Temperature at Large Scale." *Cryosphere* 10 (5): 2291-2315.

Post, E., R. B. Alley, T. R. Christensen, M. Macias-Fauria, B. C. Forbes, M. N. Gooseff, A. Iler, et al. 2019. "The Polar Regions in a 2 Degrees C Warmer World." *Science Advances* 5 (12): eaaw9883.

Potvin, L. R., E. S. Kane, R. A. Chimner, R. K. Kolka, and E. A. Lilleskov. 2015. "Effects of Water Table Position and Plant Functional Group on Plant Community,

Aboveground Production, and Peat Properties in a Peatland Mesocosm Experiment (PEATcosm)." *Plant and Soil* 387 (1): 277-294.

Proctor, M. 1982. "Physiological Ecology: Water Relations, Light and Temperature Responses, Carbon Balance." In *Bryophyte Ecology*, edited by A. Smith, 333-381. Dordrecht, Netherlands: Springer.

Proctor, M., Z. Nagy, Z. Csintalan, and Z. Takacs. 1998. "Water-Content Components in Bryophytes: Analysis of Pressure-Volume Relationships." *Journal of Experimental Botany* 49 (328): 1845-1854.

Proctor, M. 1999. "Water-Relations Parameters of some Bryophytes Evaluated by Thermocouple Psychrometry." *Journal of Bryology* 21: 263-270.

Proctor, M. 2000a. "The Bryophyte Paradox: Tolerance of Desiccation, Evasion of Drought." *Plant Ecology* 151 (1): 41-49.

Proctor, M. 2000b. "Physiological Ecology." In *Bryophyte Biology*, edited by A. Jonathan Shaw and Bernard Goffinet, 225-247. Cambridge: Cambridge University Press.

Proctor, M. and Z. Tuba. 2002. "Poikilohydry and Homoihydry: Antithesis Or Spectrum of Possibilities?" *New Phytologist* 156 (3): 327-349.

Proctor, M., M. Oliver, A. Wood, A. Peter, L. Stark, N. Cleavitt, and B. Mishler. 2007. "Invited Review: Desiccation-Tolerance in Bryophytes: A Review." *The Bryologist* 110 (4): 595-621.

Raynolds, M. K., D. A. Walker, H. E. Epstein, J. E. Pinzon, and C. J. Tucker. 2012. "A New Estimate of Tundra-Biome Phytomass from Trans-Arctic Field Data and AVHRR NDVI." *Remote Sensing Letters* 3 (5): 403-411.

Rees, W. G., O. V. Tutubalina, and E. I. Golubeva. 2004. "Reflectance Spectra of Subarctic Lichens between 400 and 2400 Nm." *Remote Sensing of Environment* 90 (3): 281-292.

Reski, R. 2018. "Quantitative Moss Cell Biology." *Current Opinion in Plant Biology; Cell Biology* 46: 39-47.

Riedel, S. M., H. E. Epstein, and D. A. Walker. 2005. "Biotic Controls Over Spectral Reflectance of Arctic Tundra Vegetation." *International Journal of Remote Sensing* 26 (11): 2391-2405.

Roos, R. E., K. van Zuijlen, T. Birkemoe, K. Klanderud, S. I. Lang, S. Bokhorst, D. A. Wardle, and J. Asplund. 2019. "Contrasting Drivers of Community-Level Trait Variation for Vascular Plants, Lichens and Bryophytes Across an Elevational Gradient." *Functional Ecology* 33 (12): 2430-2446.

Rydin, H. and J. K. Jeglum. 2006. *The Biology of Peatlands.* Oxford, UK: Oxford University Press.

Saunois, M., A. R. Stavert, B. Poulter, P. Bousquet, J. G. Canadell, R. B. Jackson, P. A. Raymond, et al. 2020. "The Global Methane Budget 2000--2017." *Earth System Science Data* 12 (3): 1561-1623.

Schuur, E. A. G., J. Bockheim, J. G. Canadell, E. Euskirchen, C. B. Field, S. V. Goryachkin, S. Hagemann, et al. 2008. "Vulnerability of Permafrost Carbon to Climate Change: Implications for the Global Carbon Cycle." *Bioscience* 58 (8): 701-714.

Schuur, E. A. G. and B. Abbott. 2011. "High Risk of Permafrost Thaw." *Nature* 480 (7375): 32-33.

Schuur, E. A. G., A. D. McGuire, C. Schädel, G. Grosse, J. W. Harden, D. J. Hayes, G. Hugelius, et al. 2015. "Climate Change and the Permafrost Carbon Feedback." *Nature* 520 (7546): 171-179.

Schuur, E. A. G. and M. C. Mack. 2018. "Ecological Response to Permafrost Thaw and Consequences for Local and Global Ecosystem Services." *Annual Review of Ecology, Evolution, and Systematics* 49 (1): 279-301.

Serreze, M. C. and R. G. Barry. 2014. *The Arctic Climate System.* 2nd ed. Cambridge: Cambridge University Press.

Shaw, J. and K. Renzaglia. 2004. "Phylogeny and Diversification of Bryophytes." *American Journal of Botany* 91 (10): 1557-1581.

Siewert, M. B. and J. Olofsson. 2020. "Scale-Dependency of Arctic Ecosystem Properties Revealed by UAV." *Environmental Research Letters* 15 (9).

Sim, T. G., G. T. Swindles, P. J. Morris, M. Galka, D. Mullan, and J. M. Galloway. 2019. "Pathways for Ecological Change in Canadian High Arctic Wetlands Under Rapid Twentieth Century Warming." *Geophysical Research Letters* 46 (9): 4726-4737.

Singh, C. P. and C. Prabakaran. 2015. "Reflectance Spectra of High-Altitude Lichens Based on in Situ Measurements." In *Recent Advances in Lichenology*, edited by D. Upreti, P. Divakar, V. Shukla and R. Bajpai, 181-188. New Delhi: Springer.

Slate, M. L., B. W. Sullivan, and R. M. Callaway. 2019. "Desiccation and Rehydration of Mosses Greatly Increases Resource Fluxes that Alter Soil Carbon and Nitrogen Cycling." *Journal of Ecology* 107 (4): 1767-1778.

Snelgar, W. P. and T. G. A. Green. 1980. "Carbon Dioxide Exchange in Lichens: Low Carbon Dioxide Compensation Levels and Lack of Apparent Photorespiratory Activity in some Lichens." *The Bryologist* 83 (4): 505-507.

Song, X., F. M. Hoffman, C. M. Iversen, Y. Yin, J. Kumar, C. Ma, and X. Xu. 2017. "Significant Inconsistency of Vegetation Carbon Density in CMIP5 Earth System Models Against Observational Data." *Journal of Geophysical Research: Biogeosciences* 122 (9): 2282-2297.

Stow, D. A., A. Hope, A. D. McGuire, D. Verbyla, J. Gamon, F. Huemmrich, S. Houston, et al. 2004. "Remote Sensing of Vegetation and Land-Cover Change in Arctic Tundra Ecosystems." *Remote Sensing of Environment* 89 (3): 281-308.

Stoy, P. C., L. E. Street, A. V. Johnson, A. Prieto-Blanco, and S. A. Ewing. 2012. "Temperature, Heat Flux, and Reflectance of Common Subarctic Mosses and Lichens Under Field Conditions: Might Changes to Community Composition Impact Climate-Relevant Surface Fluxes?" *Arctic, Antarctic, and Alpine Research* 44 (4): 500-508.

Street, L. E., P. C. Stoy, M. Sommerkorn, B. J. Fletcher, V. L. Sloan, T. C. Hill, and M. Williams. 2012. "Seasonal Bryophyte Productivity in the Sub-Arctic: A Comparison with Vascular Plants." *Functional Ecology* 26 (2): 365-378.

Tape, K., M. Sturm, and C. Racine. 2006. "The Evidence for Shrub Expansion in Northern Alaska and the Pan-Arctic." *Global Change Biology* 12 (4): 686-702.

Tarnocai, C. 2009. "The Impact of Climate Change on Canadian Peatlands." *Canadian Water Resources Journal* 34 (4): 453-466.

Thenkabail, P. S., R. B. Smith, and E. D. Pauw. 2000. "Hyperspectral Vegetation Indices and their Relationships with Agricultural Crop Characteristics." *Remote Sensing of Environment* 71 (2): 158-182.

Tilman, D., J. Knops, D. Wedin, P. Reich, M. Ritchie, and E. Siemann. 1997. "The Influence of Functional Diversity and Composition on Ecosystem Processes." *Science* 277 (5330): 1300.

Treat, C. C., T. Kleinen, N. Broothaerts, A. S. Dalton, R. Dommain, T. A. Douglas, J. Z. Drexler, et al. 2019. "Widespread Global Peatland Establishment and Persistence Over the Last 130,000 Y." *Proceedings of the National Academy of Sciences of the United States of America* 116 (11): 4822-4827.

Turetsky, M. R. 2003. "The Role of Bryophytes in Carbon and Nitrogen Cycling." *The Bryologist* 106 (3): 395-409.

Turetsky, M. R., M. C. Mack, T. N. Hollingsworth, and J. W. Harden. 2010. "The Role of Mosses in Ecosystem Succession and Function in Alaska's Boreal forestThis Article is One of a Selection of Papers from the Dynamics of Change in Alaska's Boreal Forests: Resilience and Vulnerability in Response to Climate Warming." *Canadian Journal of Forest Research* 40 (7): 1237-1264.

Turetsky, M. R., B. Bond-Lamberty, E. Euskirchen, J. Talbot, S. Frolking, A. D. McGuire, and E-S Tuittila. 2012. "The Resilience and Functional Role of Moss in Boreal and Arctic Ecosystems." *New Phytologist* 196 (1): 49-67.

Turetsky, M. R., B. W. Abbott, M. C. Jones, K. W. Anthony, D. Olefeldt, E. A. G. Schuur, G. Grosse, et al. 2020. "Carbon Release through Abrupt Permafrost Thaw." *Nature Geoscience* 13 (2): 138-143.

Ustin, S. L., D. Riaño, and E. R. Hunt. 2012. "Estimating Canopy Water Content from Spectroscopy." *Israel Journal of Plant Sciences* 60 (1-2): 9-23.

van Breemen, N. 1995. "How Sphagnum Bogs Down Other Plants." *Trends in Ecology & Evolution* 10 (7): 270-275.

Van Gaalen, K. E., L. B. Flanagan, and D. R. Peddle. 2007. "Photosynthesis, Chlorophyll Fluorescence and Spectral Reflectance in Sphagnum Moss at Varying Water Contents." *Oecologia* 153 (1): 19-28.

van Huissteden, J. and A. J. Dolman. 2012. "Soil Carbon in the Arctic and the Permafrost Carbon Feedback." *Current Opinion in Environmental Sustainability* 4 (5): 545-551.

Vierling, L. A., D. W. Deering, and T. F. Eck. 1997. "Differences in Arctic Tundra Vegetation Type and Phenology as seen using Bidirectional Radiometry in the Early Growing Season." *Remote Sensing of Environment* 60 (1): 71-82.

Vitt, D. H. 2006. "Functional Characteristics and Indicators of Boreal Peatlands." In *Boreal Peatland Ecosystems*, edited by R. K. Wieder and D. H. Vitt, 9-24. Berlin, Heidelberg: Springer Berlin Heidelberg.

Vitt, D. H. 2007. "Estimating Moss and Lichen Ground Layer Net Primary Production in Tundra, Peatlands, and Forests." In *Principles and Standards for Measuring Primary Production*, edited by T. Fahey and A. Knapp. New York: Oxford University Press.

Vogelmann, J. E. and D. M. Moss. 1993. "Spectral Reflectance Measurements in the Genus Sphagnum." *Remote Sensing of Environment* 45 (3): 273-279.

Waite, M. and L. Sack. 2010. "How does Moss Photosynthesis Relate to Leaf and Canopy Structure? Trait Relationships for 10 Hawaiian Species of Contrasting Light Habitats." *New Phytologist* 185 (1): 156-172.

Walker, D. A., M. K. Raynolds, F. J. A. Daniëls, E. Einarsson, A. Elvebakk, W. A. Gould, A. E. Katenin, et al. 2005. "The Circumpolar Arctic Vegetation Map." *Journal of Vegetation Science* 16 (3): 267-282.

Washburn, A. L. 1947. *Reconnaissance Geology of Portions of Victoria Island and Adjacent Regions, Arctic Canada.* Geological Society of America.

Westergaard-Nielsen, A., M. Lund, S. H. Pedersen, N. M. Schmidt, S. Klosterman, J. Abermann, and B. U. Hansen. 2017. "Transitions in High-Arctic Vegetation Growth Patterns and Ecosystem Productivity Tracked with Automated Cameras from 2000 to 2013." *Ambio* 46 (1): 39-52.

White, J. R., R. D. Shannon, J. F. Weltzin, J. Pastor, and S. D. Bridgham. 2008. "Effects of Soil Warming and Drying on Methane Cycling in a Northern Peatland Mesocosm Study." *Journal of Geophysical Research-Biogeosciences* 113: G00A06.

Wikström, N., X. He-Nygrén, and A. Shaw. 2009. "Liverworts (Marchantiophyta)." In *The Timetree of Life*, edited by S. B. Hedges and S. Kumar, 146-152. New York: Oxford University Press.

Williams, M., R. Bell, L. Spadavecchia, L. E. Street, and M. T. Van Wijk. 2008. "Upscaling Leaf Area Index in an Arctic Landscape through Multiscale Observations." *Global Change Biology* 14 (7): 1517-1530.

Winkler, A. J., R. B. Myneni, G. A. Alexandrov, and V. Brovkin. 2019. "Earth System Models Underestimate Carbon Fixation by Plants in the High Latitudes." *Nature Communications* 10 (1): 885.

Wood, A. J. 2007. "Invited Essay: New Frontiers in Bryology and Lichenology: The Nature and Distribution of Vegetative Desiccation-Tolerance in Hornworts, Liverworts and Mosses." *The Bryologist* 110 (2): 163-177.

Wullschleger, S. D., H. E. Epstein, E. O. Box, E. S. Euskirchen, S. Goswami, C. M. Iversen, J. Kattge, R. J. Norby, P. M. van Bodegom, and X. Xu. 2014. "Plant Functional Types in Earth System Models: Past Experiences and Future Directions for Application of Dynamic Vegetation Models in High-Latitude Ecosystems." *Annals of Botany* 114 (1): 1-16.

Xie, Y., Z. Sha, and M. Yu. 2008. "Remote Sensing Imagery in Vegetation Mapping: A Review." *Journal of Plant Ecology* 1 (1): 9-23.

Xu, J., P. J. Morris, J. Liu, and J. Holden. 2018. "PEATMAP: Refining Estimates of Global Peatland Distribution Based on a Meta-Analysis." *Catena* 160: 134-140.

Xue, J. and B. Su. 2017. "Significant Remote Sensing Vegetation Indices: A Review of Developments and Applications." *Journal of Sensors* 2017.

Yu, Z., D. W. Beilman, and M. C. Jones. 2009. "Sensitivity of Northern Peatland Carbon Dynamics to Holocene Climate Change." *Carbon Cycling in Northern Peatlands* 184: 55-69.

Yu, Z., J. Loisel, D. P. Brosseau, D. W. Beilman, and S. J. Hunt. 2010. "Global Peatland Dynamics since the Last Glacial Maximum." *Geophysical Research Letters* 37: L13402.

Zagajewski, B., H. Tømmervik, J. W. Bjerke, E. Raczko, Z. Bochenek, A. Kłos, A. Jarocióska, S. Lavender, and D. Ziółkowski. 2017. "Intraspecific Differences in Spectral Reflectance Curves as Indicators of Reduced Vitality in High-Arctic Plants." *Remote Sensing* 9 (12): 1289.

Zagajewski, B., M. Kycko, H. Tømmervik, Z. Bochenek, B. Wojtuń, J. W. Bjerke, and A. Kłos. 2018. "Feasibility of Hyperspectral Vegetation Indices for the Detection of Chlorophyll Concentration in Three High Arctic Plants: Salix Polaris, Bistorta Vivipara, and Dryas Octopetala." *Acta Societatis Botanicorum Poloniae* 87 (4): 1-19.

Zechmeister, H. G., K. Grodzińska, and G. Szarek-Łukaszewska. 2003. "Chapter 10 Bryophytes." *Trace Metals and Other Contaminants in the Environment* 6: 329-375.

Zeng, L., B. D. Wardlow, D. Xiang, S. Hu, and D. Li. 2020. "A Review of Vegetation Phenological Metrics Extraction using Time-Series, Multispectral Satellite Data." *Remote Sensing of Environment* 237: 111511.

Zhang, E., X. Zhang, S. Yang, and S. Wang. 2014. "Improving Hyperspectral Image Classification using Spectral Information Divergence." *IEEE Geoscience and Remote Sensing Letters* 11 (1): 249-253.

Zhang, Y., M. Migliavacca, J. Penuelas, and W. Ju. 2021. "Advances in Hyperspectral Remote Sensing of Vegetation Traits and Functions." *Remote Sensing of Environment* 252: 112121.

Zhang, Z., N. E. Zimmermann, A. Stenke, X. Li, E. L. Hodson, G. Zhu, C. Huang, and B. Poulter. 2017. "Emerging Role of Wetland Methane Emissions in Driving 21st Century Climate Change." *Proceedings of the National Academy of Sciences* 114 (36): 9647.

Zoltai, S. C., L. A. Morrissey, G. P. Livingston, and W. J. Groot. 1998. "Effects of Fires on Carbon Cycling in North American Boreal Peatlands." *Environmental Reviews* 6 (1): 13-24.

APPENDIX A

OBJECTIVE 1 AND 2 ADDITIONAL RESULTS

Average Spectra

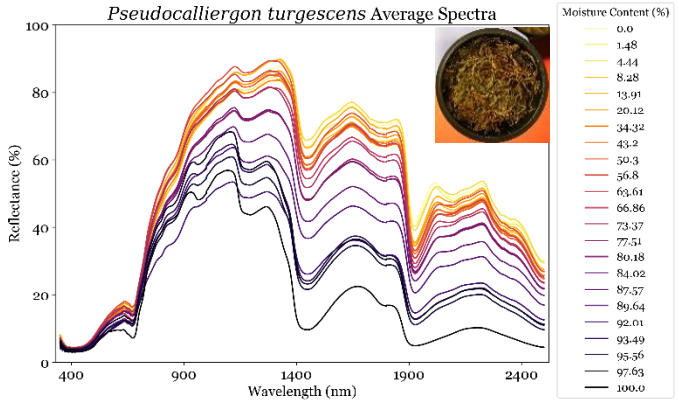

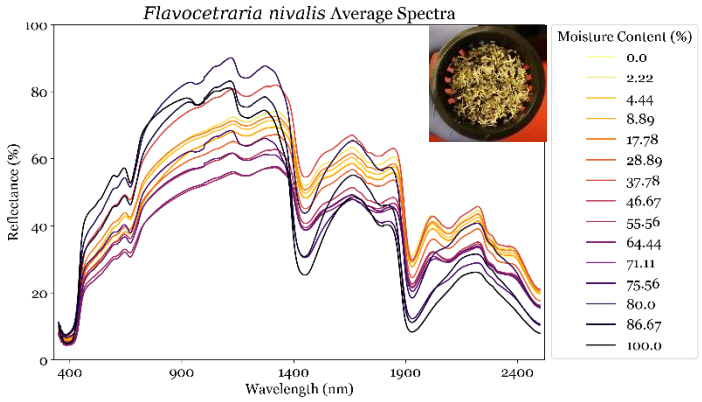

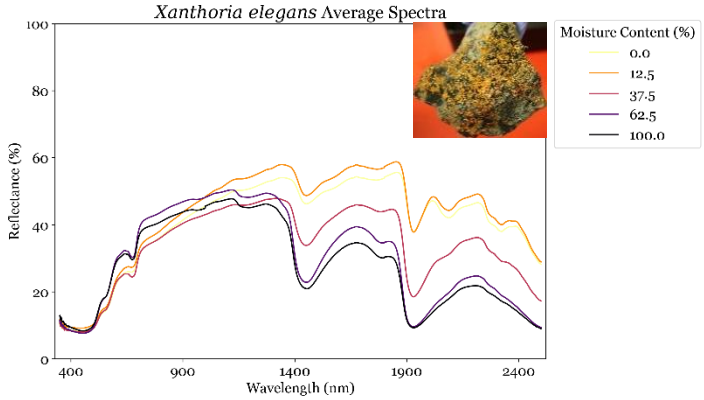

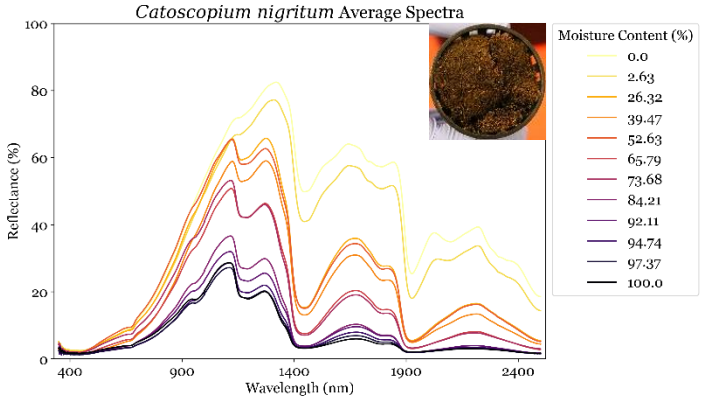

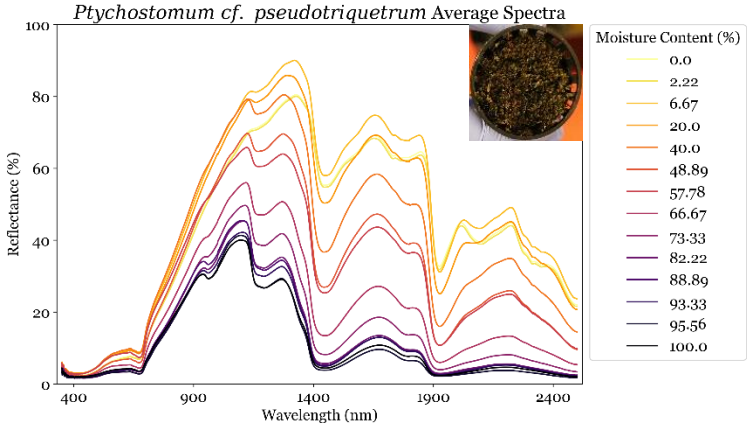
Ptychostomum cf. pseudotriquetrum Average Spectra
Reflectance (%)
Wavelength (nm)
Moisture Content (%)
0.0
2.22
6.67
20.0
40.0
48.89
57.78
66.67
73.33
82.22
88.89
93.33
95.56
100.0

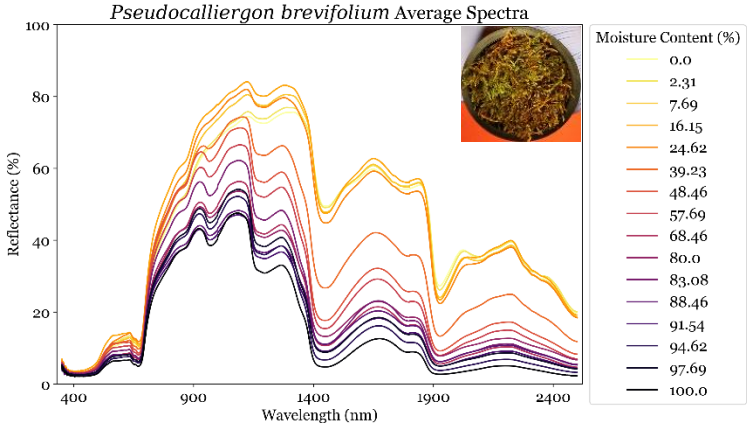
Pseudocalliergon brevifolium Average Spectra
Reflectance (%)
Wavelength (nm)
Moisture Content (%)
0.0
2.31
7.69
16.15
24.62
39.23
48.46
57.69
68.46
80.0
83.08
88.46
91.54
94.62
97.69
100.0

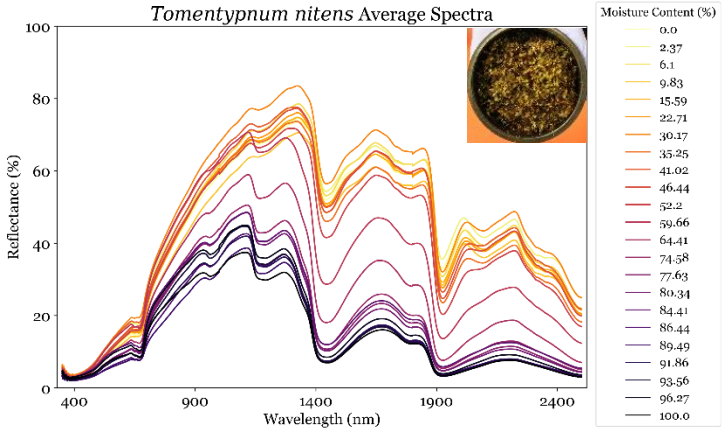
Tomentypnum nitens Average Spectra
Reflectance (%)
Wavelength (nm)
Moisture Content (%)
0.0
2.37
6.1
9.83
15.59
22.71
30.17
35.25
41.02
46.44
52.2
59.66
64.41
74.58
77.63
80.34
84.41
86.44
89.49
91.86
93.56
96.27
100.0

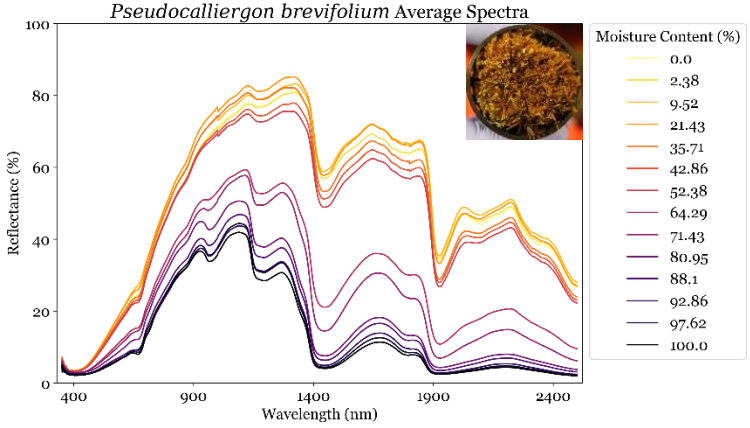
Pseudocalliergon brevifolium Average Spectra
Reflectance (%)
Wavelength (nm)
Moisture Content (%)
0.0
2.38
9.52
21.43
35.71
42.86
52.38
64.29
71.43
80.95
88.1
92.86
97.62
100.0

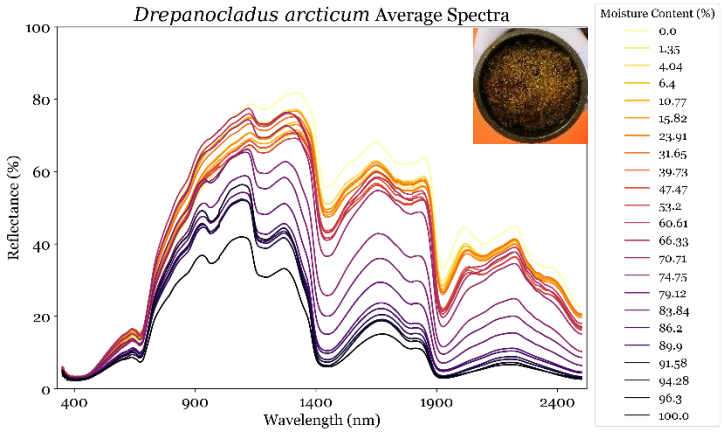
Drepanocladus arcticum Average Spectra
Reflectance (%)
Wavelength (nm)
Moisture Content (%)
0.0
1.35
4.04
6.4
10.77
15.82
23.91
31.65
39.73
47.47
53.2
60.61
66.33
70.71
74.75
79.12
83.84
86.2
89.9
91.58
94.28
96.3
100.0

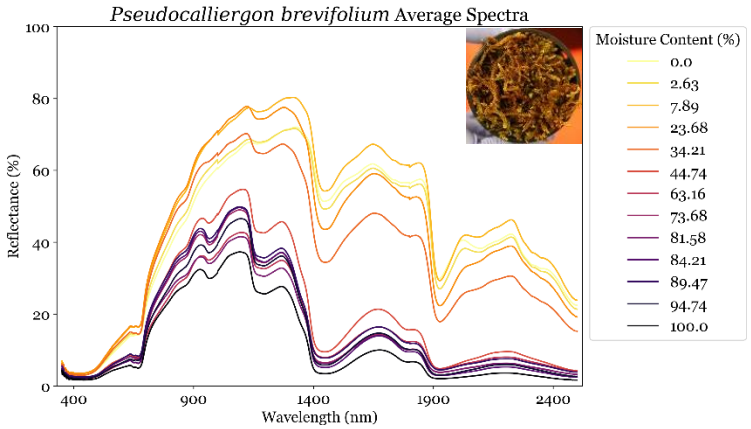
Pseudocalliergon brevifolium Average Spectra
Reflectance (%)
Wavelength (nm)
Moisture Content (%)
0.0
2.63
7.89
23.68
34.21
44.74
63.16
73.68
81.58
84.21
89.47
94.74
100.0

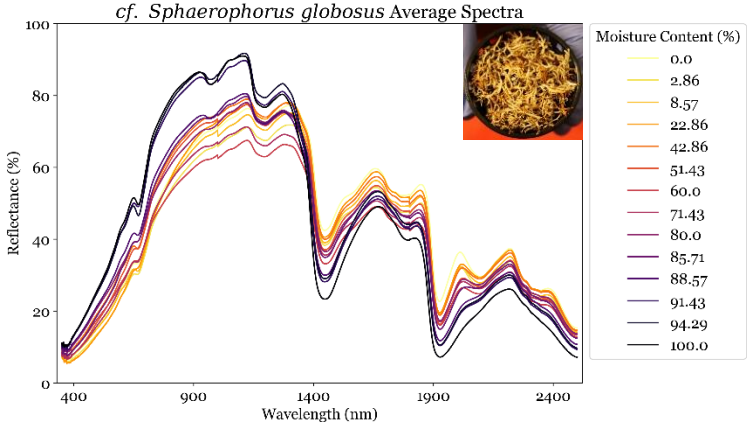
cf. Sphaerophorus globosus Average Spectra
Reflectance (%)
Wavelength (nm)
Moisture Content (%)
0.0
2.86
8.57
22.86
42.86
51.43
60.0
71.43
80.0
85.71
88.57
91.43
94.29
100.0

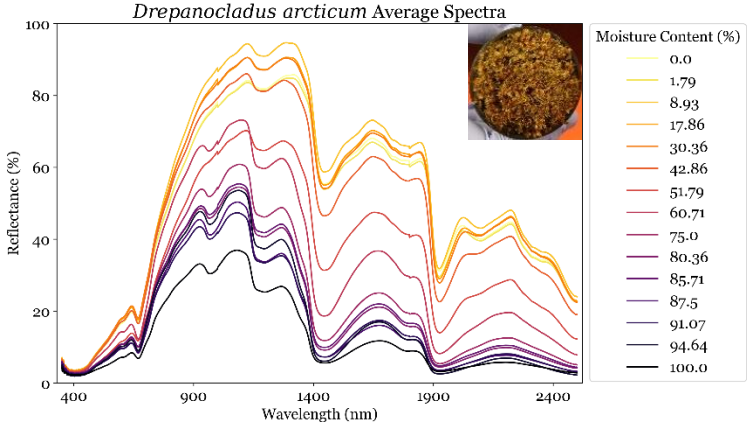
Drepanocladus arcticum Average Spectra
Reflectance (%)
Wavelength (nm)
Moisture Content (%)
0.0
1.79
8.93
17.86
30.36
42.86
51.79
60.71
75.0
80.36
85.71
87.5
91.07
94.64
100.0

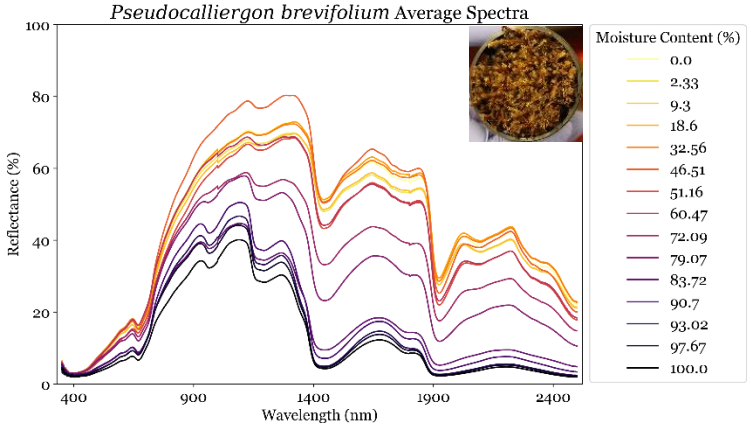

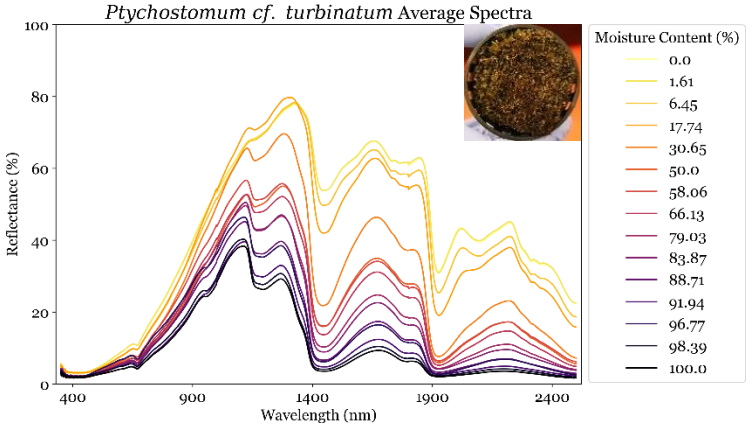

Derivatives of Average Spectra

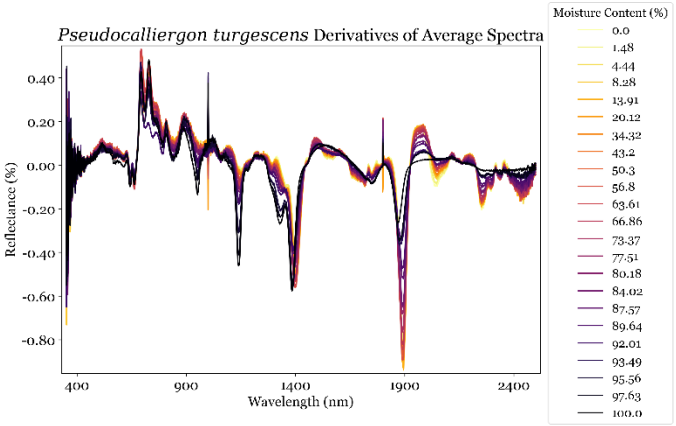

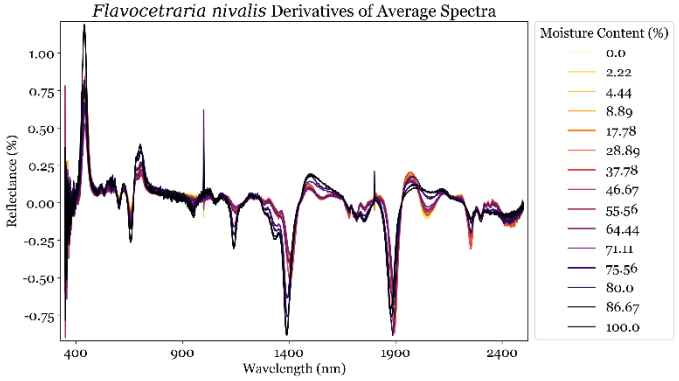

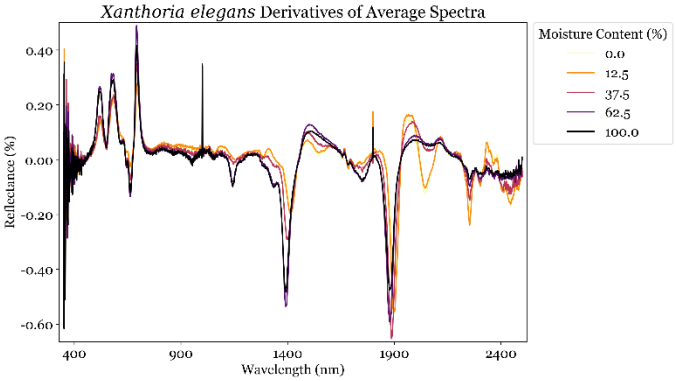
Xanthoria elegans Derivatives of Average Spectra
Reflectance (%)
0.40
0.20
0.00
-0.20
-0.40
-0.60
400
900
1400
1900
2400
Wavelength (nm)
Moisture Content (%)
0.0
12.5
37.5
62.5
100.0

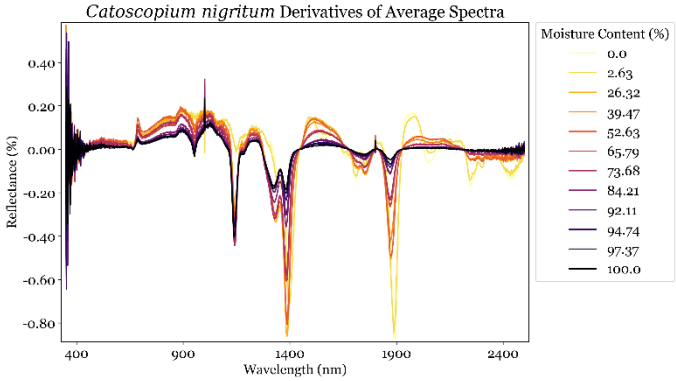
Catoscopium nigritum Derivatives of Average Spectra
Reflectance (%)
0.40
0.20
0.00
-0.20
-0.40
-0.60
-0.80
400
900
1400
1900
2400
Wavelength (nm)
Moisture Content (%)
0.0
2.63
26.32
39.47
52.63
65.79
73.68
84.21
92.11
94.74
97.37
100.0

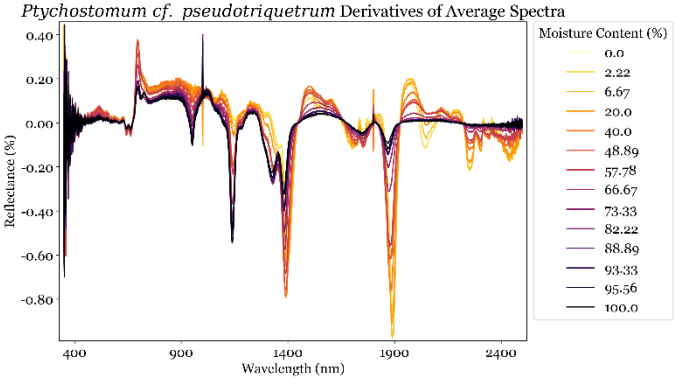
Ptychostomum cf. pseudotriquetrum Derivatives of Average Spectra
Reflectance (%)
0.40
0.20
0.00
-0.20
-0.40
-0.60
-0.80
400
900
1400
1900
2400
Wavelength (nm)
Moisture Content (%)
0.0
2.22
6.67
20.0
40.0
48.89
57.78
66.67
73.33
82.22
88.89
93.33
95.56
100.0

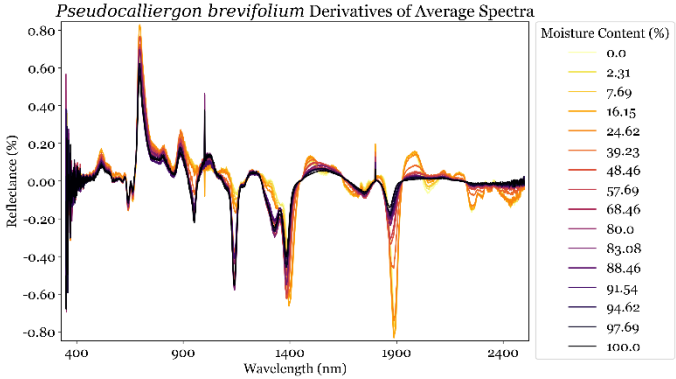
Pseudocalliergon brevifolium Derivatives of Average Spectra
Reflectance (%)
0.80
0.60
0.40
0.20
0.00
-0.20
-0.40
-0.60
-0.80
400
900
1400
1900
2400
Wavelength (nm)
Moisture Content (%)
0.0
2.31
7.69
16.15
24.62
39.23
48.46
57.69
68.46
80.0
83.08
88.46
91.54
94.62
97.69
100.0

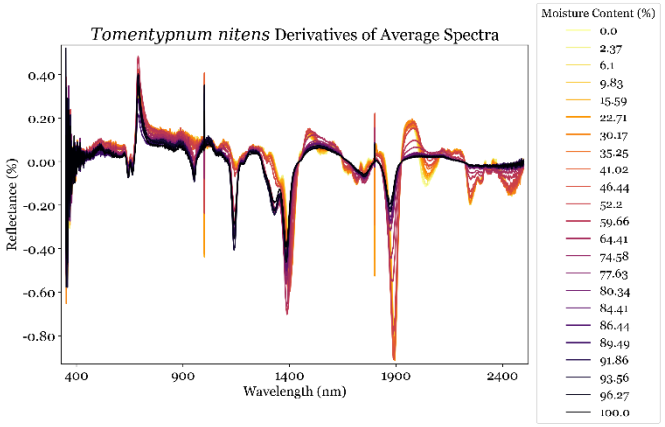
Tomentypnum nitens Derivatives of Average Spectra
Reflectance (%)
0.40
0.20
0.00
-0.20
-0.40
-0.60
-0.80
400
900
1400
1900
2400
Wavelength (nm)
Moisture Content (%)
0.0
2.37
6.1
9.83
15.59
22.71
30.17
35.25
41.02
46.44
52.2
59.66
64.41
74.58
77.63
80.34
84.41
86.44
89.49
91.86
93.56
96.27
100.0

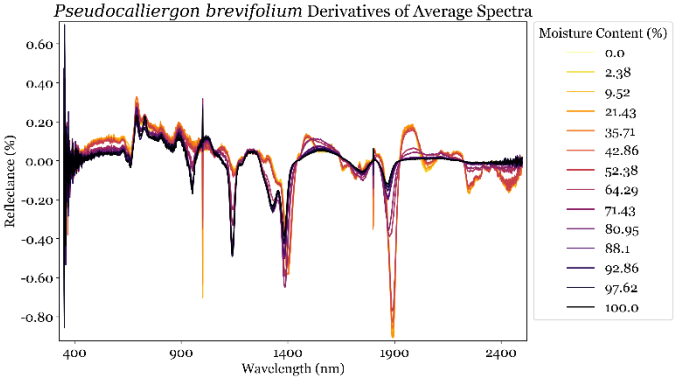
Pseudocalliergon brevifolium Derivatives of Average Spectra
Reflectance (%)
0.60
0.40
0.20
0.00
-0.20
-0.40
-0.60
-0.80
400
900
1400
1900
2400
Wavelength (nm)
Moisture Content (%)
0.0
2.38
9.52
21.43
35.71
42.86
52.38
64.29
71.43
80.95
88.1
92.86
97.62
100.0

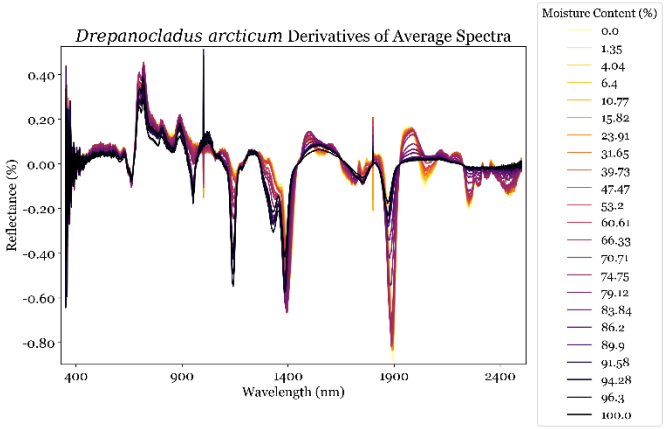
Drepanocladus arcticum Derivatives of Average Spectra
Reflectance (%)
0.40
0.20
0.00
-0.20
-0.40
-0.60
-0.80
400
900
1400
1900
2400
Wavelength (nm)
Moisture Content (%)
0.0
1.35
4.04
6.4
10.77
15.82
23.91
31.65
39.73
47.47
53.2
60.61
66.33
70.71
74.75
79.12
83.84
86.2
89.9
91.58
94.28
96.3
100.0

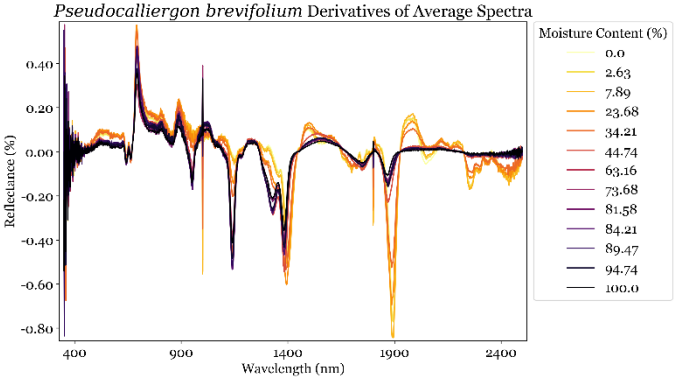
Pseudocalliergon brevifolium Derivatives of Average Spectra
Reflectance (%)
0.40
0.20
0.00
-0.20
-0.40
-0.60
-0.80
400
900
1400
1900
2400
Wavelength (nm)
Moisture Content (%)
0.0
2.63
7.89
23.68
34.21
44.74
63.16
73.68
81.58
84.21
89.47
94.74
100.0

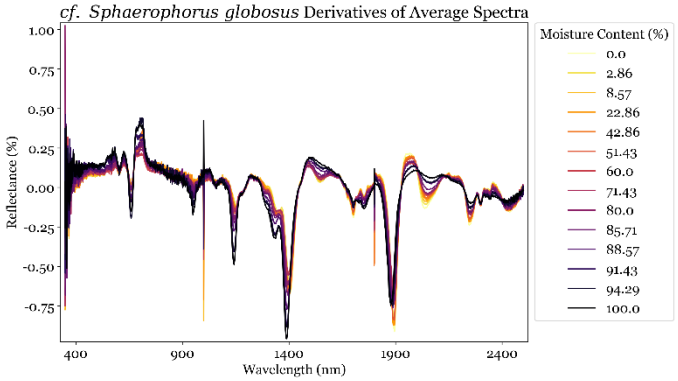
cf. Sphaerophorus globosus Derivatives of Average Spectra
Reflectance (%)
1.00
0.75
0.50
0.25
0.00
-0.25
-0.50
-0.75
400
900
1400
1900
2400
Wavelength (nm)
Moisture Content (%)
0.0
2.86
8.57
22.86
42.86
51.43
60.0
71.43
80.0
85.71
88.57
91.43
94.29
100.0

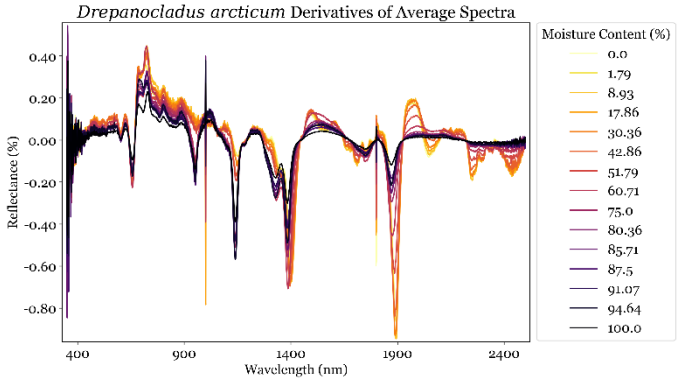
Drepanocladus arcticum Derivatives of Average Spectra
Reflectance (%)
0.40
0.20
0.00
-0.20
-0.40
-0.60
-0.80
400
900
1400
1900
2400
Wavelength (nm)
Moisture Content (%)
0.0
1.79
8.93
17.86
30.36
42.86
51.79
60.71
75.0
80.36
85.71
87.5
91.07
94.64
100.0

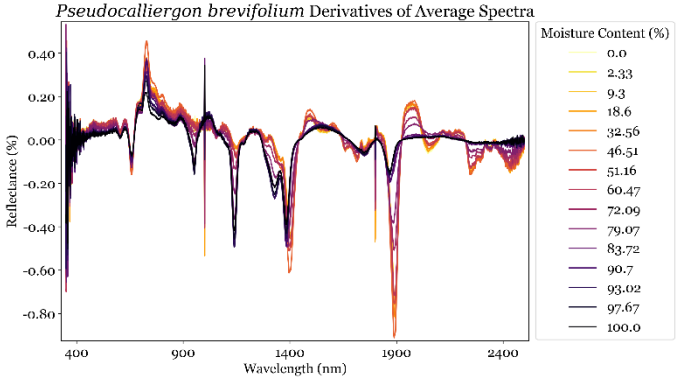
Pseudocalliergon brevifolium Derivatives of Average Spectra
Reflectance (%)
0.40
0.20
0.00
-0.20
-0.40
-0.60
-0.80
400
900
1400
1900
2400
Wavelength (nm)
Moisture Content (%)
0.0
2.33
9.3
18.6
32.56
46.51
51.16
60.47
72.09
79.07
83.72
90.7
93.02
97.67
100.0

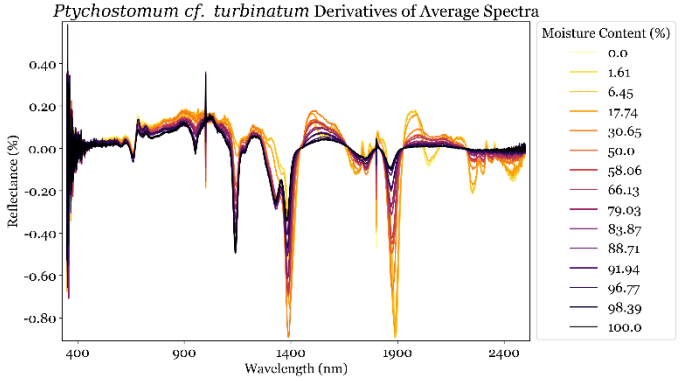
Ptychostomum cf. turbinatum Derivatives of Average Spectra
Reflectance (%)
0.40
0.20
0.00
-0.20
-0.40
-0.60
-0.80
400
900
1400
1900
2400
Wavelength (nm)
Moisture Content (%)
0.0
1.61
6.45
17.74
30.65
50.0
58.06
66.13
79.03
83.87
88.71
91.94
96.77
98.39
100.0

Within-Species SID (Full Spectral Range and 100nm Window) Analyses

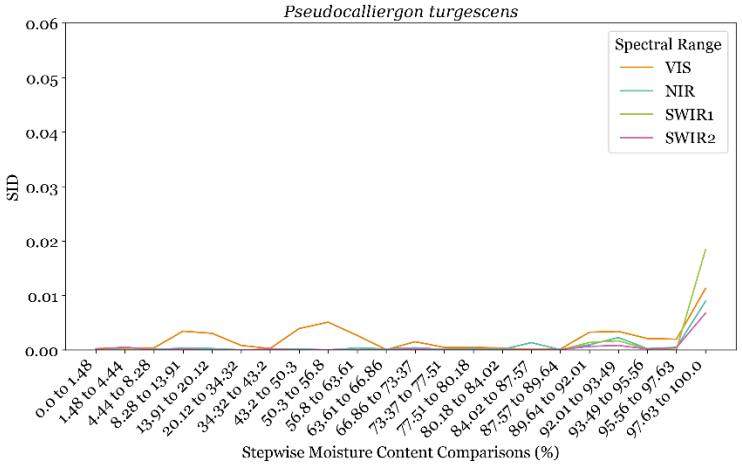

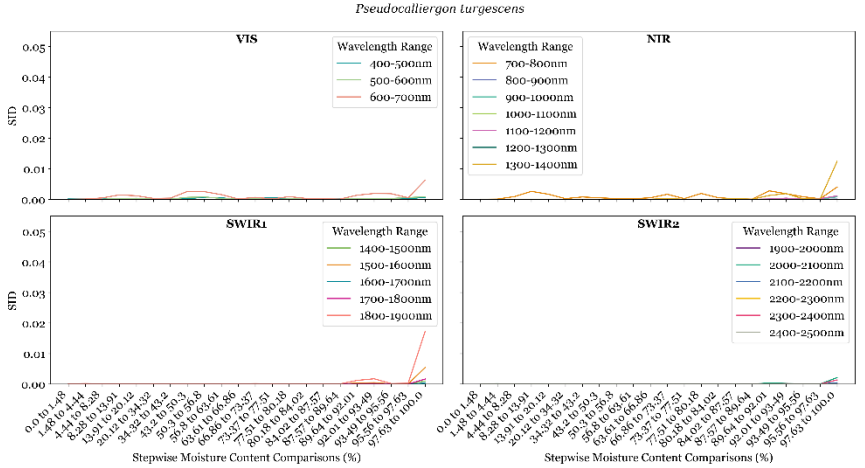

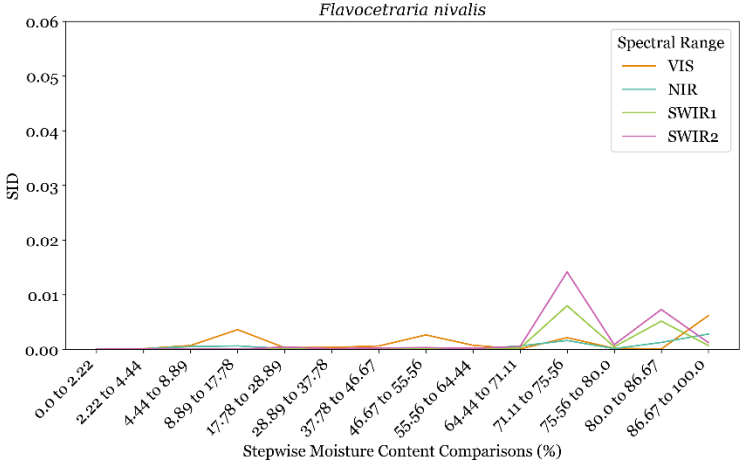

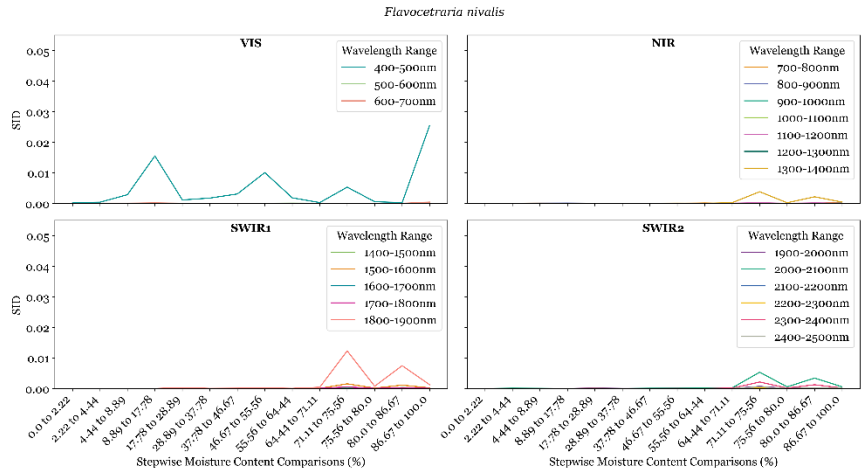

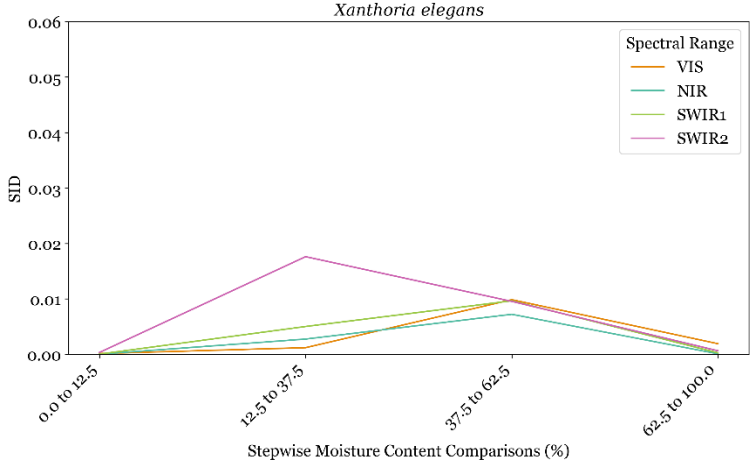
Xanthoria elegans
Spectral Range
VIS
NIR
SWIR1
SWIR2
SID
0.06
0.05
0.04
0.03
0.02
0.01
0.00
0.0 to 12.5
12.5 to 37.5
37.5 to 62.5
62.5 to 100.0
Stepwise Moisture Content Comparisons (%)

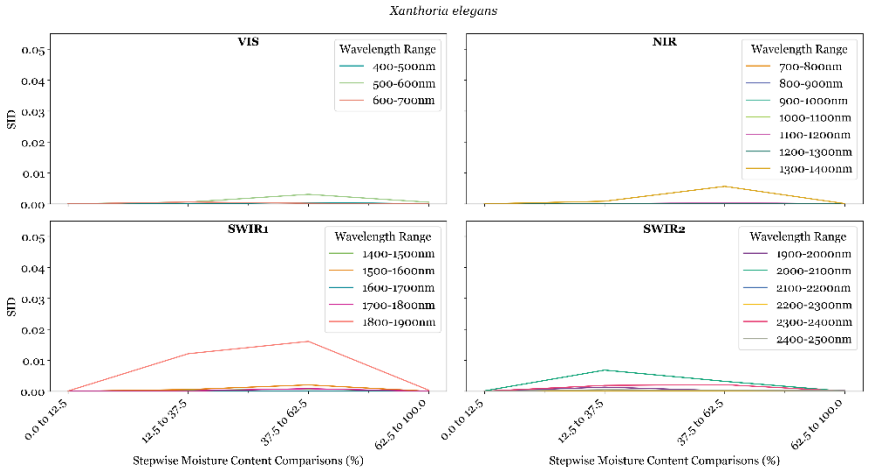
Xanthoria elegans
VIS
Wavelength Range
400-500nm
500-600nm
600-700nm
NIR
Wavelength Range
700-800nm
800-900nm
900-1000nm
1000-1100nm
1100-1200nm
1200-1300nm
1300-1400nm
SWIR1
Wavelength Range
1400-1500nm
1500-1600nm
1600-1700nm
1700-1800nm
1800-1900nm
SWIR2
Wavelength Range
1900-2000nm
2000-2100nm
2100-2200nm
2200-2300nm
2300-2400nm
2400-2500nm
SID
0.06
0.05
0.04
0.03
0.02
0.01
0.00
0.0 to 12.5
12.5 to 37.5
37.5 to 62.5
62.5 to 100.0
Stepwise Moisture Content Comparisons (%)

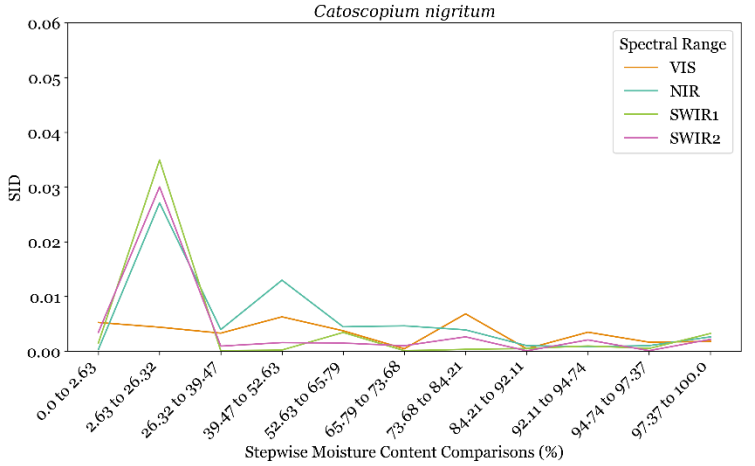
Catoscopium nigritum
Spectral Range
VIS
NIR
SWIR1
SWIR2
SID
0.06
0.05
0.04
0.03
0.02
0.01
0.00
0.0 to 2.63
2.63 to 26.32
26.32 to 39.47
39.47 to 52.63
52.63 to 65.79
65.79 to 73.68
73.68 to 84.21
84.21 to 92.11
92.11 to 94.74
94.74 to 97.37
97.37 to 100.0
Stepwise Moisture Content Comparisons (%)

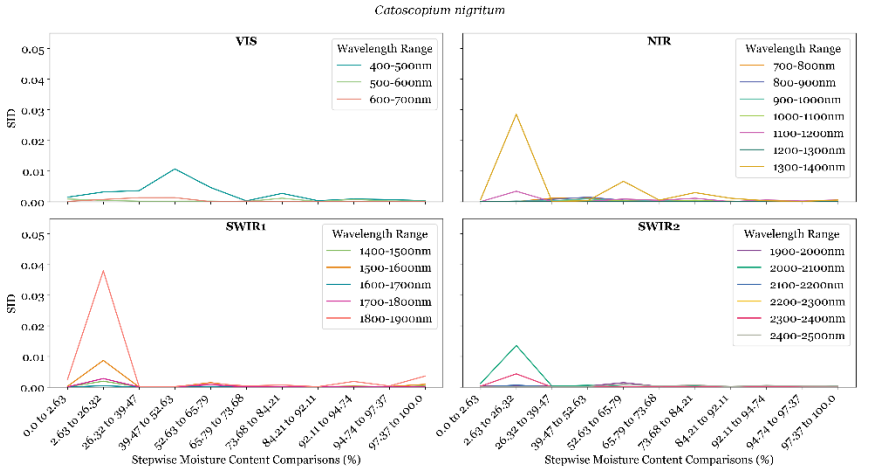
Catoscopium nigritum
VIS
Wavelength Range
400-500nm
500-600nm
600-700nm
NIR
Wavelength Range
700-800nm
800-900nm
900-1000nm
1000-1100nm
1100-1200nm
1200-1300nm
1300-1400nm
SWIR1
Wavelength Range
1400-1500nm
1500-1600nm
1600-1700nm
1700-1800nm
1800-1900nm
SWIR2
Wavelength Range
1900-2000nm
2000-2100nm
2100-2200nm
2200-2300nm
2300-2400nm
2400-2500nm
SID
0.06
0.05
0.04
0.03
0.02
0.01
0.00
0.0 to 2.63
2.63 to 26.32
26.32 to 39.47
39.47 to 52.63
52.63 to 65.79
65.79 to 73.68
73.68 to 84.21
84.21 to 92.11
92.11 to 94.74
94.74 to 97.37
97.37 to 100.0
Stepwise Moisture Content Comparisons (%)

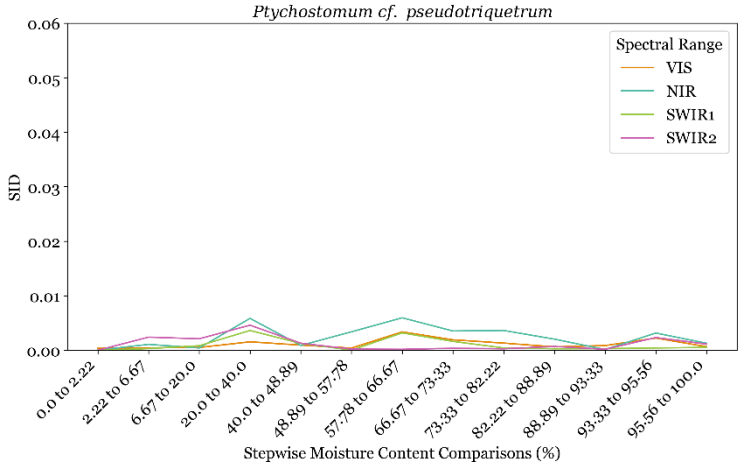
Ptychostomum cf. pseudotriquetrum
Spectral Range
VIS
NIR
SWIR1
SWIR2
SID
0.06
0.05
0.04
0.03
0.02
0.01
0.00
0.0 to 2.22
2.22 to 6.67
6.67 to 20.0
20.0 to 40.0
40.0 to 48.89
48.89 to 57.78
57.78 to 66.67
66.67 to 73.33
73.33 to 82.22
82.22 to 88.89
88.89 to 93.33
93.33 to 95.56
95.56 to 100.0
Stepwise Moisture Content Comparisons (%)

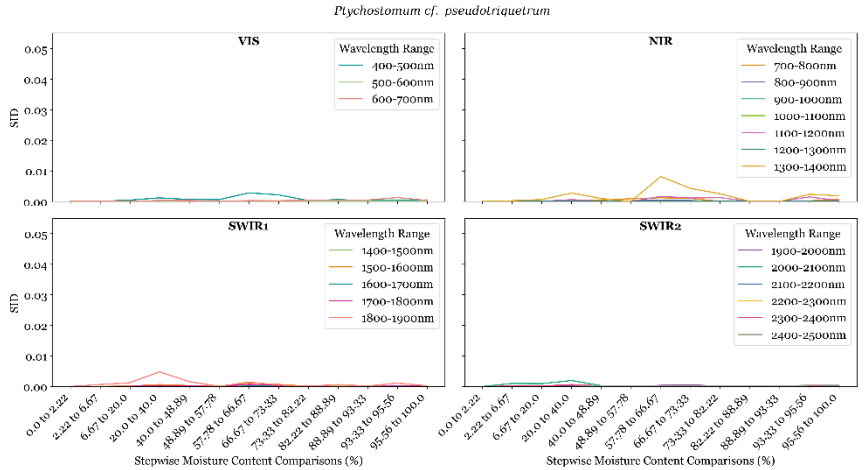
Ptychostomum cf. pseudotriquetrum
VIS
Wavelength Range
400-500nm
500-600nm
600-700nm
NIR
Wavelength Range
700-800nm
800-900nm
900-1000nm
1000-1100nm
1100-1200nm
1200-1300nm
1300-1400nm
SWIR1
Wavelength Range
1400-1500nm
1500-1600nm
1600-1700nm
1700-1800nm
1800-1900nm
SWIR2
Wavelength Range
1900-2000nm
2000-2100nm
2100-2200nm
2200-2300nm
2300-2400nm
2400-2500nm
SID
Stepwise Moisture Content Comparisons (%)

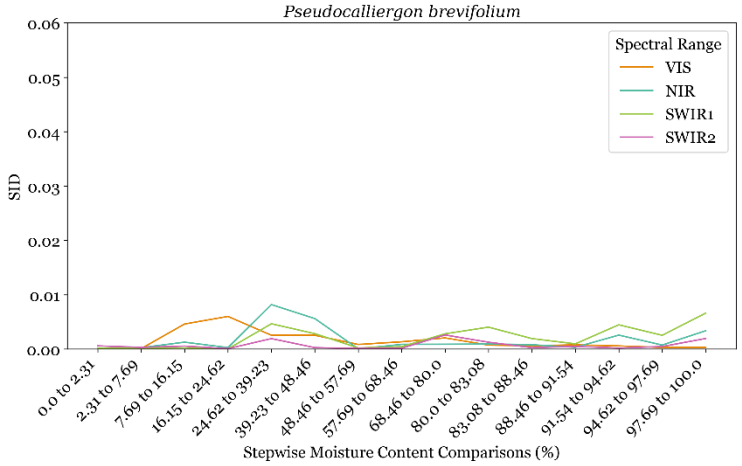
Pseudocalliergon brevifolium
Spectral Range
VIS
NIR
SWIR1
SWIR2
SID
0.06
0.05
0.04
0.03
0.02
0.01
0.00
0.0 to 2.31
2.31 to 7.69
7.69 to 16.15
16.15 to 24.62
24.62 to 39.23
39.23 to 48.46
48.46 to 57.69
57.69 to 68.46
68.46 to 80.0
80.0 to 83.08
83.08 to 88.46
88.46 to 91.54
91.54 to 94.62
94.62 to 97.69
97.69 to 100.0
Stepwise Moisture Content Comparisons (%)

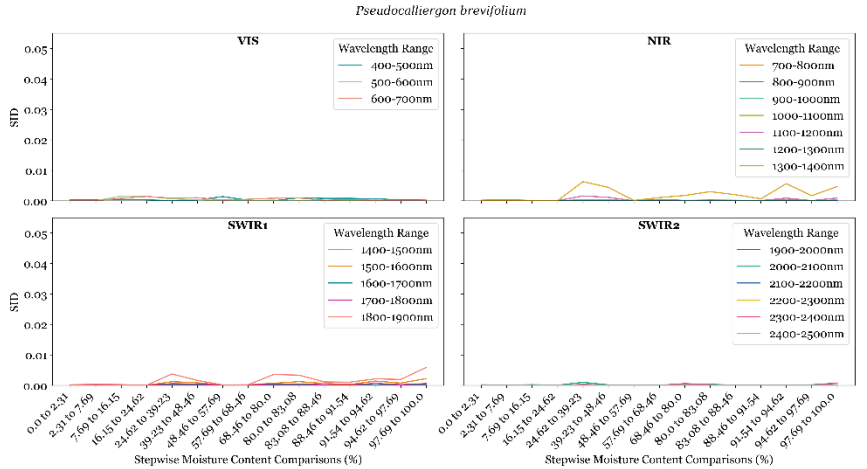
Pseudocalliergon brevifolium
VIS
Wavelength Range
400-500nm
500-600nm
600-700nm
NIR
Wavelength Range
700-800nm
800-900nm
900-1000nm
1000-1100nm
1100-1200nm
1200-1300nm
1300-1400nm
SWIR1
Wavelength Range
1400-1500nm
1500-1600nm
1600-1700nm
1700-1800nm
1800-1900nm
SWIR2
Wavelength Range
1900-2000nm
2000-2100nm
2100-2200nm
2200-2300nm
2300-2400nm
2400-2500nm
SID
Stepwise Moisture Content Comparisons (%)

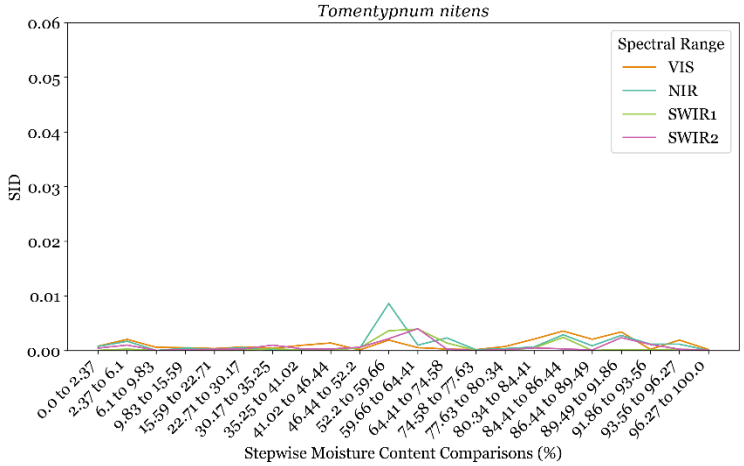
Tomentypnum nitens
SID
Stepwise Moisture Content Comparisons (%)
Spectral Range
VIS
NIR
SWIR1
SWIR2

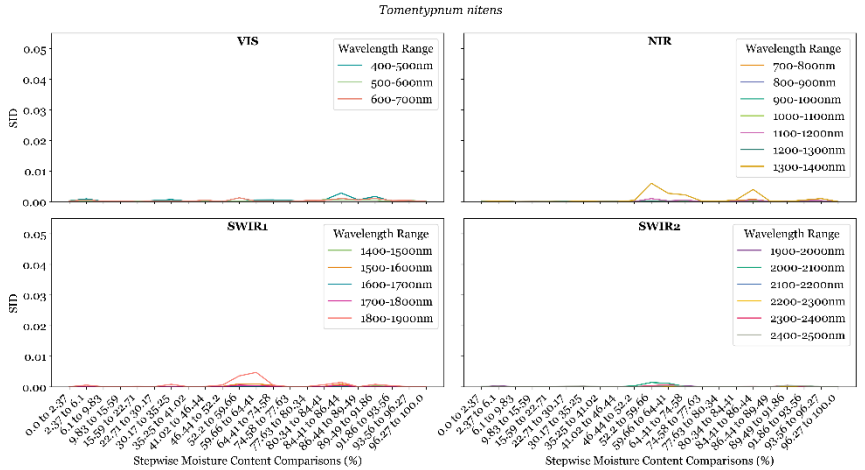
Tomentypnum nitens
VIS
NIR
SWIR1
SWIR2
SID
Stepwise Moisture Content Comparisons (%)
Wavelength Range

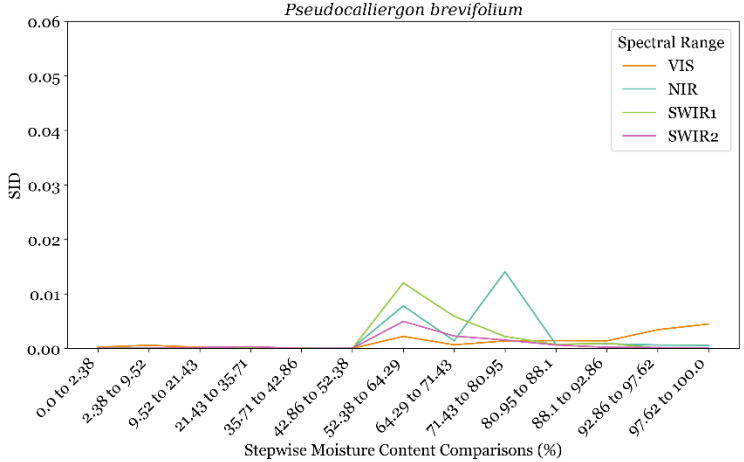
Pseudocalliergon brevifolium
SID
Stepwise Moisture Content Comparisons (%)
Spectral Range
VIS
NIR
SWIR1
SWIR2

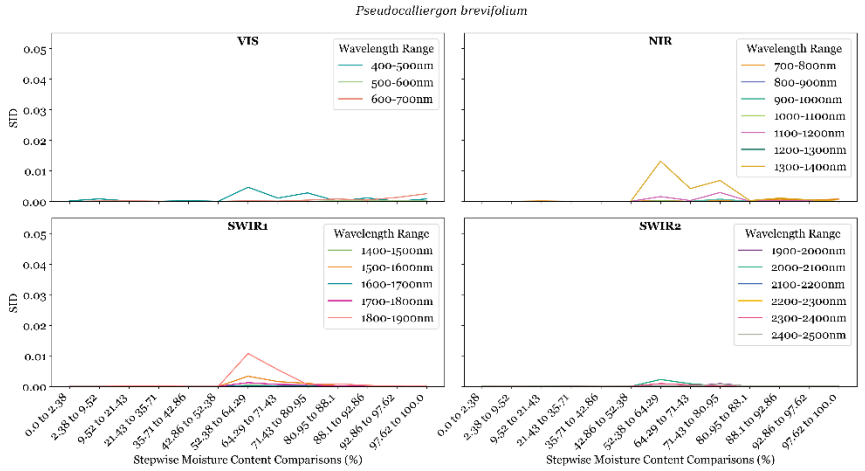
Pseudocalliergon brevifolium
VIS
NIR
SWIR1
SWIR2
SID
Stepwise Moisture Content Comparisons (%)
Wavelength Range

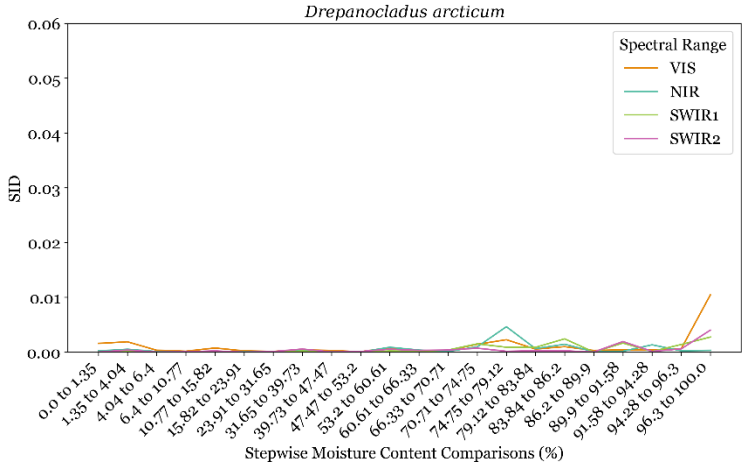
Drepanocladus arcticum
Spectral Range
VIS
NIR
SWIR1
SWIR2
SID
Stepwise Moisture Content Comparisons (%)

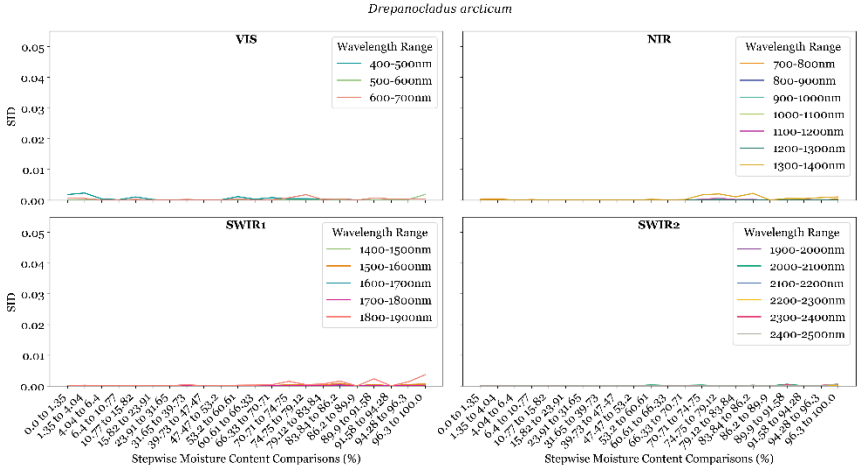
Drepanocladus arcticum
VIS
NIR
SWIR1
SWIR2
Wavelength Range
SID
Stepwise Moisture Content Comparisons (%)

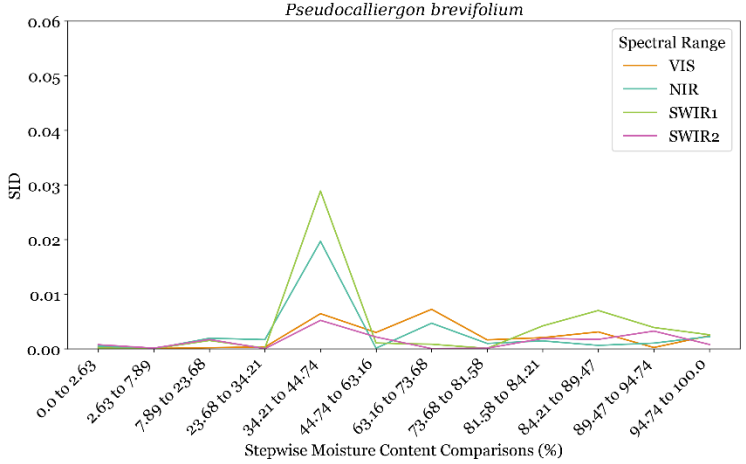
Pseudocalliergon brevifolium
Spectral Range
VIS
NIR
SWIR1
SWIR2
SID
Stepwise Moisture Content Comparisons (%)

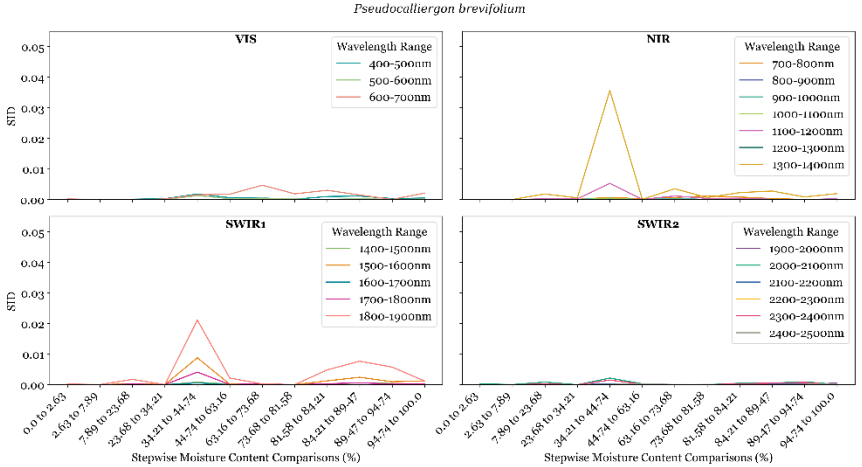
Pseudocalliergon brevifolium
VIS
NIR
SWIR1
SWIR2
Wavelength Range
SID
Stepwise Moisture Content Comparisons (%)

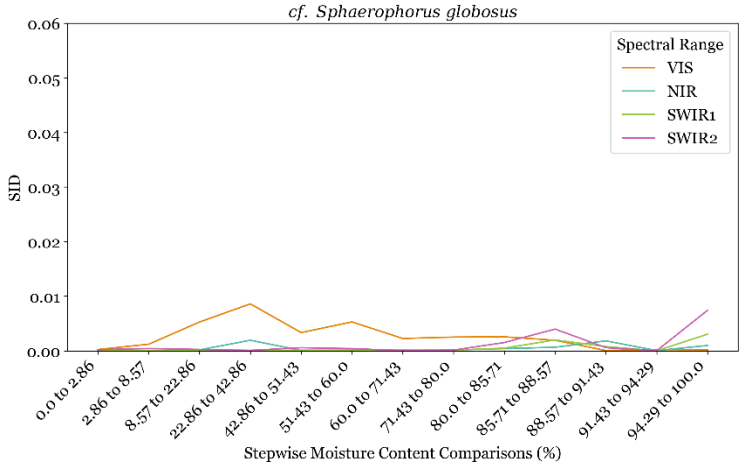
cf. Sphaerophorus globosus
Spectral Range
VIS
NIR
SWIR1
SWIR2
SID
Stepwise Moisture Content Comparisons (%)

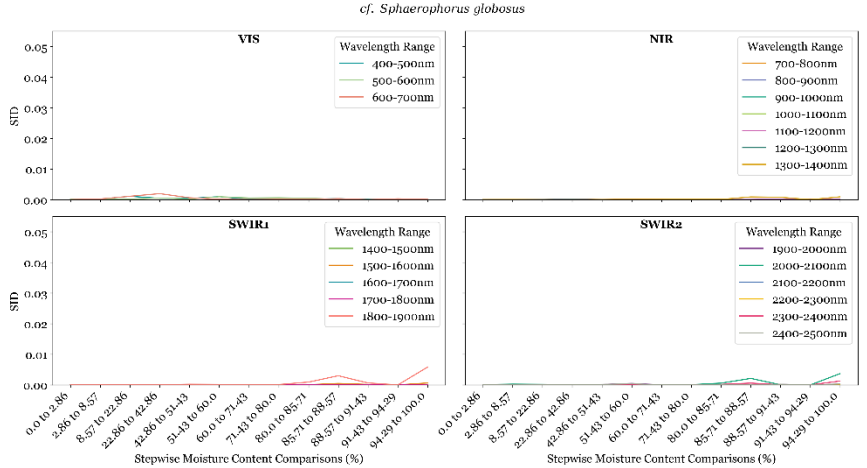
cf. Sphaerophorus globosus
VIS
NIR
SWIR1
SWIR2
Wavelength Range
SID
Stepwise Moisture Content Comparisons (%)

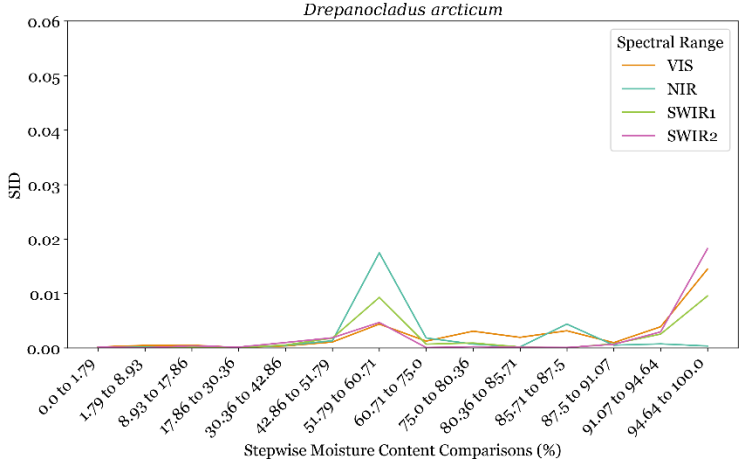
Drepanocladus arcticum
Spectral Range
VIS
NIR
SWIR1
SWIR2
SID
Stepwise Moisture Content Comparisons (%)

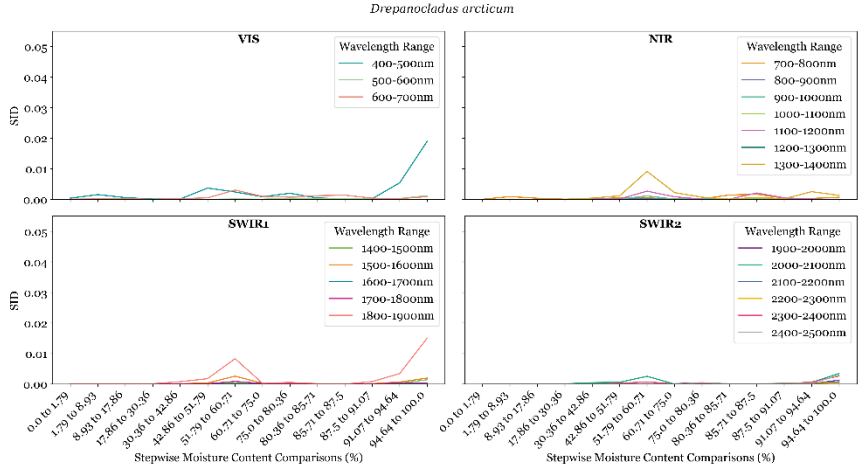
Drepanocladus arcticum
VIS
NIR
SWIR1
SWIR2
Wavelength Range
SID
Stepwise Moisture Content Comparisons (%)

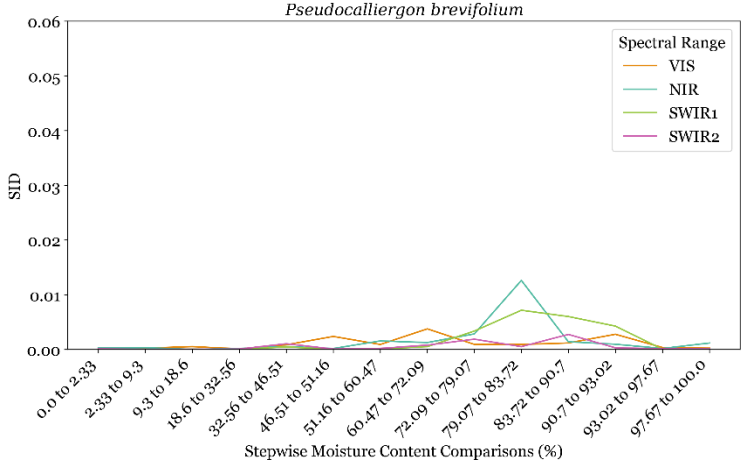
Pseudocalliergon brevifolium
Spectral Range
VIS
NIR
SWIR1
SWIR2
SID
Stepwise Moisture Content Comparisons (%)

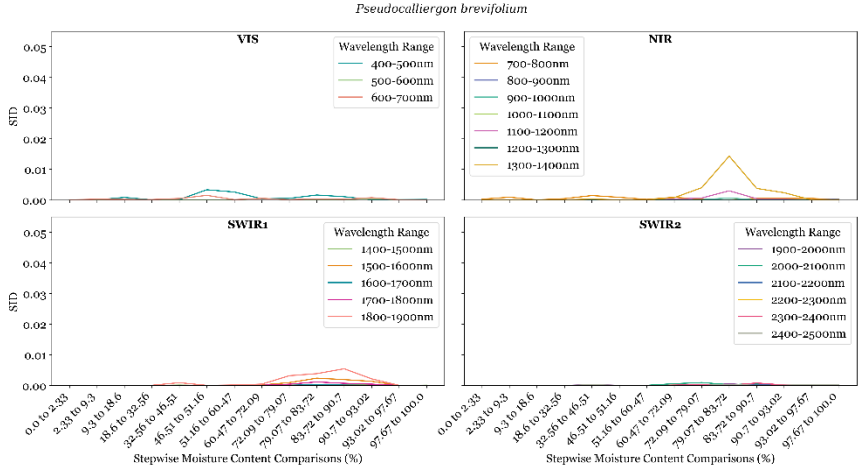
Pseudocalliergon brevifolium
VIS
NIR
SWIR1
SWIR2
Wavelength Range
SID
Stepwise Moisture Content Comparisons (%)

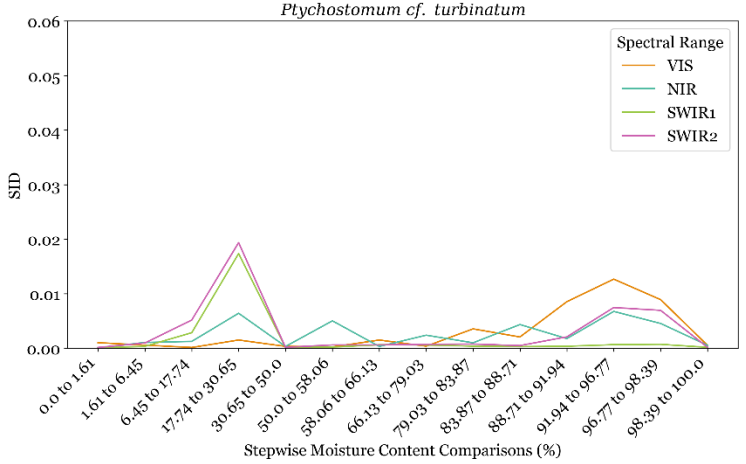
Ptychostomum cf. turbinatum
Spectral Range
VIS
NIR
SWIR1
SWIR2
SID
Stepwise Moisture Content Comparisons (%)

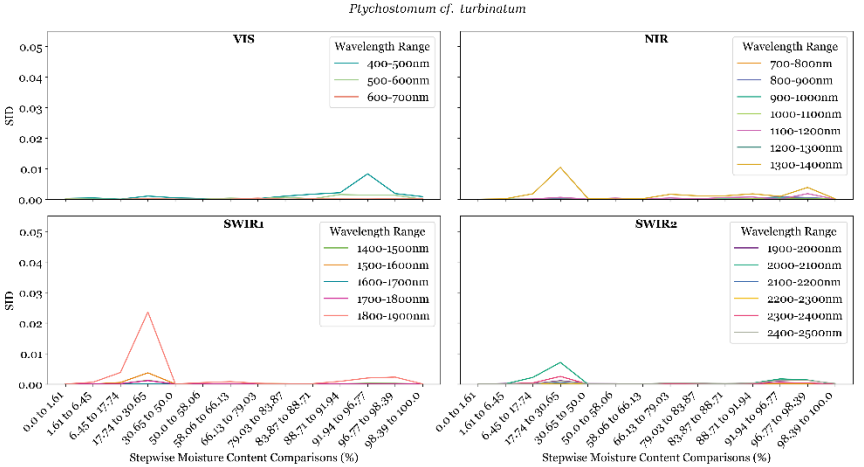
Ptychostomum cf. turbinatum
VIS
NIR
SWIR1
SWIR2
Wavelength Range
SID
Stepwise Moisture Content Comparisons (%)

Convex Hull Maxima Points

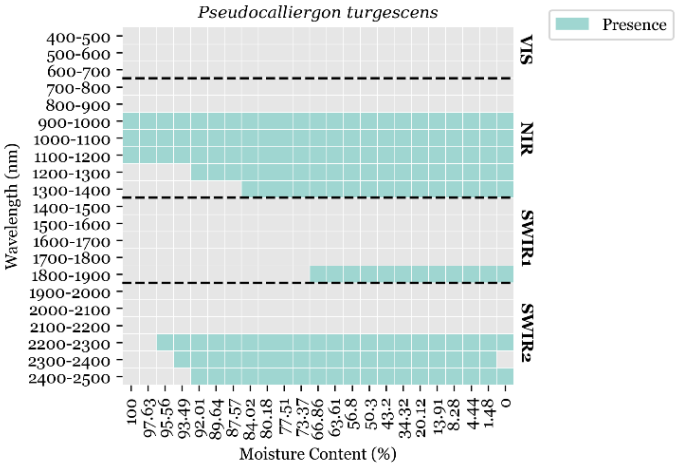

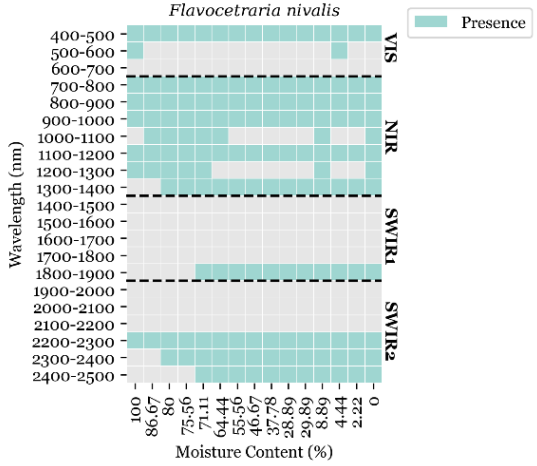

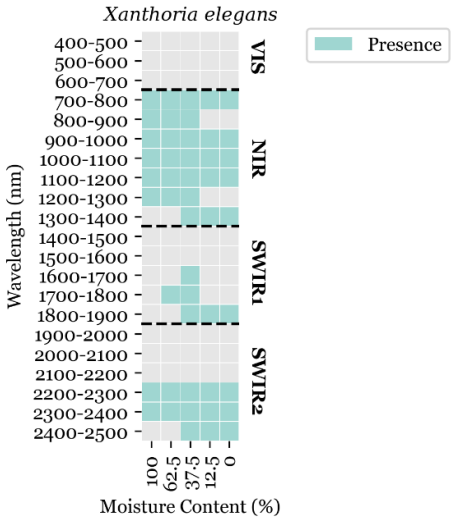

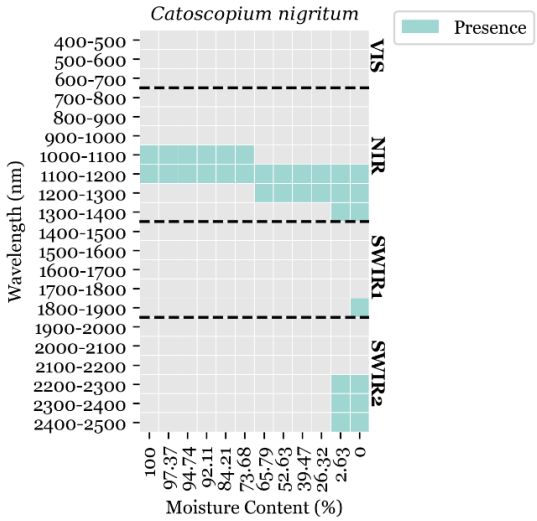

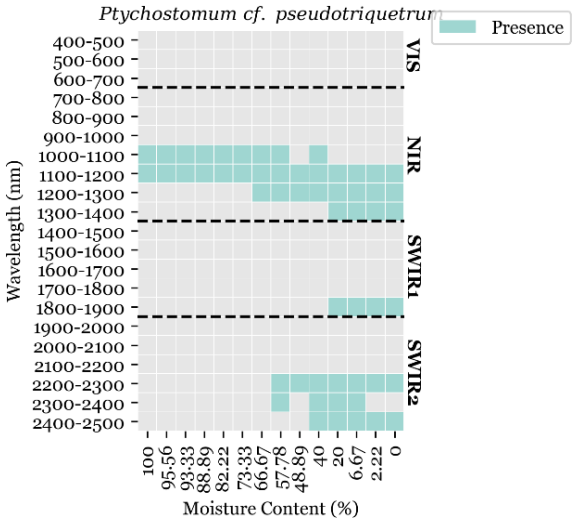
Ptychostomum cf. pseudotriquetrum
Presence
Wavelength (nm)
400-500
500-600
600-700
700-800
800-900
900-1000
1000-1100
1100-1200
1200-1300
1300-1400
1400-1500
1500-1600
1600-1700
1700-1800
1800-1900
1900-2000
2000-2100
2100-2200
2200-2300
2300-2400
2400-2500
VIS
NIR
SWIR1
SWIR2
100
95.56
93.33
88.89
82.22
73.33
66.67
57.78
48.89
40
20
6.67
2.22
0
Moisture Content (%)

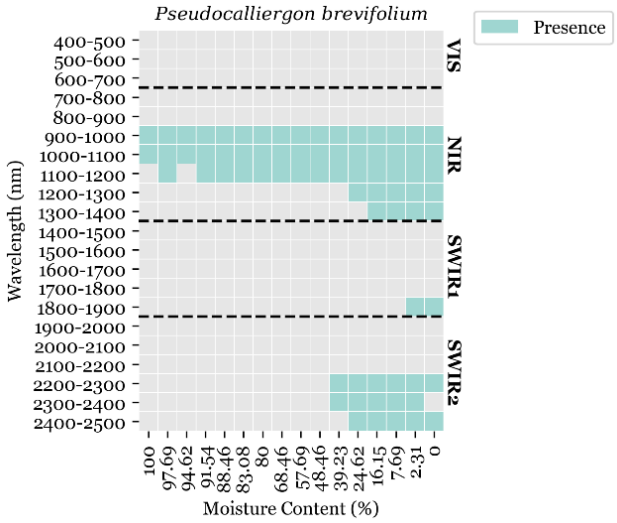
Pseudocalliergon brevifolium
Presence
Wavelength (nm)
400-500
500-600
600-700
700-800
800-900
900-1000
1000-1100
1100-1200
1200-1300
1300-1400
1400-1500
1500-1600
1600-1700
1700-1800
1800-1900
1900-2000
2000-2100
2100-2200
2200-2300
2300-2400
2400-2500
VIS
NIR
SWIR1
SWIR2
100
97.69
94.62
91.54
88.46
83.08
80
68.46
57.69
48.46
39.23
24.62
16.15
7.69
2.31
0
Moisture Content (%)

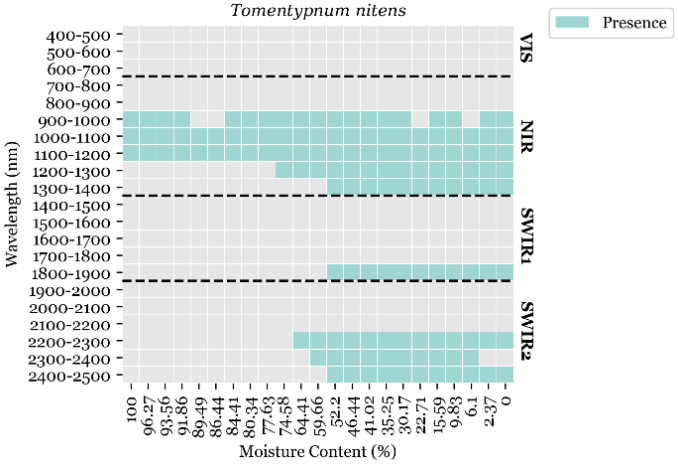
Tomentypnum nitens
Presence
Wavelength (nm)
400-500
500-600
600-700
700-800
800-900
900-1000
1000-1100
1100-1200
1200-1300
1300-1400
1400-1500
1500-1600
1600-1700
1700-1800
1800-1900
1900-2000
2000-2100
2100-2200
2200-2300
2300-2400
2400-2500
VIS
NIR
SWIR1
SWIR2
100
96.27
93.56
91.86
89.49
86.44
84.41
80.34
77.63
74.58
64.41
59.66
52.2
46.44
41.02
35.25
30.17
22.71
15.59
9.83
6.1
2.37
0
Moisture Content (%)

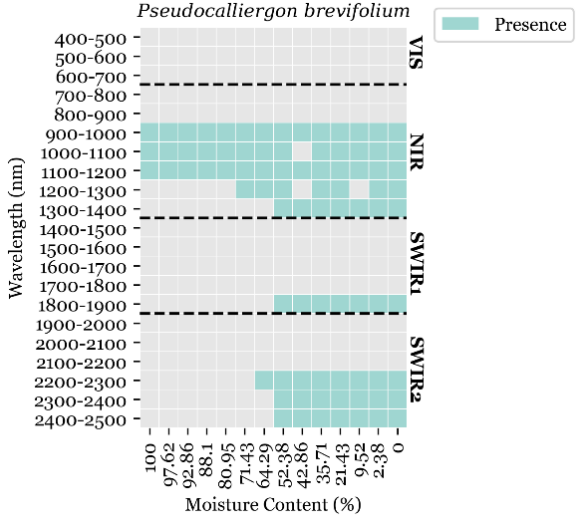
Pseudocalliergon brevifolium
Presence
Wavelength (nm)
400-500
500-600
600-700
700-800
800-900
900-1000
1000-1100
1100-1200
1200-1300
1300-1400
1400-1500
1500-1600
1600-1700
1700-1800
1800-1900
1900-2000
2000-2100
2100-2200
2200-2300
2300-2400
2400-2500
VIS
NIR
SWIR1
SWIR2
100
97.62
92.86
88.1
80.95
71.43
64.29
52.38
42.86
35.71
21.43
9.52
2.38
0
Moisture Content (%)

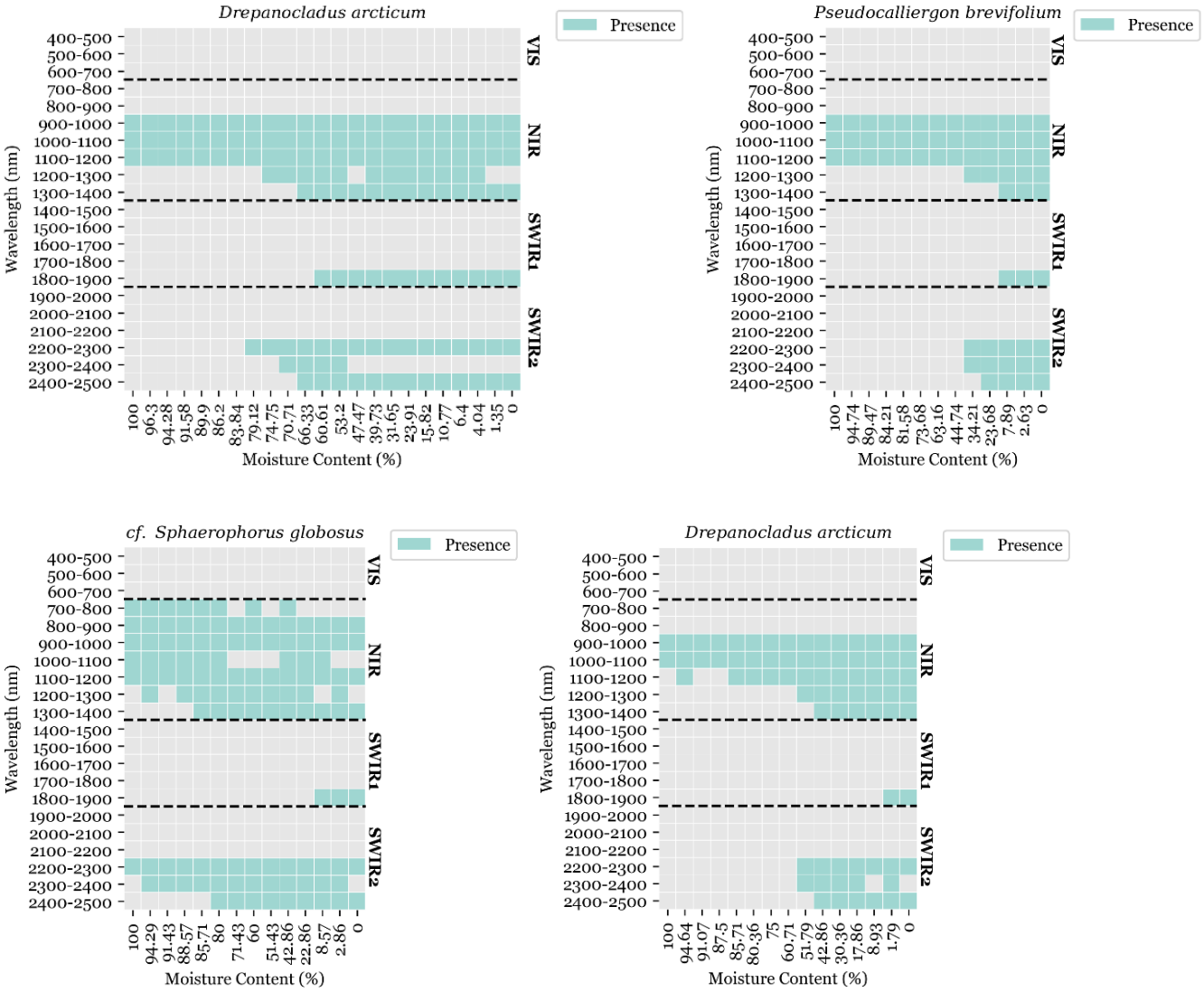
Drepanocladus arcticum
Presence
Wavelength (nm)
400-500
500-600
600-700
700-800
800-900
900-1000
1000-1100
1100-1200
1200-1300
1300-1400
1400-1500
1500-1600
1600-1700
1700-1800
1800-1900
1900-2000
2000-2100
2100-2200
2200-2300
2300-2400
2400-2500
VIS
NIR
SWIR1
SWIR2
100 96.3 94.28 91.58 89.9 86.2 83.84 79.12 74.75 70.71 66.33 60.61 53.2 47.47 39.73 31.65 23.91 15.82 10.77 6.4 4.04 1.35 0
Moisture Content (%)
Pseudocalliergon brevifolium
Presence
Wavelength (nm)
VIS
NIR
SWIR1
SWIR2
100 94.74 89.47 84.21 81.58 73.68 63.16 44.74 34.21 23.68 7.89 2.63 0
Moisture Content (%)
cf. Sphaerophorus globosus
Presence
Wavelength (nm)
VIS
NIR
SWIR1
SWIR2
100 94.29 91.43 88.57 85.71 80 71.43 60 51.43 42.86 22.86 8.57 2.86 0
Moisture Content (%)
Drepanocladus arcticum
Presence
Wavelength (nm)
VIS
NIR
SWIR1
SWIR2
100 94.64 91.07 87.5 85.71 80.36 75 60.71 51.79 42.86 30.36 17.86 8.93 1.79 0
Moisture Content (%)

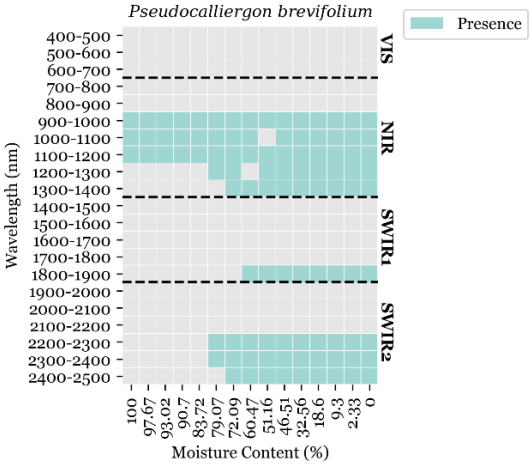

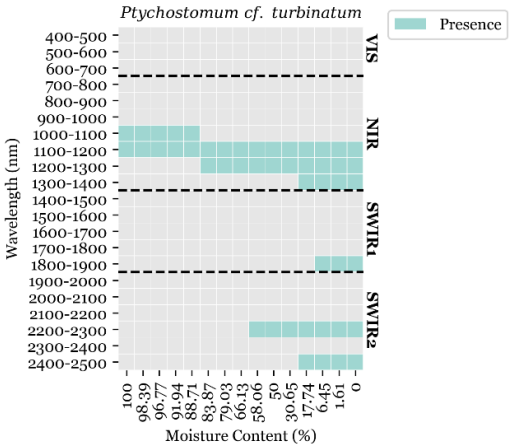

10% Binned Spectra

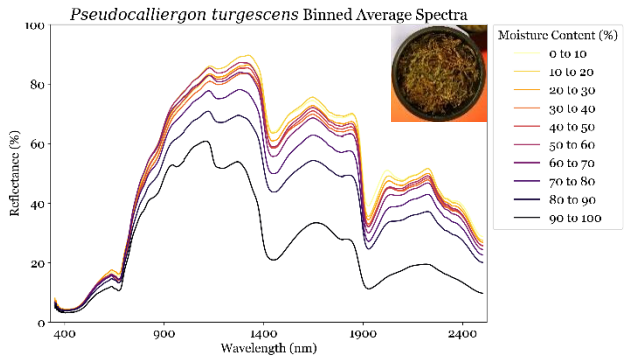

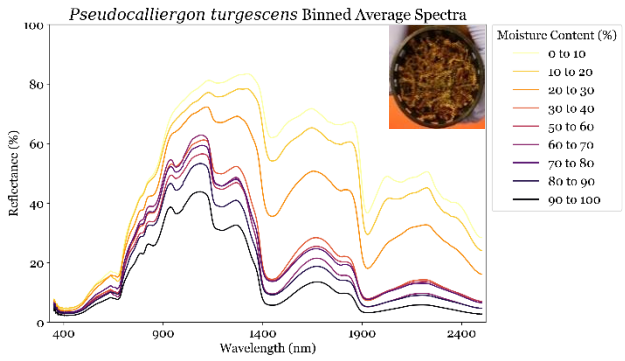

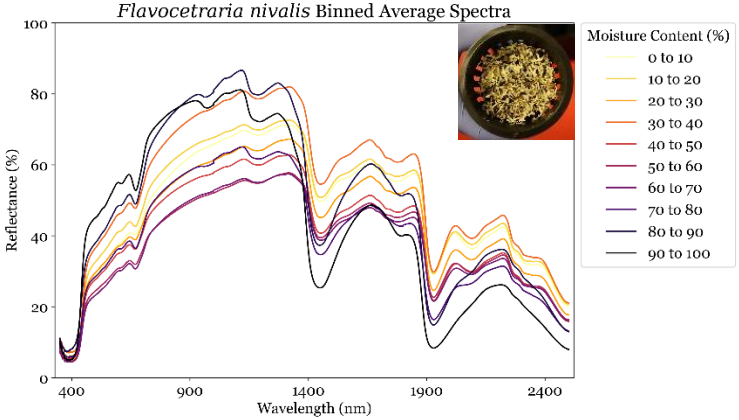
Flavocetraria nivalis Binned Average Spectra
Reflectance (%)
Wavelength (nm)
Moisture Content (%)
0 to 10
10 to 20
20 to 30
30 to 40
40 to 50
50 to 60
60 to 70
70 to 80
80 to 90
90 to 100

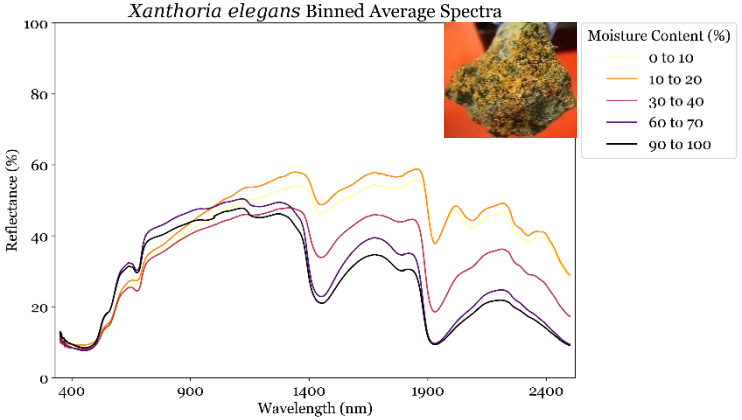
Xanthoria elegans Binned Average Spectra
Reflectance (%)
Wavelength (nm)
Moisture Content (%)
0 to 10
10 to 20
30 to 40
60 to 70
90 to 100

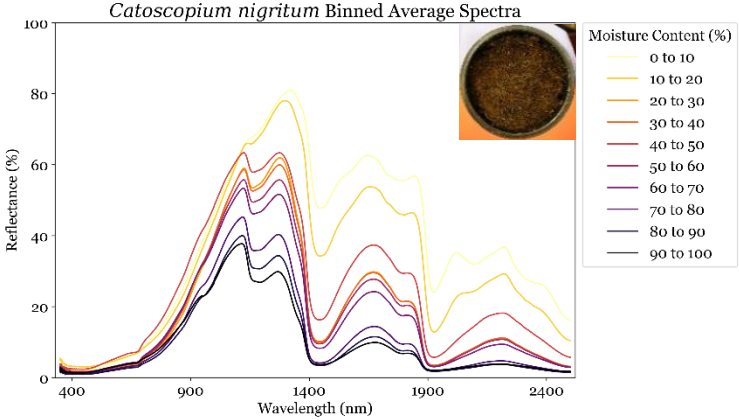
Catoscopium nigritum Binned Average Spectra
Reflectance (%)
Wavelength (nm)
Moisture Content (%)
0 to 10
10 to 20
20 to 30
30 to 40
40 to 50
50 to 60
60 to 70
70 to 80
80 to 90
90 to 100

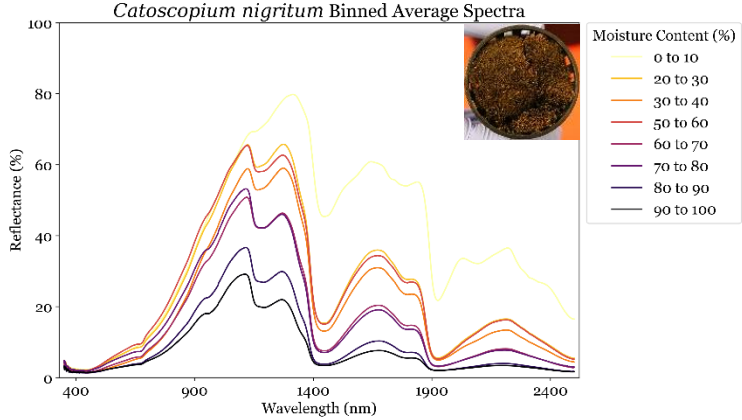
Catoscopium nigritum Binned Average Spectra
Reflectance (%)
Wavelength (nm)
Moisture Content (%)
0 to 10
20 to 30
30 to 40
50 to 60
60 to 70
70 to 80
80 to 90
90 to 100

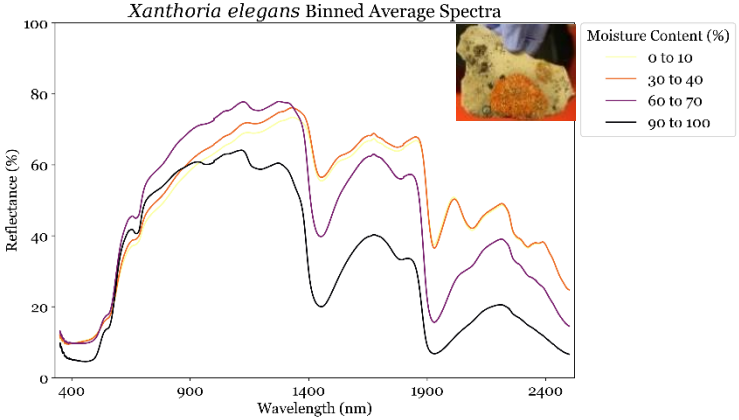
Xanthoria elegans Binned Average Spectra
Reflectance (%)
Wavelength (nm)
Moisture Content (%)
0 to 10
30 to 40
60 to 70
90 to 100

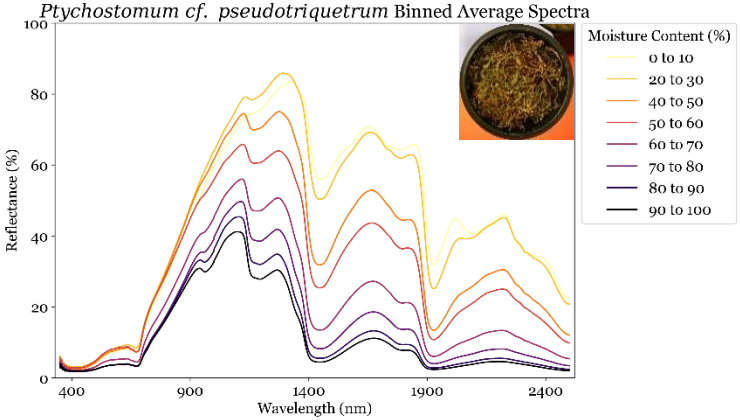
Ptychostomum cf. pseudotriquetrum Binned Average Spectra
Reflectance (%)
Wavelength (nm)
Moisture Content (%)
0 to 10
20 to 30
40 to 50
50 to 60
60 to 70
70 to 80
80 to 90
90 to 100

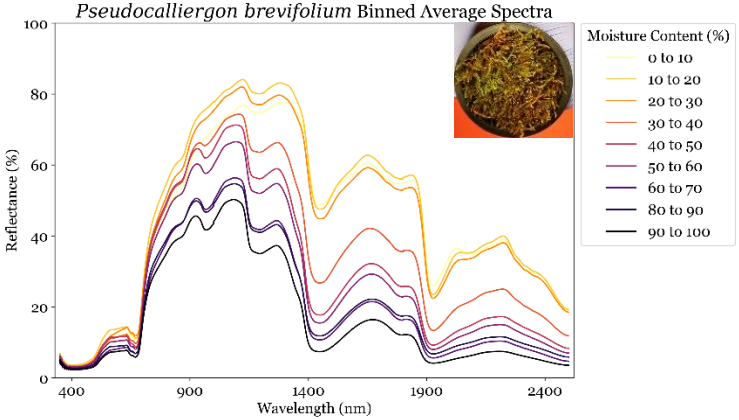
Pseudocalliergon brevifolium Binned Average Spectra
Reflectance (%)
Wavelength (nm)
Moisture Content (%)
0 to 10
10 to 20
20 to 30
30 to 40
40 to 50
50 to 60
60 to 70
80 to 90
90 to 100

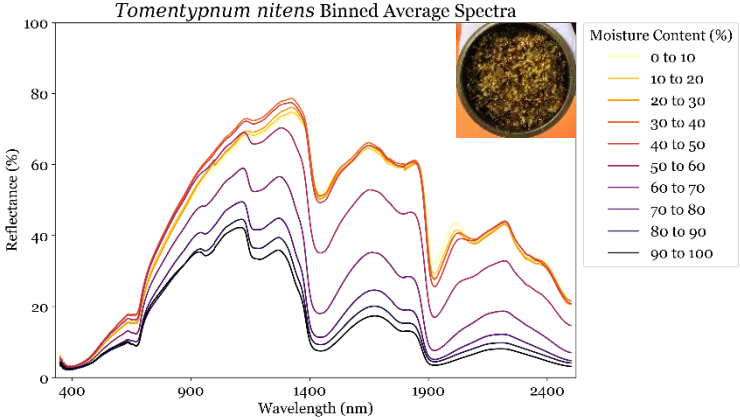
Tomentypnum nitens Binned Average Spectra
Reflectance (%)
Wavelength (nm)
Moisture Content (%)
0 to 10
10 to 20
20 to 30
30 to 40
40 to 50
50 to 60
60 to 70
70 to 80
80 to 90
90 to 100

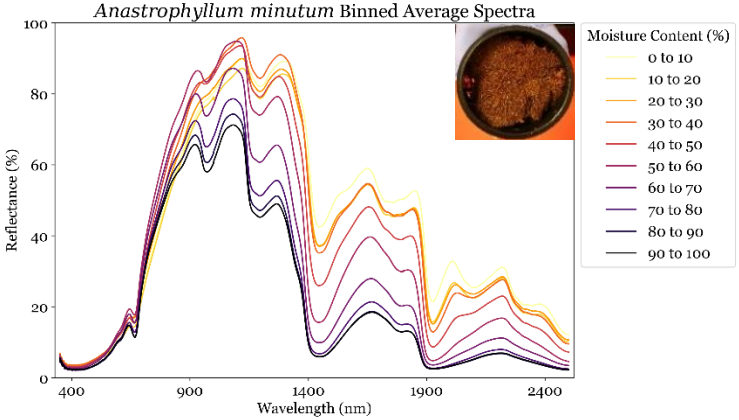
Anastrophyllum minutum Binned Average Spectra
Reflectance (%)
Wavelength (nm)
Moisture Content (%)
0 to 10
10 to 20
20 to 30
30 to 40
40 to 50
50 to 60
60 to 70
70 to 80
80 to 90
90 to 100

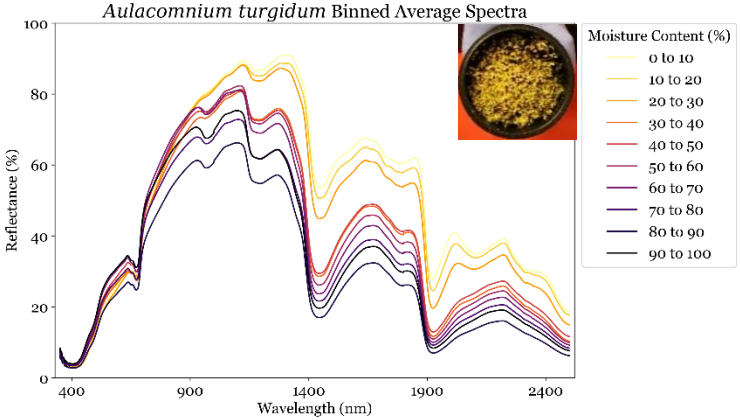
Aulacomnium turgidum Binned Average Spectra
Reflectance (%)
Wavelength (nm)
Moisture Content (%)
0 to 10
10 to 20
20 to 30
30 to 40
40 to 50
50 to 60
60 to 70
70 to 80
80 to 90
90 to 100

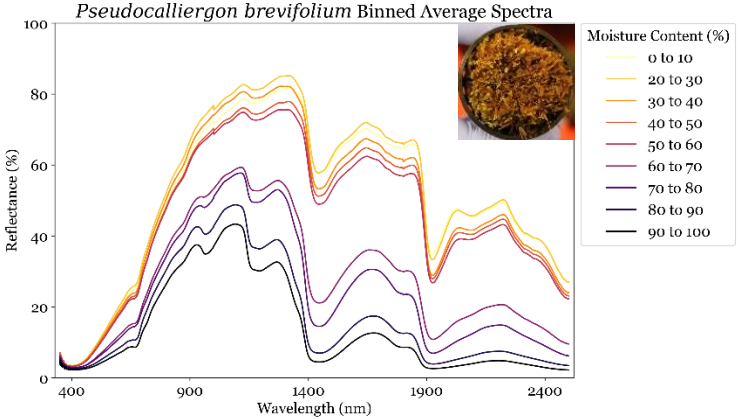
Pseudocalliergon brevifolium Binned Average Spectra
Reflectance (%)
Wavelength (nm)
Moisture Content (%)
0 to 10
20 to 30
30 to 40
40 to 50
50 to 60
60 to 70
70 to 80
80 to 90
90 to 100

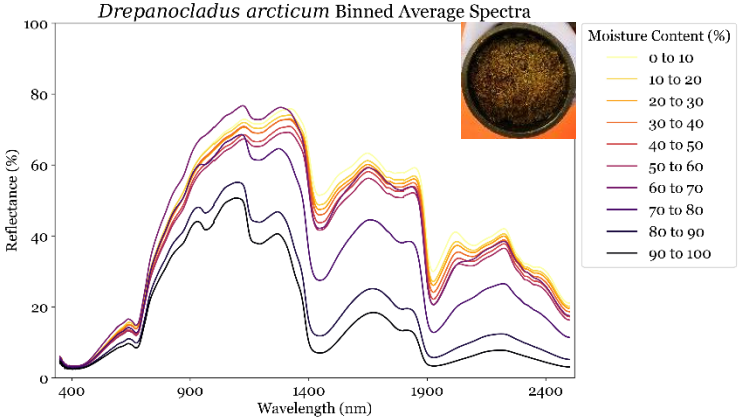
Drepanocladus arcticum Binned Average Spectra
Reflectance (%)
Wavelength (nm)
Moisture Content (%)
0 to 10
10 to 20
20 to 30
30 to 40
40 to 50
50 to 60
60 to 70
70 to 80
80 to 90
90 to 100

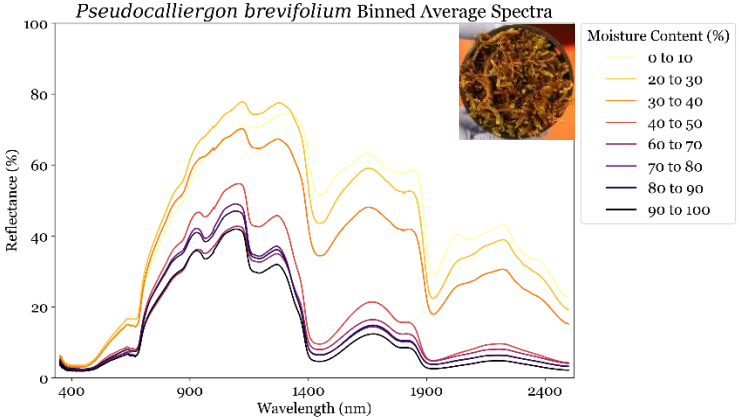
Pseudocalliergon brevifolium Binned Average Spectra
Reflectance (%)
Wavelength (nm)
Moisture Content (%)
0 to 10
20 to 30
30 to 40
40 to 50
60 to 70
70 to 80
80 to 90
90 to 100

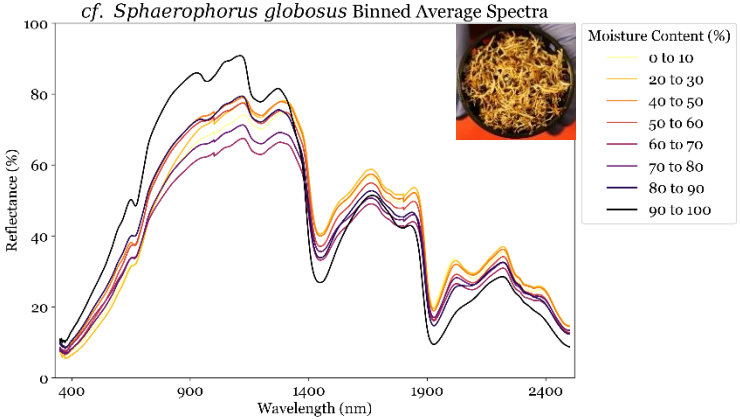
cf. Sphaerophorus globosus Binned Average Spectra
Reflectance (%)
Wavelength (nm)
Moisture Content (%)
0 to 10
20 to 30
40 to 50
50 to 60
60 to 70
70 to 80
80 to 90
90 to 100

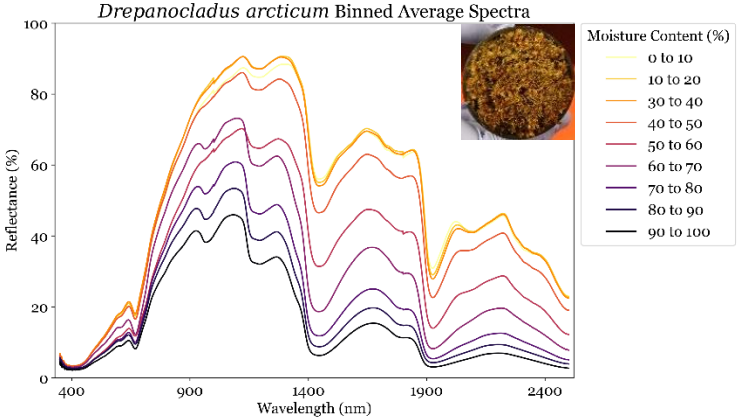
Drepanocladus arcticum Binned Average Spectra
Reflectance (%)
Wavelength (nm)
Moisture Content (%)
0 to 10
10 to 20
30 to 40
40 to 50
50 to 60
60 to 70
70 to 80
80 to 90
90 to 100

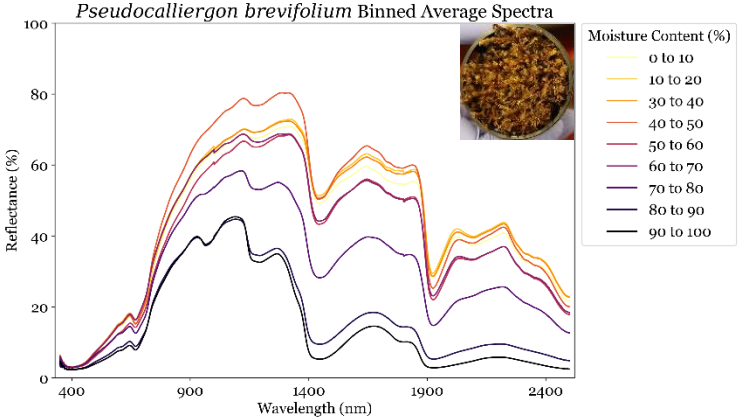
Pseudocalliergon brevifolium Binned Average Spectra
Reflectance (%)
Wavelength (nm)
Moisture Content (%)
0 to 10
10 to 20
30 to 40
40 to 50
50 to 60
60 to 70
70 to 80
80 to 90
90 to 100

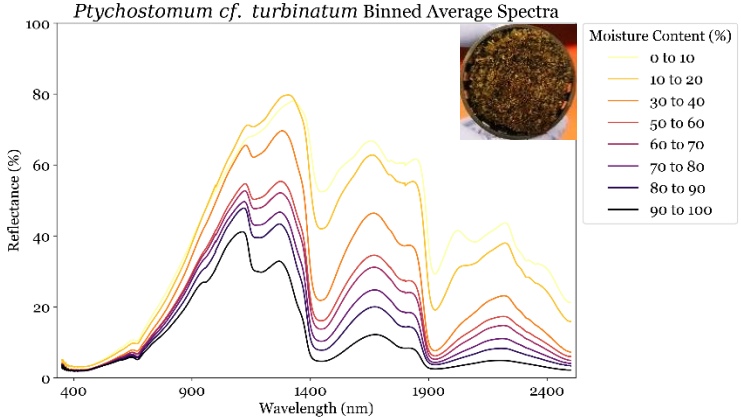

Convex Hull Maxima Points of Binned Spectra

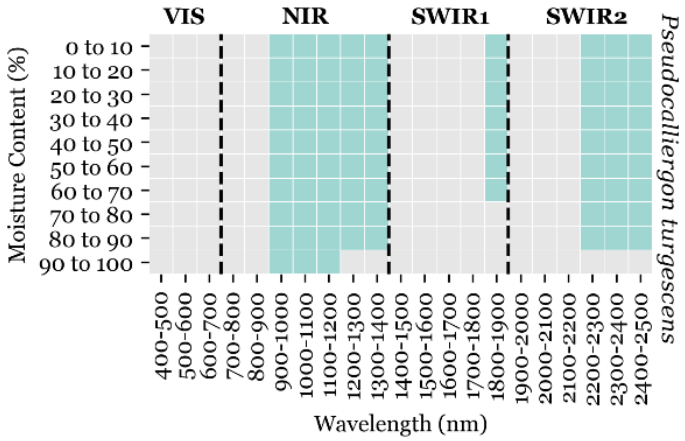

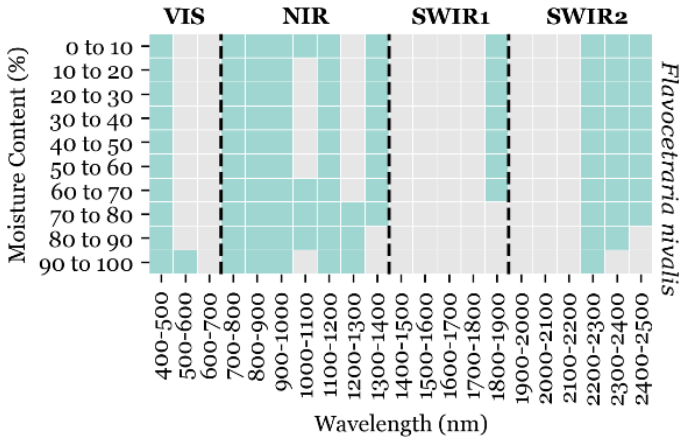

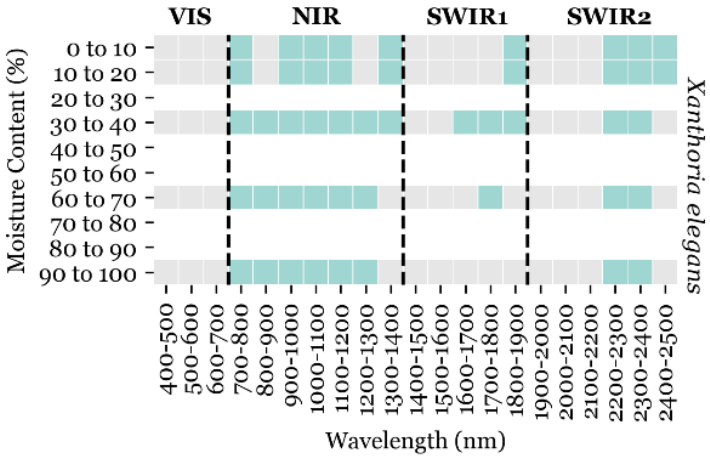
VIS
NIR
SWIR1
SWIR2
Moisture Content (%)
0 to 10
10 to 20
20 to 30
30 to 40
40 to 50
50 to 60
60 to 70
70 to 80
80 to 90
90 to 100
400-500
500-600
600-700
700-800
800-900
900-1000
1000-1100
1100-1200
1200-1300
1300-1400
1400-1500
1500-1600
1600-1700
1700-1800
1800-1900
1900-2000
2000-2100
2100-2200
2200-2300
2300-2400
2400-2500
Wavelength (nm)
Xanthoria elegans

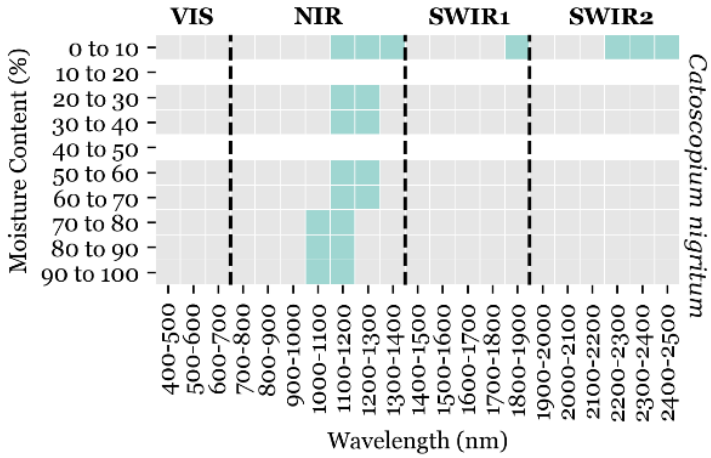
VIS
NIR
SWIR1
SWIR2
Moisture Content (%)
0 to 10
10 to 20
20 to 30
30 to 40
40 to 50
50 to 60
60 to 70
70 to 80
80 to 90
90 to 100
400-500
500-600
600-700
700-800
800-900
900-1000
1000-1100
1100-1200
1200-1300
1300-1400
1400-1500
1500-1600
1600-1700
1700-1800
1800-1900
1900-2000
2000-2100
2100-2200
2200-2300
2300-2400
2400-2500
Wavelength (nm)
Catoscopium nigritum

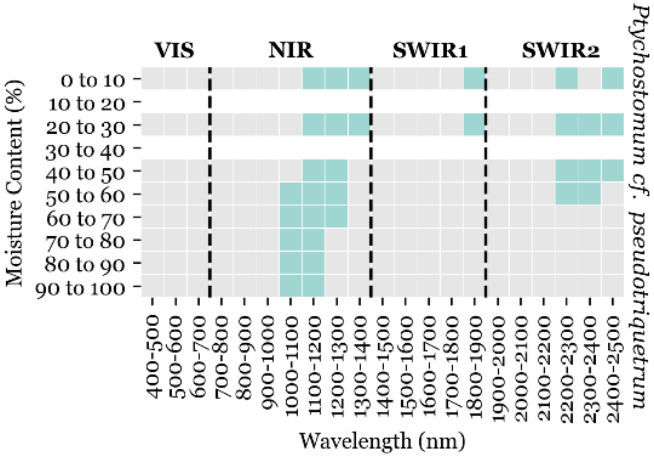
VIS
NIR
SWIR1
SWIR2
Moisture Content (%)
0 to 10
10 to 20
20 to 30
30 to 40
40 to 50
50 to 60
60 to 70
70 to 80
80 to 90
90 to 100
400-500
500-600
600-700
700-800
800-900
900-1000
1000-1100
1100-1200
1200-1300
1300-1400
1400-1500
1500-1600
1600-1700
1700-1800
1800-1900
1900-2000
2000-2100
2100-2200
2200-2300
2300-2400
2400-2500
Wavelength (nm)
Pohlia cf. pseudotorquescens

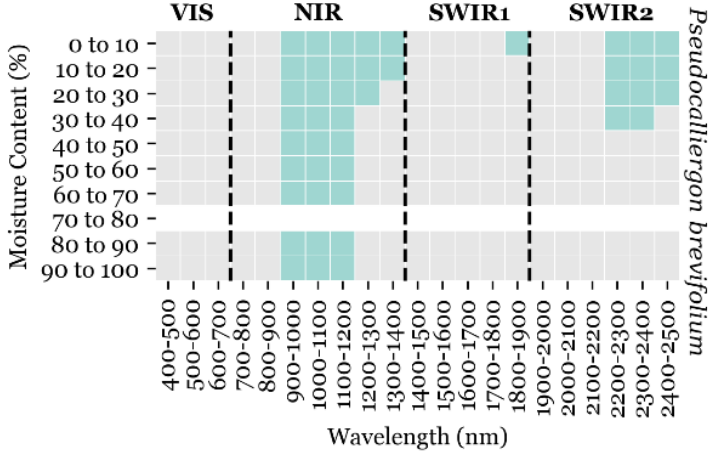
VIS
NIR
SWIR1
SWIR2
Moisture Content (%)
0 to 10
10 to 20
20 to 30
30 to 40
40 to 50
50 to 60
60 to 70
70 to 80
80 to 90
90 to 100
400-500
500-600
600-700
700-800
800-900
900-1000
1000-1100
1100-1200
1200-1300
1300-1400
1400-1500
1500-1600
1600-1700
1700-1800
1800-1900
1900-2000
2000-2100
2100-2200
2200-2300
2300-2400
2400-2500
Wavelength (nm)
Pseudocalliergon brevifolium

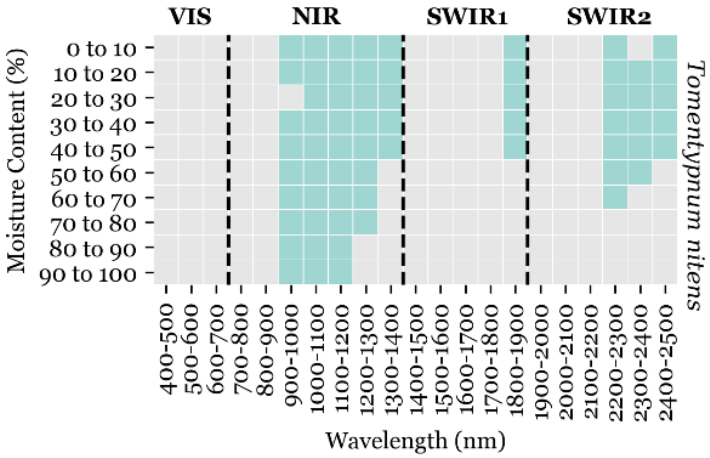
VIS
NIR
SWIR1
SWIR2
Moisture Content (%)
0 to 10
10 to 20
20 to 30
30 to 40
40 to 50
50 to 60
60 to 70
70 to 80
80 to 90
90 to 100
400-500
500-600
600-700
700-800
800-900
900-1000
1000-1100
1100-1200
1200-1300
1300-1400
1400-1500
1500-1600
1600-1700
1700-1800
1800-1900
1900-2000
2000-2100
2100-2200
2200-2300
2300-2400
2400-2500
Wavelength (nm)
Tomentypnum nitens

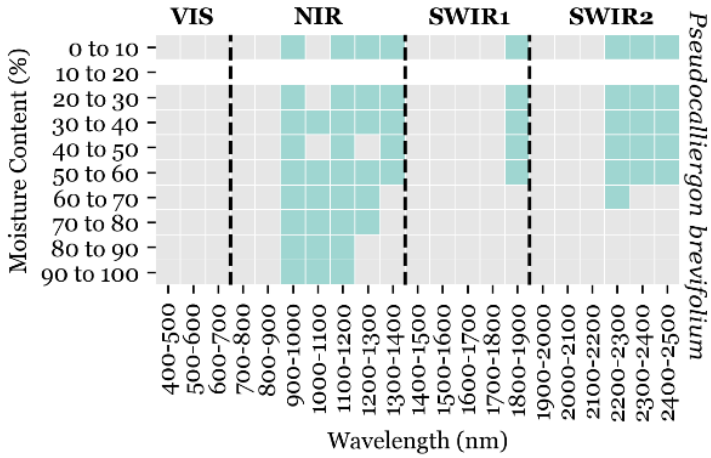
VIS
NIR
SWIR1
SWIR2
Moisture Content (%)
0 to 10
10 to 20
20 to 30
30 to 40
40 to 50
50 to 60
60 to 70
70 to 80
80 to 90
90 to 100
400-500
500-600
600-700
700-800
800-900
900-1000
1000-1100
1100-1200
1200-1300
1300-1400
1400-1500
1500-1600
1600-1700
1700-1800
1800-1900
1900-2000
2000-2100
2100-2200
2200-2300
2300-2400
2400-2500
Wavelength (nm)
Pseudocalliergon brevifolium

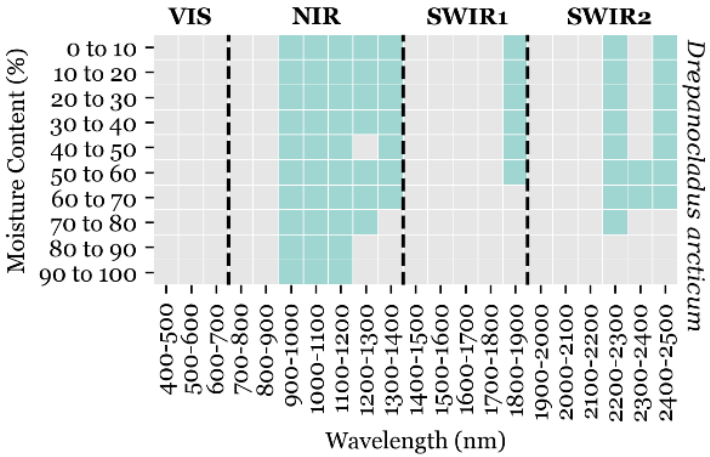
VIS
NIR
SWIR1
SWIR2
Moisture Content (%)
0 to 10
10 to 20
20 to 30
30 to 40
40 to 50
50 to 60
60 to 70
70 to 80
80 to 90
90 to 100
400-500
500-600
600-700
700-800
800-900
900-1000
1000-1100
1100-1200
1200-1300
1300-1400
1400-1500
1500-1600
1600-1700
1700-1800
1800-1900
1900-2000
2000-2100
2100-2200
2200-2300
2300-2400
2400-2500
Wavelength (nm)
Drepanocladus arcticum

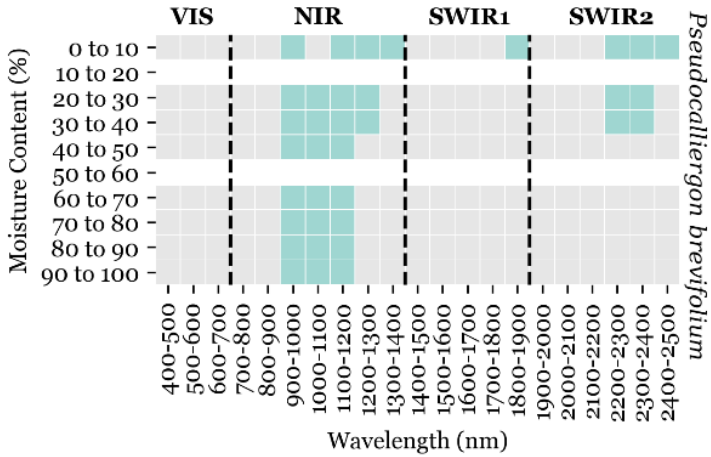
VIS
NIR
SWIR1
SWIR2
Moisture Content (%)
0 to 10
10 to 20
20 to 30
30 to 40
40 to 50
50 to 60
60 to 70
70 to 80
80 to 90
90 to 100
400-500
500-600
600-700
700-800
800-900
900-1000
1000-1100
1100-1200
1200-1300
1300-1400
1400-1500
1500-1600
1600-1700
1700-1800
1800-1900
1900-2000
2000-2100
2100-2200
2200-2300
2300-2400
2400-2500
Wavelength (nm)
Pseudocalliergon brevifolium

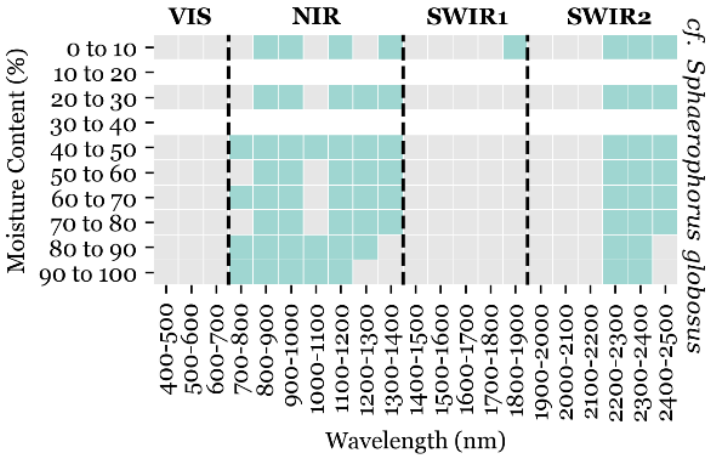
VIS
NIR
SWIR1
SWIR2
Moisture Content (%)
0 to 10
10 to 20
20 to 30
30 to 40
40 to 50
50 to 60
60 to 70
70 to 80
80 to 90
90 to 100
400-500
500-600
600-700
700-800
800-900
900-1000
1000-1100
1100-1200
1200-1300
1300-1400
1400-1500
1500-1600
1600-1700
1700-1800
1800-1900
1900-2000
2000-2100
2100-2200
2200-2300
2300-2400
2400-2500
Wavelength (nm)
cf. Sphaerophorus globosus

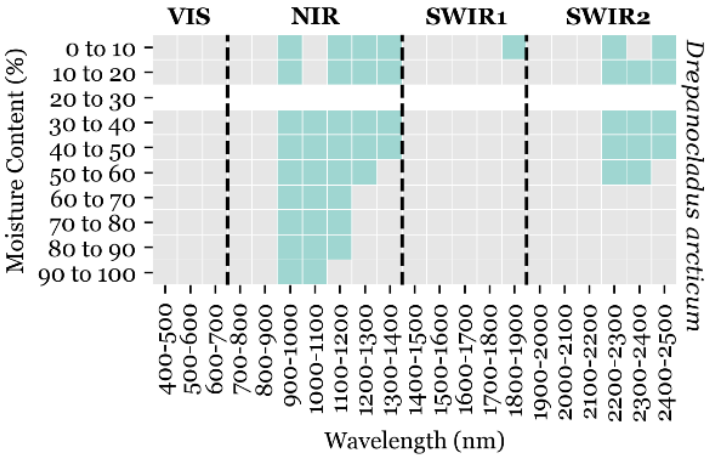
VIS
NIR
SWIR1
SWIR2
Moisture Content (%)
0 to 10
10 to 20
20 to 30
30 to 40
40 to 50
50 to 60
60 to 70
70 to 80
80 to 90
90 to 100
400-500
500-600
600-700
700-800
800-900
900-1000
1000-1100
1100-1200
1200-1300
1300-1400
1400-1500
1500-1600
1600-1700
1700-1800
1800-1900
1900-2000
2000-2100
2100-2200
2200-2300
2300-2400
2400-2500
Wavelength (nm)
Drepanocladus arcticum

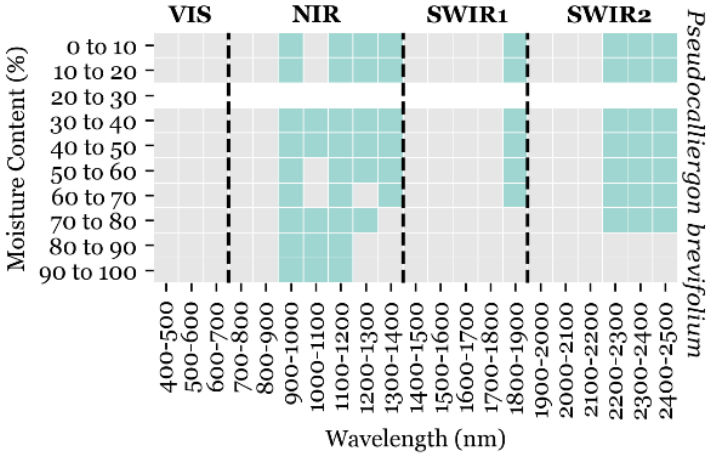
VIS
NIR
SWIR1
SWIR2
Moisture Content (%)
0 to 10
10 to 20
20 to 30
30 to 40
40 to 50
50 to 60
60 to 70
70 to 80
80 to 90
90 to 100
400-500
500-600
600-700
700-800
800-900
900-1000
1000-1100
1100-1200
1200-1300
1300-1400
1400-1500
1500-1600
1600-1700
1700-1800
1800-1900
1900-2000
2000-2100
2100-2200
2200-2300
2300-2400
2400-2500
Wavelength (nm)
Pseudocalliergon brevifolium

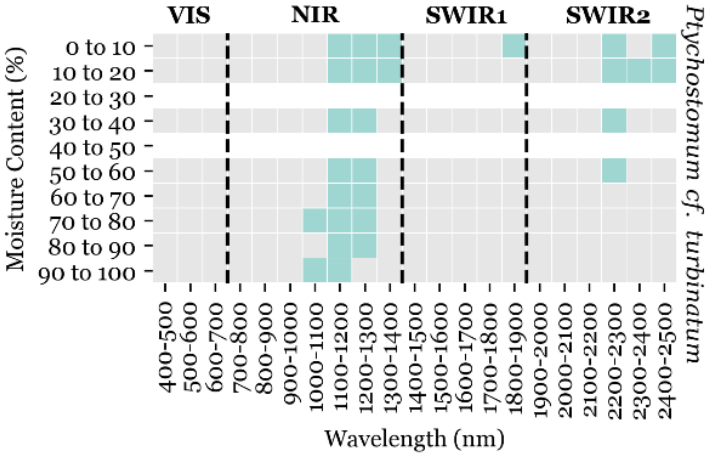
VIS
NIR
SWIR1
SWIR2
Moisture Content (%)
0 to 10
10 to 20
20 to 30
30 to 40
40 to 50
50 to 60
60 to 70
70 to 80
80 to 90
90 to 100
400-500
500-600
600-700
700-800
800-900
900-1000
1000-1100
1100-1200
1200-1300
1300-1400
1400-1500
1500-1600
1600-1700
1700-1800
1800-1900
1900-2000
2000-2100
2100-2200
2200-2300
2300-2400
2400-2500
Wavelength (nm)
Ptychostomum cf. turbinatum